DUDLEY
NAV
N

NAVAL POSTGRADUATE SCHOOL
Monterey, California

THESIS

UNDERWATER ACOUSTIC PROPAGATION
IN THE KOREA STRAIT

by

Sae Hun. Park

September 1983

Thesis Advisor: J. V. Sanders

Approved for public release; distribution unlimited

T215665

SECURITY CLASSIFICATION OF THIS PAGE (When Data Entered)

REPORT DOCUMENTATION PAGE

READ INSTRUCTIONS BEFORE COMPLETING FORM

1. REPORT NUMBER

2. GOVT ACCESSION NO.

3. RECIPIENT'S CATALOG NUMBER

4. TITLE (and Subtitle)

Underwater Acoustic Propagation in the Korea Strait

5. TYPE OF REPORT & PERIOD COVERED

Master's Thesis
September 1983

6. PERFORMING ORG. REPORT NUMBER

7. AUTHOR(s)

Sae Hun. Park

8. CONTRACT OR GRANT NUMBER(s)

9. PERFORMING ORGANIZATION NAME AND ADDRESS

Naval Postgraduate School
Monterey, CA 93943

10. PROGRAM ELEMENT, PROJECT, TASK AREA & WORK UNIT NUMBERS

11. CONTROLLING OFFICE NAME AND ADDRESS

Naval Postgraduate School
Monterey, CA 93943

12. REPORT DATE

September 1983

13. NUMBER OF PAGES

135

14. MONITORING AGENCY NAME & ADDRESS(if different from Controlling Office)

15. SECURITY CLASS. (of this report)

15a. DECLASSIFICATION/DOWNGRADING SCHEDULE

16. DISTRIBUTION STATEMENT (of this Report)

Approved for public release; distribution unlimited

17. DISTRIBUTION STATEMENT (of the abstract entered in Block 20, if different from Report)

18. SUPPLEMENTARY NOTES

19. KEY WORDS (Continue on reverse side if necessary and identify by block number)

Korea Strait, Underwater sound, Transmission Loss Models, Shallow Water Acoustics, Parabolic Equation

20. ABSTRACT (Continue on reverse side if necessary and identify by block number)

On 17 September 1980, a transmission loss (TL) experiment was conducted in the Korea Strait as a joint project between the Naval Air Development Center, U.S., and Agency for Defense Development, Korea. Two propagation paths were measured; the first parallel to the Korea Trench and the second across the trench. The TL, calculated by NADC is greater across the trench

DD FORM 1 JAN 73 1473 EDITION OF 1 NOV 65 IS OBSOLETE

S/N 0102-LF-014-6601

SECURITY CLASSIFICATION OF THIS PAGE (When Data Entered)

than parallel to the trench. A representative Sound Velocity Profile was selected after examination of twelve locations close to the experimental track. This SVP, bottom type, and bathymetry were used in three computer models and the predictions of TL compared to experimental results. A split-step FFT parabolic equation model and a ray mode model shows little difference in the two directions. An implicit finite difference parabolic equation model showed a significant difference. Agreement along the path parallel to the trench was excellent when 30 dB were added to the experimental results. Agreement across the trench was less satisfactory.

Approved for public release; distribution unlimited

Underwater Acoustic Propagation in the Korea Strait

by

Sae Hun. Park
Lieutenant Commander, Republic of Korea Navy
B. S., Republic of Korea Naval Academy, 1972

Submitted in partial fulfillment of the
requirements for the degree of

MASTER OF SCIENCE IN OCEANOGRAPHY

from the

NAVAL POSTGRADUATE SCHOOL
September 1983

Thesis
P157552
c.1

DUDLEY KNOX LIBRARY
NAVAL POSTGRADUATE SCHOOL
MONTEREY, CALIFORNIA 93943

ABSTRACT

On 17 September 1983, a transmission loss (TL) experiment was conducted in the Korea Strait as a joint project between the Naval Air Development Center, U.S. and Agency for Defense Development, Korea. Two propagation paths were measures; the first parallel to the Korea Trench and the second across the trench. The TL, calculated by NADC is greater across the trench than parallel to the trench. A representative Sound Velocity Profile (SVP) was selected after examination of twelve locations close to the experimental track. This SVP, bottom type, and bathymetry were used in three computer models and the predictions of TL compared to experimental results. A split-step FFT parabolic equation model and a ray mode model shows little difference in the two directions. An implicit finite difference parabolic equation model showed a significant difference. Agreement along the path parallel to the trench was excellent when 30 dB were added to the experimental results. Agreement across the trench was less satisfactory.

TABLE OF CONTENTS

I. INTRODUCTION ---------- 16

A. FORWARD ---------- 16

B. DATA ACQUISITION ---------- 18

C. DATA PROCESSING ---------- 18

D. OBJECTIVES ---------- 18

II. GEOPHYSICAL FEATURES OF THE KOREA STRAIT ---------- 20

A. OCEANOGRAPHY ---------- 20

1. General ---------- 20

2. Sea Bottom Topography and Sediment ---------- 21

3. Ocean Current ---------- 26

4. Tide ---------- 31

5. Salinity ---------- 34

6. Sound Velocity Profiles (SVP) ---------- 37

7. Thermal Structure ---------- 40

a. Sea-Surface Temperature ---------- 40

b. Mixed Layer Depth (MLD) ---------- 47

B. ACOUSTICS ---------- 49

1. Ambient Noise ---------- 49

a. Wind-Related Noise ---------- 51

b. Biological Noise ---------- 57

c. Shipping and Industrial Noise ---------- 63

2. Acoustic Effects of the Bottom ---------- 65

3. Signal Fluctuation ---------- 69

III. MEASUREMENT OF TRANSMISSION LOSS IN THE KOREA STRAIT ----- 76

IV. COMPARISON WITH COMPUTER MODELS ---------- 85

V. CONCLUSIONS AND RECOMMENDATIONS ---------- 111

A. CONCLUSIONS ---------- 111

B. RECOMMENDATIONS ---------- 111

APPENDIX A ---------- 113

APPENDIX B ---------- 119

LIST OF REFERENCES ---------- 131

BIBLIOGRAPHY ---------- 133

INITIAL DISTRIBUTION LIST ---------- 134

LIST OF TABLES

1. Summary of Background Noise at Sea ---------- 51

2. Monthly Mean Wind Speed and Direction in September in the Korea Strait ---------- 55

3. Annual Mean Wind Speed and Direction in September in the Korea Strait ---------- 56

4. Summary of the Sensitivity Check of JAEGER Model ---------- 102

LIST OF FIGURES

1. Geographical Location of the Korea Strait ---------- 22

2. Geographical Location of the Korea Strait with Sea of Japan ---------- 23

3. Bathymetry around Korean Peninsula ---------- 24

4. Bathymetry in the Korea Strait ---------- 25

5. Distribution of Sediments in the Korea Strait and around Coastal Korean Peninsula ---------- 27

6. Seasonal Predominant Ocean Circulation Pattern Around the Korean Peninsula ---------- 29

7. Monthly Mean Surface Current Speed in the Western Channel of the Korea Strait ---------- 30

8. General Ocean Circulation around Korean Peninsula ---------- 32

9. Average Tidal Range around Korea Peninsula ---------- 33

10. T-S Diagram in the Korea Strait ---------- 35

11. Typical Temperature, Salinity, Density Profile in Shallow Water ---------- 39

12. SVP at the Korea Trench in September ---------- 41

13. Schematic Picture of Factors Affecting Ocean Thermal Structure ---------- 42

14. Limiting Ray Paths in Different SVP ---------- 43

15. Generalized Seasonal, Monthly Change of Thermal Structure --- 45

16. Mean Monthly Sea Surface Temperature Distribution around the Korean Peninsula in March and September ---------- 46

17. Average Ambient Noise Level in the Korea Strait (1) on-shore location (34 47 N - 128 45 E) and (2) off-shore location (34 42 N - 128 00 E) ---------- 50

18. Conceptual Diagram of Sources of Deep Water Ambient Noise ---- 50

19. Wind-related Ambient Noise Spectra at Coastal Locations ------ 52

20. Wind Dominated Ambient Noise Level ---------- 52

21. Standard Deviation of Ambient Noise with Winds, Shipping Contribution ---------- 54

22. Distribution of Sound-Producing Fish around the Korean Peninsula ---------- 58

23. Biological Distribution around the Korean Peninsula ---------- 59

24. Migration Months and Route of Common Fish in the Korea Strait ---------- 60

25. Overall Diurnal Variation of Shrimp Noise Level at Various Locations ---------- 60

26. Distribution of Marine Mammals around the Korean Peninsula in Summer ---------- 62

27. Distribution of Marine Mammals around the Korean Peninsula in Winter ---------- 62

28. Comparison of Ambient Noise Standard Deviation Dominated by Shipping and Wind at Different Locations ---------- 64

29. Average Ambient Noise Level at the Entrance of Pusan --------- 64

30. Average Ambient Noise Level at the Entrance of Ulsan Harbor -- 65

31. Measured Bottom Backscattering Strength of Various Bottom Materials ---------- 67

32. Bottom Loss Classification for Frequency 1 - 4 khz ---------- 67

33. Typical Bottom Loss in Korea Strait ---------- 68

34. Diurnal Variation of Fish Attenuation ---------- 71

35. Drop Pattern Diagram for Transmission Loss Measurement in the Korea Strait ---------- 78

36. Bottom Contour in NE Direction ---------- 79

37. Bottom Contour in SE Direction ---------- 80

38. Measured Transmission Loss in NE Direction ---------- 81

39. Measured Transmission Loss in SE Direction ---------- 82

40. Historical September BT Plot in the Korea Strait ---------- 83

41. Maximum and Minimum Temperature Profile in the Korea Strait ---------- 84

42. Ray Path in the NE Direction with Single SVP ---------- 87

43. Ray Path in the SE Direction with Single SVP ---------- 88

44. Incoherent TL in NE Direction, 200 hz ---------- 89

45. Incoherent TL in SE Direction, 200 hz ---------- 90

46. TL Comparison in 100 hz, Half-beam Width 60 Degree, in both Directions by NEWPE Model ---------- 92

47. TL in the NE Direction, 50 hz, N=4000, smooth=5. KS1 ------- 94

48. TL in the SE Direction, 50 hz, N=4000, smooth=5 ---------- 95

49. Comparison of Smoothed NEWPE Prediction with Measurements 50 hz, 60 degrees half-beam Width ---------- 97

50. Comparison of Smoothed NEWPE Prediction with Measurements 100 hz, 60 degrees Half-beam Width ---------- 98

51. Comparison of Smoothed NEWPE Prediction with Measurements 200 hz, 60 degrees Half-beam Width ---------- 99

52. Comparison of TL with MEDUSA Model and Measurements -------- 100

53. The Effect of the Number of Vertical Grid Points, 200 hz --- 103

54. The Effect of the Number of Vertical Grid Points, 800 hz --- 104

55. TL Comparison of the Effect with Different Bottom Profile -- 105

56. TL Comparison with Flat Bottom, in Both Directions, 50 hz -- 107

57. TL Comparison with JAEGER Model and Measurements, 50 hz ---- 108

58. TL Comparison with JAEGER Model and Measurements, 100 hz --- 109

59. TL Comparison with JAEGER Model and Measurements, 200 hz --- 110

A-1. Monthly Mean SST in January and February ---------- 113

A-2. Monthly Mean SST in March and April ---------- 114

A-3. Monthly Mean SST in May and June ---------- 115

A-4. Monthly Mean SST in July and August ---------- 116

A-5. Monthly Mean SST in September and October ---------- 117

A-6. Monthly Mean SST in November and December ---------- 118

B-1. Historical SVP in September (34.8N-129.7E) ---------- 119

B-2. Historical SVP in September (34.9N-129.5E) ---------- 120

B-3. Historical SVP in September (34.9N-129.6E) ---------- 121

B-4. Historical SVP in September (34.9N-129.7E) ---------- 122

B-5. Historical SVP in September (35.0N-129.3E) ---------- 123

B-6. Historical SVP in September (35.0N-129.4E) ---------- 124

B-7. Historical SVP in September (35.0N-129.5E) ---------- 125

B-8. Historical SVP in September (35.1N-129.2E) ---------- 126

B-9. Historical SVP in September (35.1N-129.3E) ---------- 127

B-10. Historical SVP in September (35.1N-129.5E) ---------- 128

B-11. Historical SVP in September (35.2N-129.6E) ---------- 129

B-12. Historical SVP in September (35.3N-129.7E) ---------- 130

ABBREVIATIONS

1. ROK: Republic of Korea
2. ASW: Anti-Submarine Warfare
3. SAR: Search and Rescue
4. SVP: Sound Velocity Profile
5. SUS: Signal, Underwater Sound
6. SONAR: Sound Navigation and Ranging
7. RADAR: Radio Detection and Ranging
8. MSL: Mean Sea Level
9. FNOC: Fleet Numerical Oceanography Center
10. NADC: Naval Air Development Center
11. MLD: Mixed Layer Depth
12. DARPA: Defense Advanced Research Projects Agency
13. ADD: Agency for Defence Development in R.O.K.
14. NRL: Naval Research Laboratory
15. JASA: Journal of The Acoustic Society of America
16. NUSC: Naval Underwater System Center
17. SLOC: Sea Line of Communications
18. NAVOCEANO: Naval Oceanographic Office
19. BLUG: Bottom Loss Upgrade
20. SSMO: Summary of Synoptic Meteological Observation
21. MOODS: Master Oceanography Observation Data System
22. FACT: Fast Assymtotic Coherence Transmission
23. PE: Parabolic Equation

24. KIAS: Knots, Indicated Air Speed

25. SST: Sea Surface Temperature

26. DMAHTC: Defense Mapping Agency Hydrographic Topographic Center

27. LOFAR: Low Frequency Analyzing and Recording

28. FFT: Fast Fourier Transform

29. IFD: Implicit Finite Difference

ACKNOWLEDGEMENT

I wish to thank Professors James V. Sanders of the Physics Department and Glenn H. Jung of the Oceanography Department of the U.S. Naval Postgraduate School for their academic guidance as well as numerous practical comments.

Their close coordination, communication, and supervision made this thesis possible and I hope that the relationships remain close in the future.

I also appreciate the help of Professor A. B. Coppens of the Physics Department of the U.S. Naval Postgraduate School for his support and advice, particularly in relation to the calculation of Sound Velocity and testing the Transmission Loss Models.

I would also like to thank Lieutenant Joe Blanchard of Air Ocean Science Program Curriculum at the U. S. Naval Postgraduate School and Lieutenant Bruce Northridge of Fleet Numerical Oceanographic Center, Monterey and Mr. Eugene Brown, Bill Currie of NAVOCEANO for their assistance in acquiring data and helping with the various computer programs. Thanks also to Dr. Na J.Y. Applied Research Laboratory at Research Institute in Chinhae; Dr. D.E. Weston of the Procurement

Executive Ministry of Defence, Admiralty Underwater Weapons Establishment, Portland, United Kingdom, for supplying data and papers.

I also want to express my great thanks to the Repulic of Korea Navy and especially to my colleagues, Naval Aviators CAPT. Kwon, S.Y.; CDR Lee, K.P.; and CDR, Park, Y.K., Commander of AIRASRON 101, for their encouragement and for providing data.

I. INTRODUCTION

A. FORWARD

Underwater sound has a wide variety of applications ranging from commercial fishing to military operations. In naval operations underwater sound is employed in mine operations, search and detection efforts, and underwater communication; especially for submarine and anti-submarine warfare the understanding of the sound transmission is essential for effective search and evasion measures in the ocean.

The ROK navy conducts anti-submarine warfare, mine operations, and amphibious operations as well as counter-infiltration operations in support of national security. To accomplish these missions successfully, the understanding of environmental phenomena and how they affect the behavior of underwater sound is of prime importance for operations. The understanding of various interactions and mechanisms of how the ocean bottom properties, such as density and topography, and SVP in the water column, the generation of the waves, propagation of tides, and swells, current system, ocean fronts affect acoustic propagation in the ocean is a fundamental requirement to conduct successful naval operations.

During the last 10 years, naval officers have tried to carry out the assigned operations and exercises without sufficiently taking into account the environmental factors. However, as naval weapon systems have become sophisticated and submarine evasive measures improved, environmental considerations have become more important and sensitive for the successful conduct of naval operations, especially for ASW.

As Air-ASW platforms were introduced in the inventory of the ROK Navy, we realized during past exercises that the patterns, tactics, and operational procedures which were developed for use in the deep oceans were not applicable to the shallow Korean waters. We strongly feel the need to develop for shallow water use tactics which will maximize the ASW readiness not only for the air platform but also the jointly coordinated ASW task. The growing interest about the environmental conditions around the Korean Peninsula lead to a series of experiments and measurements conducted by the joint efforts with ROK Navy and researchers.

In addition, mission commanders and organizational commanders need accurate and reliable environmental forecasts for the mission area, and they need to know how the environment affects the conduct of the mission. To carry out their mission better, the naval officers need to understand the geophysical characteristics in their operational areas. The understanding of oceanographic dynamical mechanisms is helpful not only for ASW but also for amphibious operations, mine operations, SAR and counter-infiltration operations and other naval operations as well.

This thesis addresses one aspect of these problems: The environmental factors necessary to compute the propagation loss of particular importance to the ROK Navy in the Korea Strait between southeastern Korean and Kyushu of Japan. This region is very important for Korea's national security, and it is an area of much greater complexity in its physical and dynamical properties than other ocean areas aurrounding Korea.

B. DATA ACQUISITION

a. The climatological Bathythermographs (BTs) were available from FNOC MOODS data.

b. Bottom Bathymetry charts were provided by the NAVOCEANO, DMAHTC, and Dr. Na of ARL Texas.

c. Bottom loss values with grazing angle at different frequencies were available from the FNOC BLUG data.

d. Sediments composition chart of the study area were also provided by Dr. Na of ARL Texas.

e. Propagation loss data were obtained from the ADD Chin-Hae, ROK.

f. Sounding charts of the Korea Strait were provided by the Commander of AIRASRON 101, ROK Navy.

C. DATA PROCESSING

a. The ray trace was plotted by the FNOC computer either MEDUSA or RP70.

b. Sound velocity profiles were plotted by TEK-618 at NPGS.

c. Transmission loss was computed by NEWPE model at the NAVOCEANO, IFD PE model (JAEGER Model) at the NPGS and by MEDUSA model at the FNOC.

D. OBJECTIVES

This thesis addresses some of oceanographic factors that influence ASW operations in the Korea Strait by attempting to:

a. Collect and summarize pertinent oceanographic data that influences acoustic propagation and detection in the Korea Strait.

b. Review those aspects of oceanographic behavior that are not usually important in deep ocean but may be of importance in the Korea Strait.

c. Acquire a basic understanding of underwater sound propagation mechanisms in the Korea Strait.

d. Evaluate and determine the validity of various computer models as applied to the problem of sound proparation in the Korea Strait.

e. Compare and analyze the propagation loss from the actual measurement and numerical model results.

II. GEOPHYSICAL FEATURES OF THE KOREA STRAIT

A. OCEANOGRAPHY

1. General

The Korea Strait is a sea area between the Sea of Japan and East Chine Sea (Yellow Sea). It is divided into two channels by Tsushima Island. The western channel is part of the Korean peninsula and the eastern channel is part of the Sea of Japan.

The Korea Strait is a relatively small and shallow sea area but has very complicated environmental features that affect underwater sound transmission. Without describing the detailed geological development of the Korea Strait, the shore line of the southern peninsula is highly indented and there are many small islands off shore that are made of hard granitic rocks.

The Naktong River, which is the major river in the southern peninsula, flows into the narrow western channel. The Naktong delta is close to Pusan harbor. The Nakton River brings muddy sediments and fresh water into the Korea Strait. Pusan Harbor, the largest commercial port in the ROK is located 5 nm east of the Naktong river. Considerable container shipping and fishing traffic go through the Korea Strait. (Figure 1)

There are many small fishing villages along the coast. Small fishing boats generate a lot of broad band noise in this region. The general ocean flow starts to separate from the strong Kuroshio Current into the Tsushima Current as it flows toward the northeast through the Korea Strait to the Sea of Japan. (See section II-A-3)

The Korea Strait is about 150 nm (280 km) in length and has a maximum width of 110 nm (200 km); the shortest distance from the southeastern tip of the Korean peninsula to the northwestern tip of Tsushima Island is 25 nm (45 km). The average water depth in the Korea Strait is 45 km (150 ft) and the maximum is 230 m (750 ft) in the western channel trench.

The Korea Strait has a very important strategic role. It allows year-round accessibility to the Sea of Japan. Vladivostok, the principal Soviet naval port in the Pacific area, is located in the Sea of Japan. The Soviet Pacific Fleet has to pass through one of four possible straits (Korea Strait, Soya Strait, Tsugaru Strait, Tatarsk Strait) to enter and return from the Pacific Ocean. (Figure 2)

2. Sea Bottom Topography and Sediment

The bathymetry at the Sea of Japan is characterized by a series of basins, plateaus, banks and troughs. The three largest basins are the Tsushima Basin at the southern end, the Yamato Basin on the eastern side, and the Japan Basin at the northern end. These basins are separated by a plateau and rise complex in the central area. The average water depth is 1500 m (5000 ft) and maximum depth is 4000 m (13000 ft) in the sea of Japan.

The bottom topography in the Korea Strait is relatively smooth except in the trench. The average water depth of the Korea Strait is 45 m (150 ft) except in the Korean Trench where the maximum depth reaches 230 m (750 ft). The western channel is deeper than the eastern channel. It starts gradually deepending from the southern Korean peninsula toward the trench and rises smoothly back up on the other side off Kyushu of Japan.

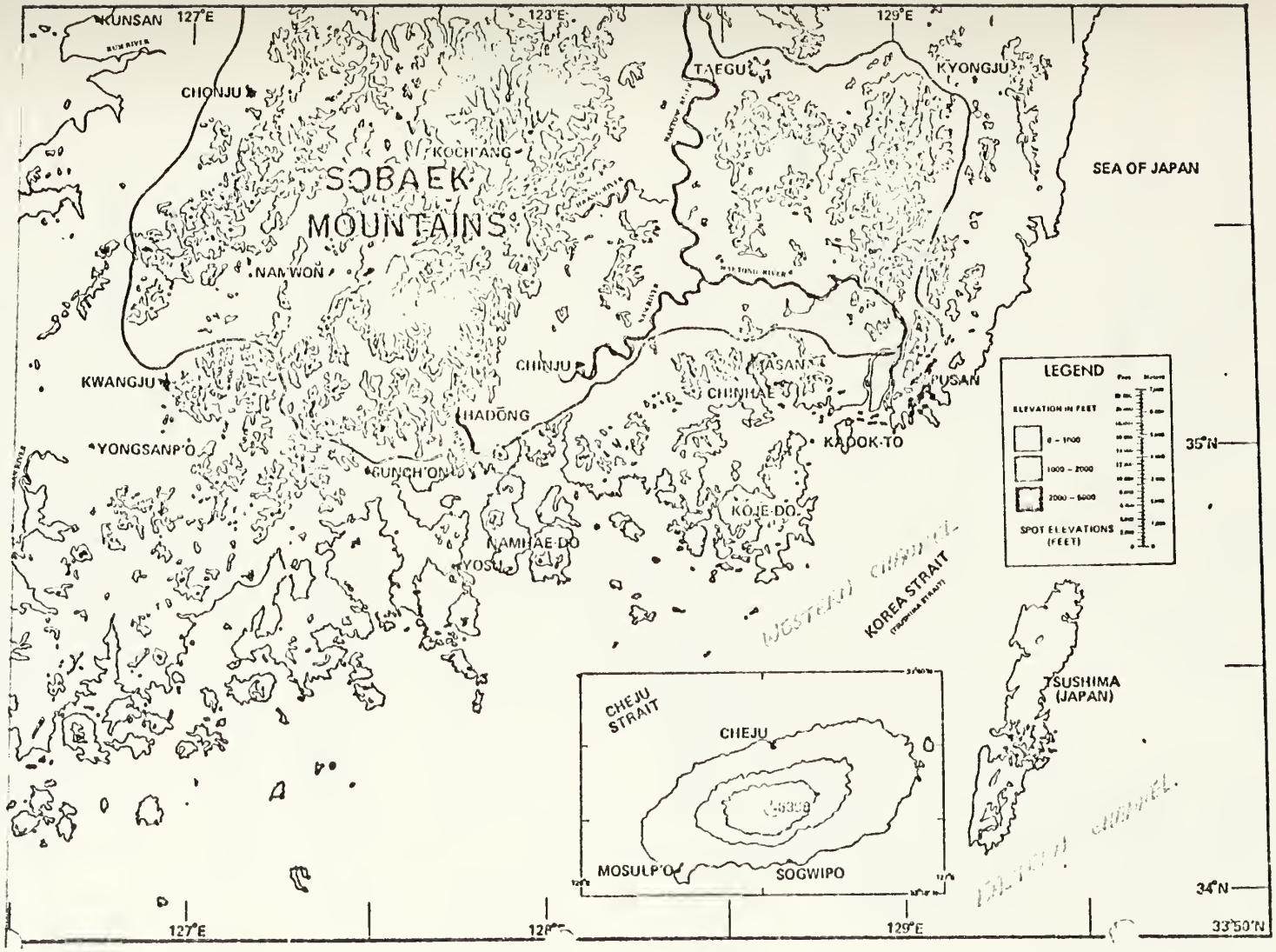

Figure 1. Geographical Location of the Korea Strait. (From Nestor, 1977)

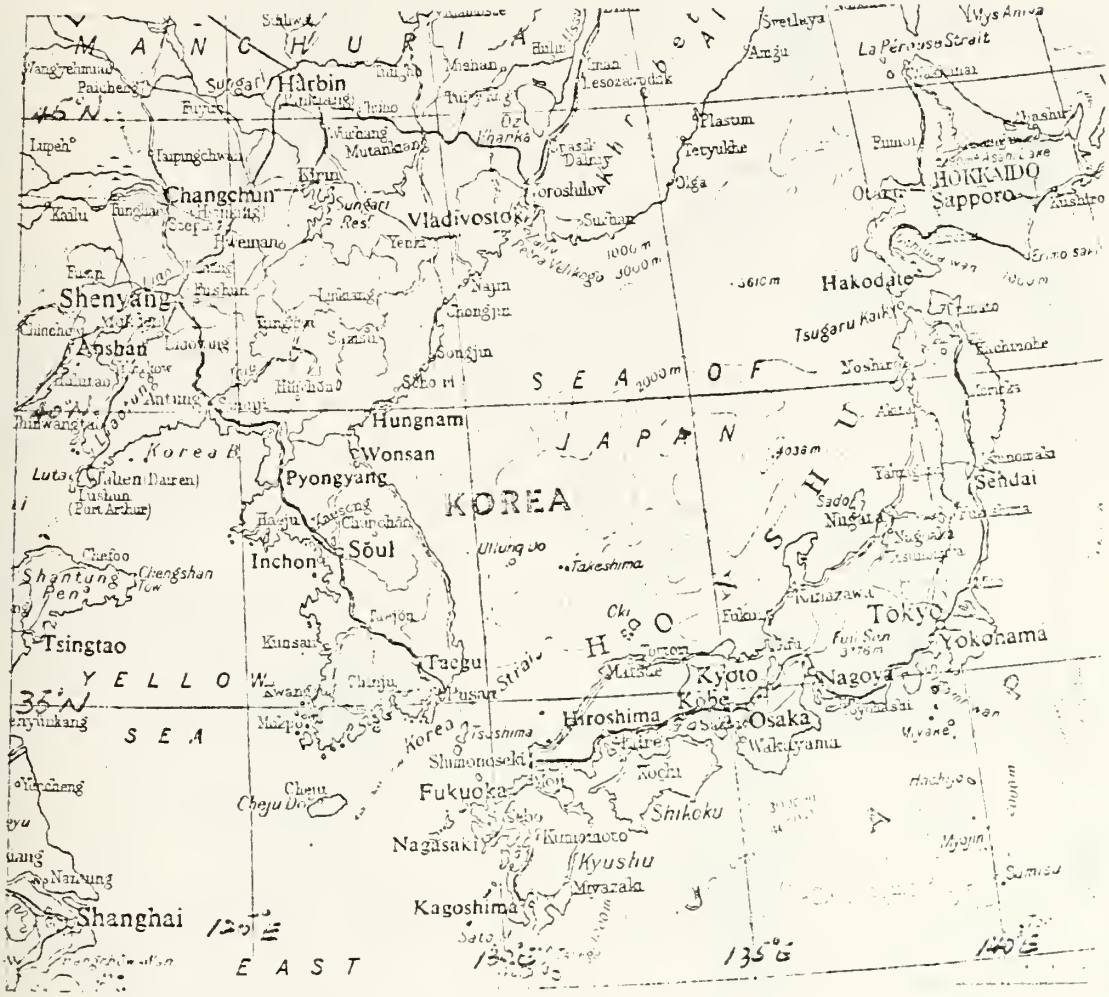

Figure 2. Geographical Location of the Korea Strait with Sea of Japan. (From The Times Atlas of the World, 1958).

The bathymetry around the Korean peninsula, Sea of Japan, and Korea Strait are shown in Figures 3 and 4.

The accurate sediment layering and composition in the Korea Strait is not well known. Most of the core samples for the world ocean show different degrees of layered structure rather than one single constant structure.

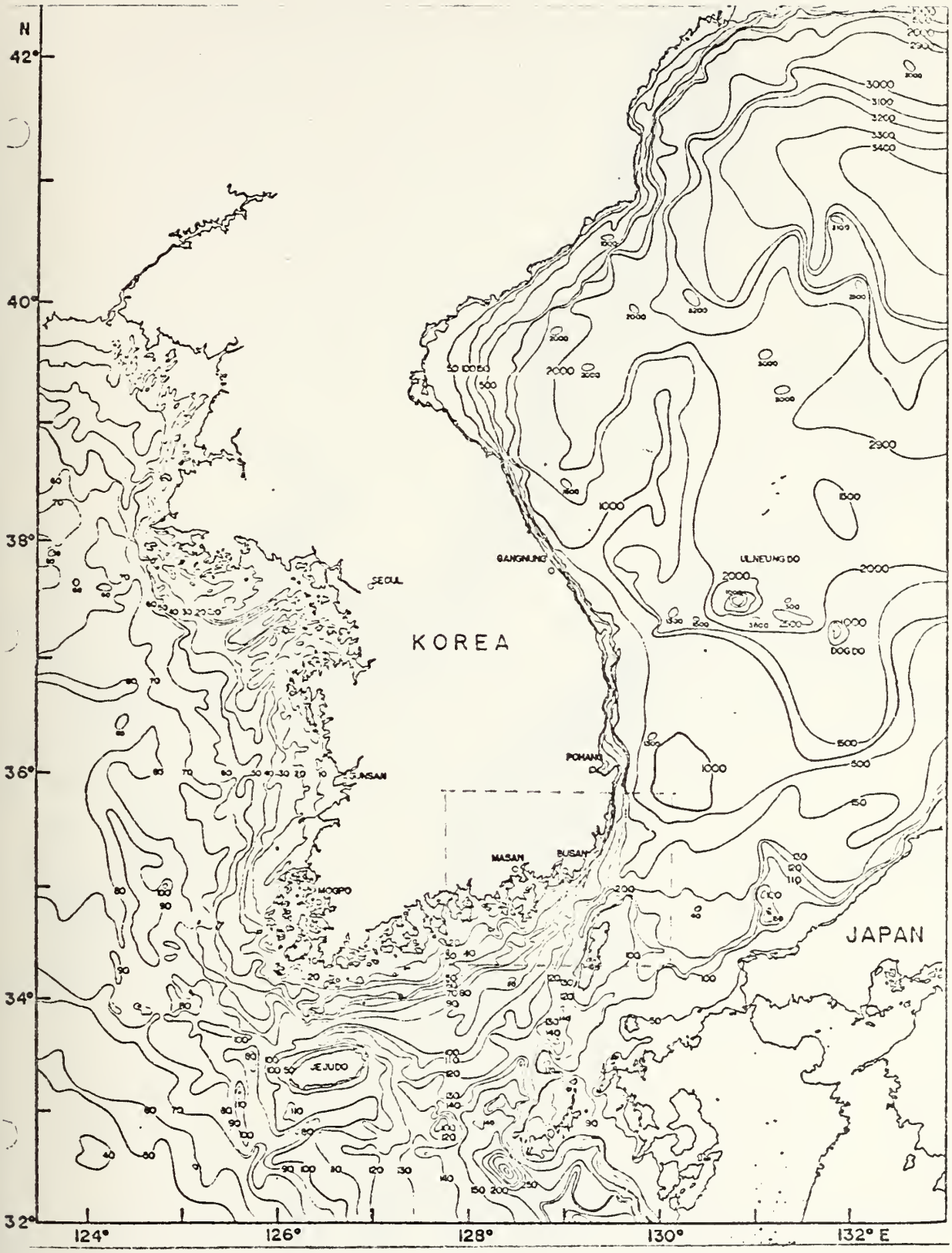

Figure 3. Bathymetry around Korean Peninsula. (From Lee, 1980)

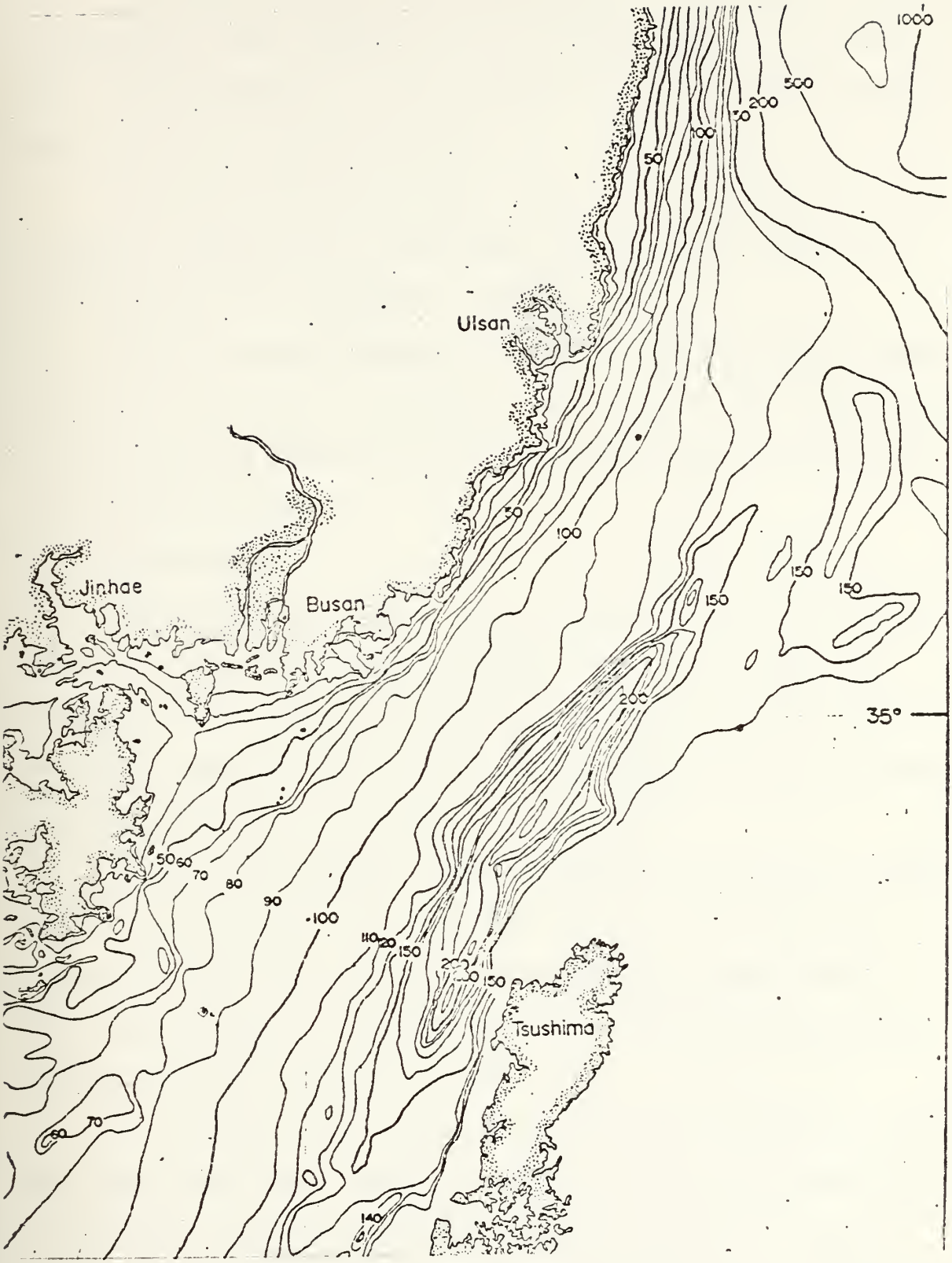

Figure 4. Bathymetry in the Korea Strait. (From Na, 1982)

The different density and sound velocity of each layer affects the underwater sound propagation loss. The Naktong River is the main source of local sediments in the Korea Strait, with additional contributions from the Yantz River in China.

The finer grain-sized sediments stay for a longer period of time in the water column and are carried away further by wave actions than are coarse-grain-sized sediments. (Figure 5)

The most dominent sediment around the Korean Peninsula is clayey silt close to the coast at the estuary of this major river. Mud and very fine sand are major sediments in the Sea of Japan and in the off-shore area in the Korea strait.

3. Ocean Current

The general ocean flow in the Korea Strait is dominated all the year round by the strong Kuroshio Current toward the northeast. The Kuroshio Current originates from the North Equatorial Current which is a relatively warm and saline flow toward the northeast passing southeast of Kyushu and Shikoku to the North Pacific Current.

At about 28-30 degrees north, the Kuoshio Current starts to bend toward the Sea of Japan. At 32 degrees north parts of the Kuroshio Current flows into the Korea Strait toward Tsushima Island, moving at about 1 knot; however, it slackens and shallows as it proceeds, forming the Tsushima Current in the Sea of Japan.

The Tsushima Current splits into two branches to the west of the Goto Islands; the eastern branch passes through the eastern channel of the Korea Strait and the western branch passes through the western channel. The Korea Strait of occupied by the Tsushima Current enroute

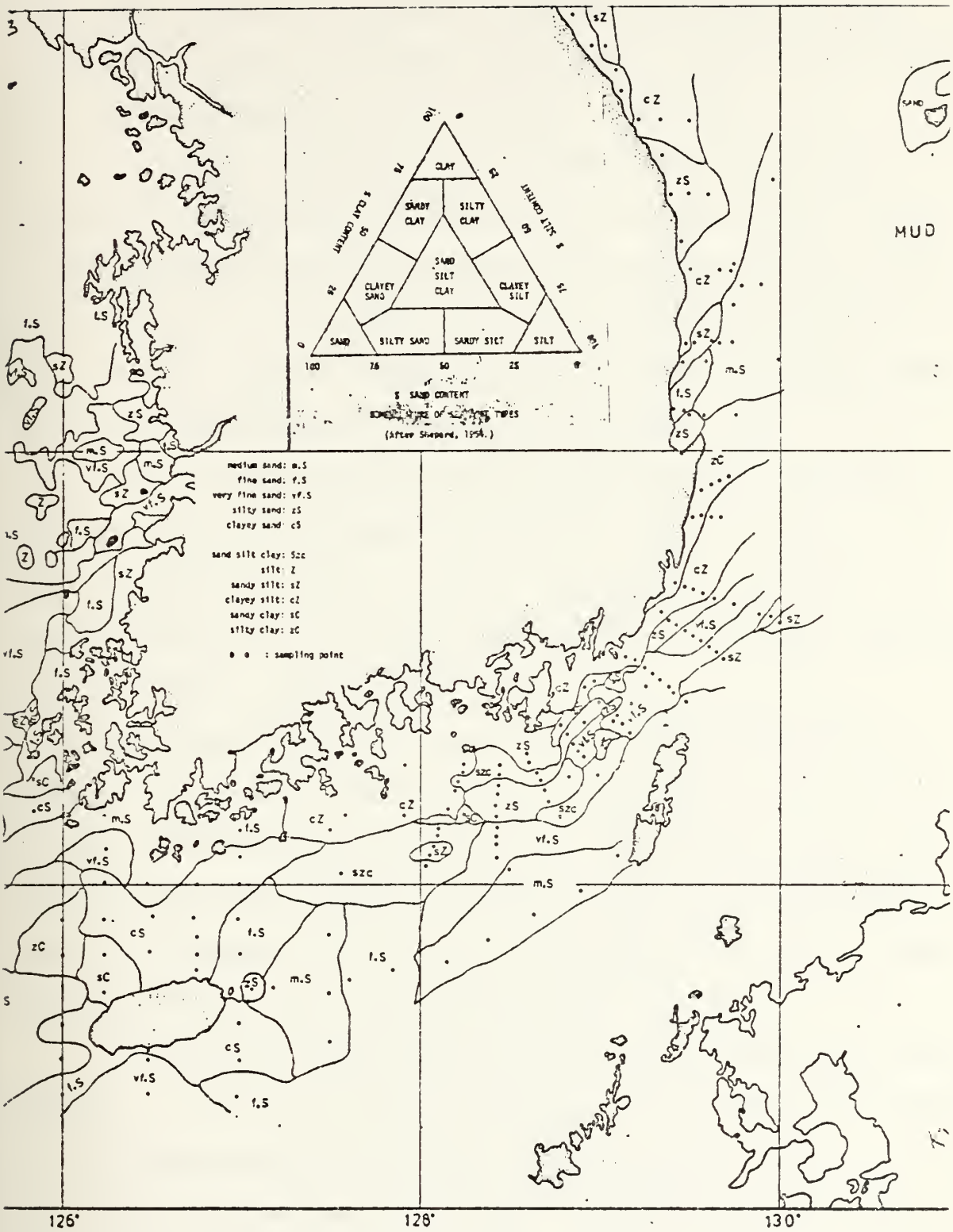

Figure 5. Distribution of Sediments in the Korea Strait and Around Coastal Korean Peninsula. (From Na, 1982)

to the Sea of Japan. The Tsushima Current flows toward Sea of Japan predominantly; during the southerly summer monsoon period the wind-driven circulation is prevailing to the northeast. (Figure 6)

The prevailing southerly winds produce coastal upwelling and turbulent mixing around 35-37 degrees north in the east coast. During the winter monsoon, northerly winds drive the Liman Current and Yellow Sea Current to the south. The Yellow Sea Current penetrates further and converges toward the Tsushima Current. The Liman Current mixes with the northeastward Tsushima Current near 35-38 degrees north.

Many scientific research efforts have been made to understand the dynamical oceanic calculation in the Korea Strait. The most recent paper explains the generation of the Tsushima Current as a result of a pressure difference between the Tsugaru and Korea Strait due to wind-driven ocean circulation. (Yoshiaki Toba et al., 1982)

The velocity of the Tsushima Current in the two channels are different. The eastern branch flows at a maximum speed of about one half of that in the western branch. The velocity in the upper layer of the western channel between Izuhara of Tsushima Island and Pusan of Korea reaches its maximum in October, and its minimum in March, with an annual mean velocity of 48 cm/s. (Kenzo Shuto, 1982) (Figure 7)

The East Korea Warm Current along the eastern coast of the Korean Peninsula is formed after passing through the Western Channel and extends up to 38 degrees north. The location varies from year to year.

Where the Tsushima Current meets the Southern Korean Coastal water it produces the Korean Coastal Front.

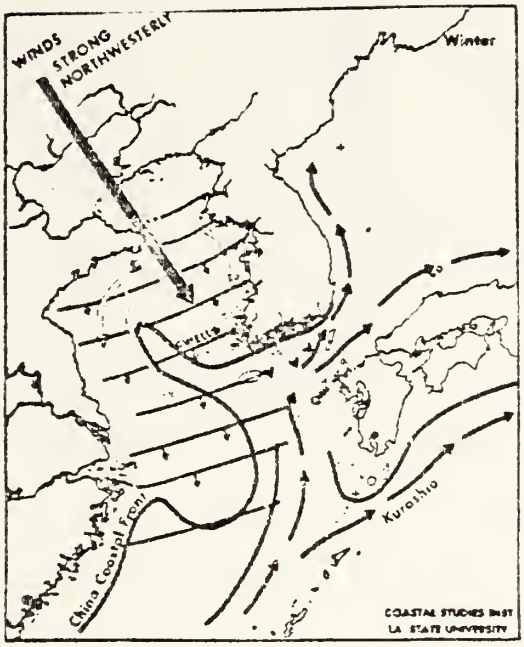

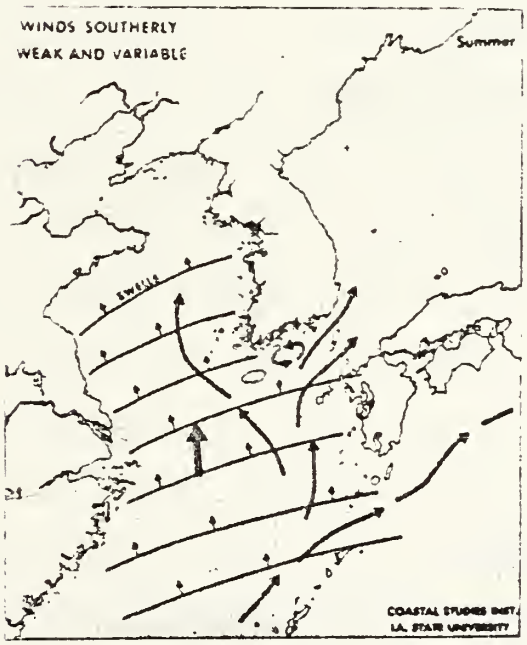

Figure 6. Seasonal Predominant Ocean Circulation Pattern Around the Korean Peninsula. (From Huh, 1982)

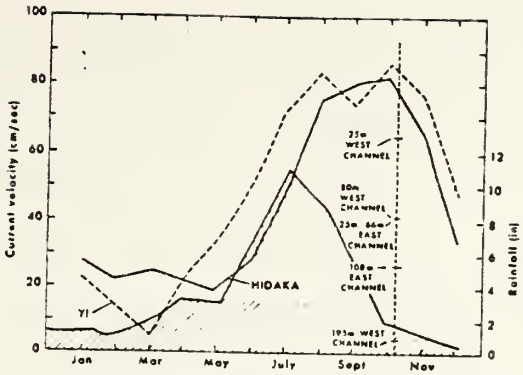

Figure 7. Monthly mean surface current speed in the western channel of the Korea Strait. (From Huh, 1982)

The Kuroshio Current flows further northwestward into the Yellow Sea area, making the Yellow Sea Warm Front when it meets with the Yellow Sea Current. The cool, fresh Oyashio Current which originated from the Sub-arctic region flows southward into the Sea of Japan.

The ocean circulation system around the Korean Peninsula varies seasonally with the typical monsoon seasons of winter and summer. During the winter, a large Continental Polar air mass develops over Siberia and generates strong northwest winds flowing into the peninsula. The strong north westerly winds generate a southerly flow of wind-driven ocean circulation (The west Yellow Sea Current and the east Oyashio Current).

The Yellow Sea (West Korean) Coastal water, freshened from summer run-off and cooled by the northerly winds is forced to flow southward. When it reaches the Korea Strait, the cool, fresh West Korean Coastal Current converges with the Tsushima Current in the western channel and forms South Korea Coastal Front. This fron is strongest and most stable in fall and winter when temperature and salinity gradients coincide. (Oscar K. Huh, 1982)

The Yellow Sea Current and Oyashio Current reach maximum speeds in the middle of December. The cold, fresh Oyashio Current penetrates beyond 38

degrees north, sometimes reaching 35 degrees north. When it meets with the warm, saline Tsushima Current moving northward, it produces the moderate Tsushima Front at around 35-38 degrees north.

By the end of March with the weakening of the wind from the north, the Yellow Sea Current and Oyashio Current change in speed and direction. This effect is not felt by the Oyashio Current until May because it is further north. During the summer, a large Maritime Tropical air mass develops in the tropical area. The southerly wind starts to dominate the whole Korean peninsula and sea area. The strong summer monsoon accelerates the northward Kuroshio Current which reaches a maximum speed of 1-2 knots and a mean water temperature of 68 F (20 C) in mid-June. At this time, the Yellow Sea Current changes its direction along the southwest coast of the Korean peninsula and begins to move northward along the west coast. The Tsushima Current becomes more extensive, reaching its maximum by July, and influences part of the domain of the Oyashio Current. The prevailing off-coast wind produces coastal upwelling at around 35 degrees north. As more and more warm water is pushed northward in the Kuroshio Current, mean water temperature is about 76 F (24.5 C), compared with 50F (15.5 C) in winter. (Figure 8)

4. Tide

Figure 9 illustrates the tidal ranges around the Korean peninsula. The mean tidal ranges vary from coast to coast. Along the east coast, in the Sea of Japan, the mean tidal range is almost negligible all the year round. The tidal range increases westward from 4 ft (1.2 m) at Pusan to 11 ft (3.3 m) at Yosu. The tidal progression along the east coast is very weak. The tide floods to the southwest and ebbs to the northeast along the east

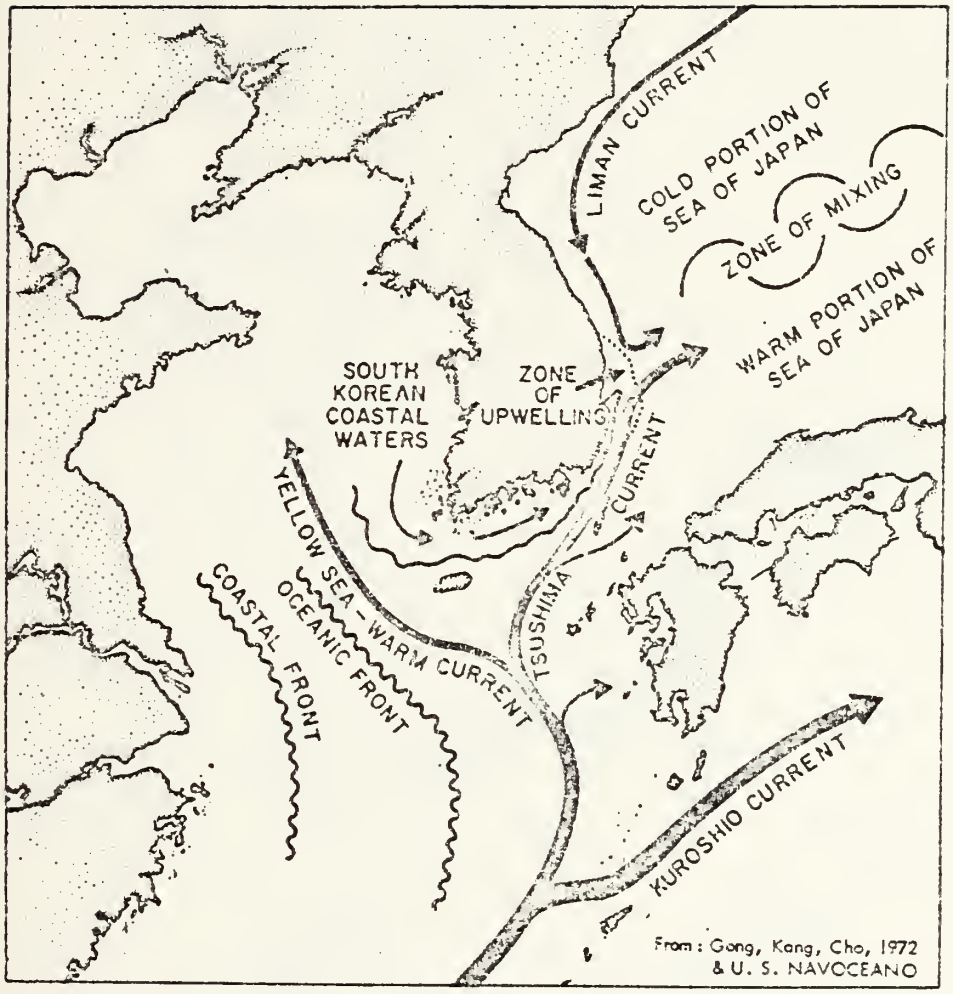

Figure 8. General Ocean Circulation around Korean Peninsula (From Nestor, 1977)

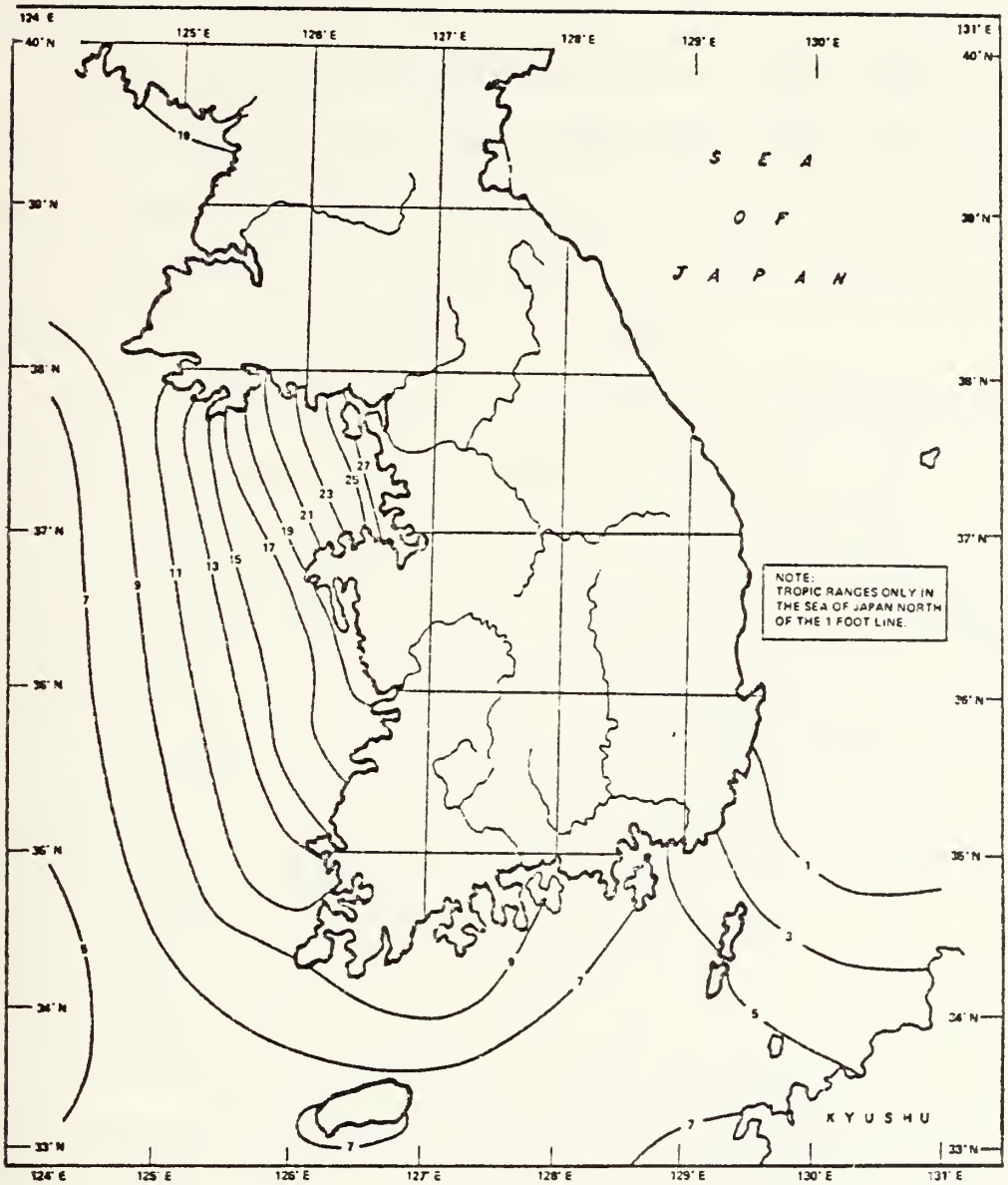

Figure 9. Average Tidal Range around Korea Peninsula. (From Nestor, 1977)

coast. The tidal flow in the Korea Strait changes twice a day near shore along the southern coast. It flows west at ebb tide and east on the flood tide with maximum flow occurring between Pusan, Korea, and Izuhara, Tushima, Japan.

On the other hand, along the west coast the mean tidal range varies from 2-21 ft. with the maximum tidal range along the west coast occurring at Inchon (37 50 N-126 40 E), about 30 ft. The mean tidal range is 3-5 ft (0.9-1.5 m) in the Korea Strait with the spring tide range reaching 11.5 ft. (3.5 m) along the south coast.

In the Korea Strait, the tidal currents are semidiurnal (two floods and two ebbs occur in each tidal day) mixed with diurnal. (Nestor, 1977) The semidiurnal tide is predominant along the west coast with flooding to north and ebbing to south. (Nestor, 1977) The tidal current speed changes from coast to coast; it varies from 1.5 kts in off-shore areas to 10 kts close to the coastal islands. The maximum flood tidal current generally occurs about three hours before high water and the maximum ebb tidal current occurs 3 hours after high water. Slack water occurs about midway between local high and low water.

5. Salinity

According to Kolpack (1982), most of the water in the Sea of Japan is relatively homogeneous and consists of deep bottom water with salinity of about 34.0 to 34.1 ppt. Above this water mass are the intermediate and surface waters, with more variable properties as a result of the influence of the cold northern Oyashio and warm Kuroshio Currents.

When the warm, salind Kuroshio Current moves northeastward through the Korea Strait it generates fairly complex oceanographic aspects in the upper water column with large variability.

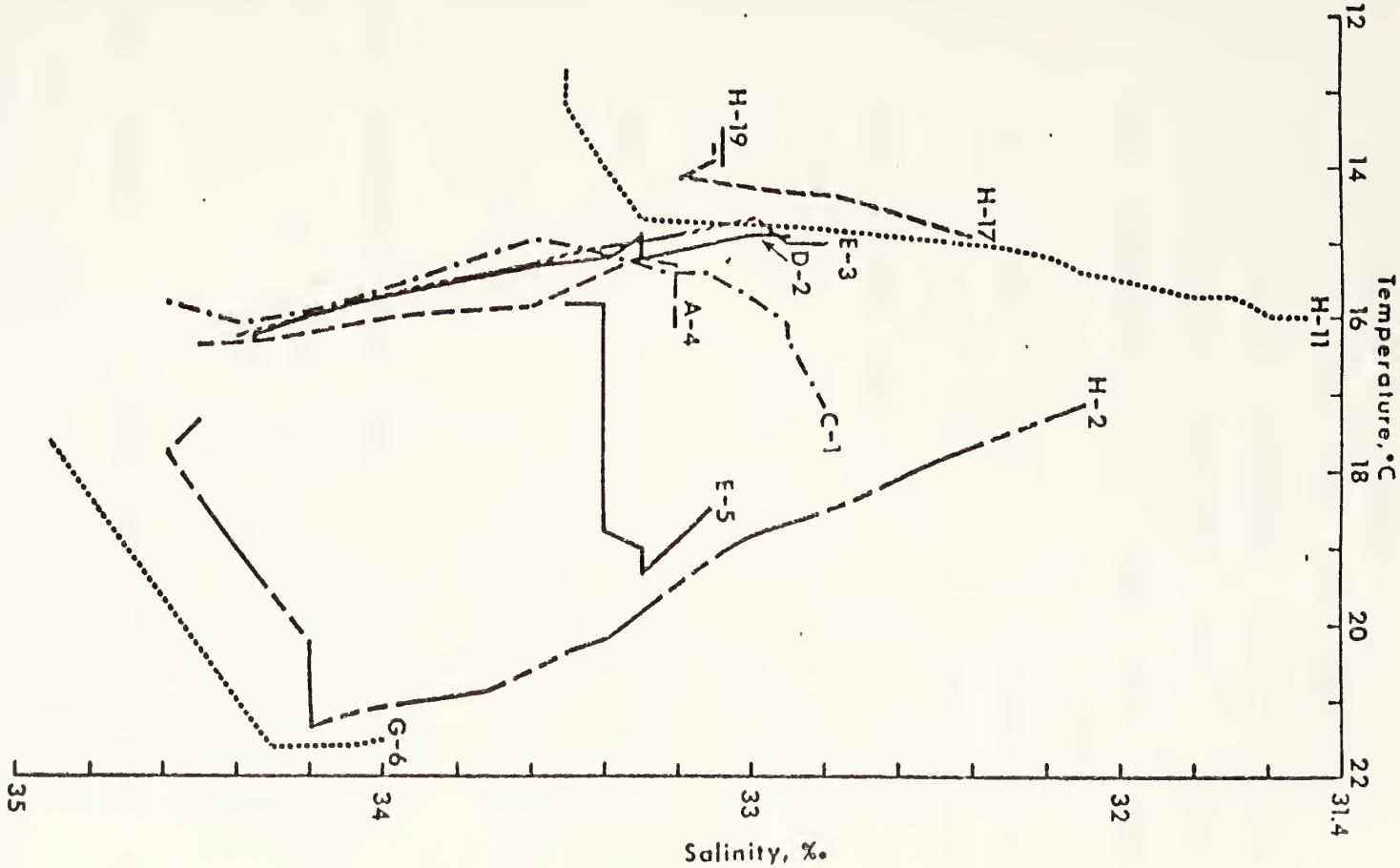

Figure 10. T-S Diagram in the Korea Strait. (From KEYRSEX80 cruise, ADD, 1980)

While attempting to understand the surface circulation in the Sea of Japan and the behavior of the Tsushima Current, Kano (1980), and Kolpack (1982) found that the distribution of salinity, particularly in the upper part of the water column, has a large variation. By analyzing the collected data during the KEYRSEX80 cruise (J.H.Na 1980) in the Korea Strait, three different water masses were encountered.

One of them is representative of the deep Tsushima Current which originated from the Kuroshio Current. The Tsushima Current waters showed higher salinity than the others and salinity even increased with depth. (G-6 in Figure 10). The other two water types are formed in the Korea Coastal water around the Korean Peninsula (E-3, D-2). In both water types, temperature and salinity increase with depth. Deeper water in these types approaches the deep Tsushima waters in temperature and salinity structure.

These three different waters mix in the Korea Strait. The less-saline Yellow Sea water meets with saline Tsushima water to mix in the upper layers in the Korea Strait (H-2). Further mixing occurs with the South Korean Coastal Water (C-1, E-5).

In the Korea Strait, the salinity is relatively low at the surface, because of the river run-off from the Korean Peninsula (Naktong River) and the inflow of the Yellow Sea Current in the upper layer. The salinity gradient shows a sharp increase in the upper layer and then remains almost constant below 60 m depth. When this situation occurs, the highest salinity is present in the eastern channel.

The maximum observed salinity in the Korea Strait is about 34.5 ppt in the eastern channel of the Korea Strait which is influenced by

the Kuroshio Current. Cool, much lower salinity water predominates in the western channel (Kolpack, 1982) due to the influx from the Yellow Sea and from the local Naktong River flow. The depth of maximum salinity in the water column shows considerable variability on a yearly basis. Generally, the depth of maximum salinity will be 50-150 m in the Korea Strait. The maximum salinity depth decreases toward the northwest and north. It is related to the interaction with the northern cool, fresh waters.

The predominant Kuroshio Current may be responsible for the variations in the flow of high salinity water through Korea Strait which ultimately influences the behavior of the Tsushima Current. So the position of ocean front in the Korea Strait is closely related to the strength of the Kuroshio Current.

The location of maximum salinity values changes in a seasonal and yearly basis. Consequently this high salinity core can be used to trace the axis of the current. In the Korea Strait, the salinity varies seasonally; low salinity occurs in the summer rainy monsoon, high salinity occurs during the dry winter monsoon.

6. Sound Velocity Profiles (SVP)

The attempts of measure of sound traveling speed in the sea water started in 1827 by Colladon in the Lake Geneva. The laboratory measurements and direct measurements were developed by mid 1900 with measuring with sound velocimeter. Many scientists tried to measure accurate sound speed in the sea by considering environmental effects (temperature, salinity, depth). Calculation of sound velocity in the Korea Strait by several different equations shows negligible change in September.

Sound energy traveling underwater follows a highly complicated path due not only to the complex medium but also to its encounters with the boundaries, at the sea surface and the sea floor. While traveling from the sound source to the receiver or to a target, the sound energy is distorted, delayed, or weakened by the various effects of internal and external underwater factors. There are several important physical characteristics of the water affecting sound travel. One of the most important factors is the water temperature; pressure (depth) and salinity also influences sound traveling in water.

The salinity variation is generally the least important and is taken constant for the sound velocity calculations most of the time in the open ocean. But in the shallow water of the Korea Strait, the Naktong River brings fresh water over the more saline ocean water; here, the salinity gradient can't be neglected. The distribution of water temperatures changes from place to place and from season to season in shallow water because of the influence of fresh water, currents, surface cooling and heating, season monsoons and other effects.

The resultant variations in sound velocity are generally greater and more variable in shallow water than over the same depth range in deep water. The temperature and salinity variations are also noticed in different deep ocean and different water masses. A typical temperature, salinity and density distribution with depth in shallow water is shown in Figure 11. The density depends on the temperature and salinity; an increase in density is proportional to a decrease in temperature and increase in salinity.

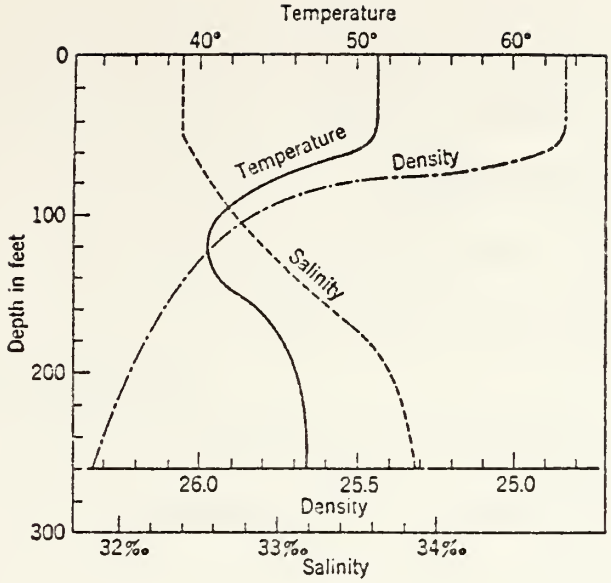

Figure 11. Typical Temperature, Salinity, Density Profile in Shallow Water. (From Officers, 1958)

The region of steep density gradient is a more stable region and less subject to change. The regions above and below this are less stable and more subject to change either through convective overturn or through other moxing processes induced by external forces. This overturn, when completed, produces thorough admixture of the water resulting in a constant distribution of temperature and salinity with depth over that region, for the upper 250 ft. of the water column (Figure 11).

This kind of situation is more dominant in deep water than in shallow water. In isothermal water conditions, the sound velocity depends only on pressure. The sound velocity increases with depth.

The other considerable factors affecting sound transmission in shallow water are the ocean bottom properties. The composition, thickness, degree of layering, roughness, and porosity change from place to place in the ocean.

The bottom sediment distribution in the Korea Strait is shown on Figure 5 (II - A-2).

The sound velocity distribution with depth (SVP) in the Korea Strait of September look quite similar in several different locations. Figure 12 shows the sound velocity profiles with the salinity and temperature profile at the Korea Trench (35 00 N-129 30 E) in September. Appendix B lists SVPs in the Korea Strait in September.

7. Thermal Structure

The temperature distribution in horizontal and vertical at sea is affected by various meteorological, oceanographic contribution. The accurate factors of ocean thermal structure is based on causative interactions between the available observations of the driving forces (Figure 13). The major factors which affect the ocean thermal structure and its changes are described in section II-7-A.

The temperature distribution in water column is very important in underwater acoustics. The temperature profile is the most predominant factor affecting acoustic propagation. The convergence zone range is affected by the sea surface temperature, the mixed-layer produces surface ducts, and a seasonal thermocline causes downward or upward refraction of rays. The gradient in the thermocline determines the limiting ray which produces shadow zones. Sound channel propagation can occur when there is a minimum in the temperature distribution. The forming of different ray paths and shadow zones strongly depends upon the subsurface thermal structure (Figure 13). Typical thermal structure in the upper ocean varies diurnally, monthly, and seasonally. (Figure 14)

a. Sea-Surface Temperature

Sea-surface temperatures are affected by many environmental factors and changes in time and places. They have a close relation with

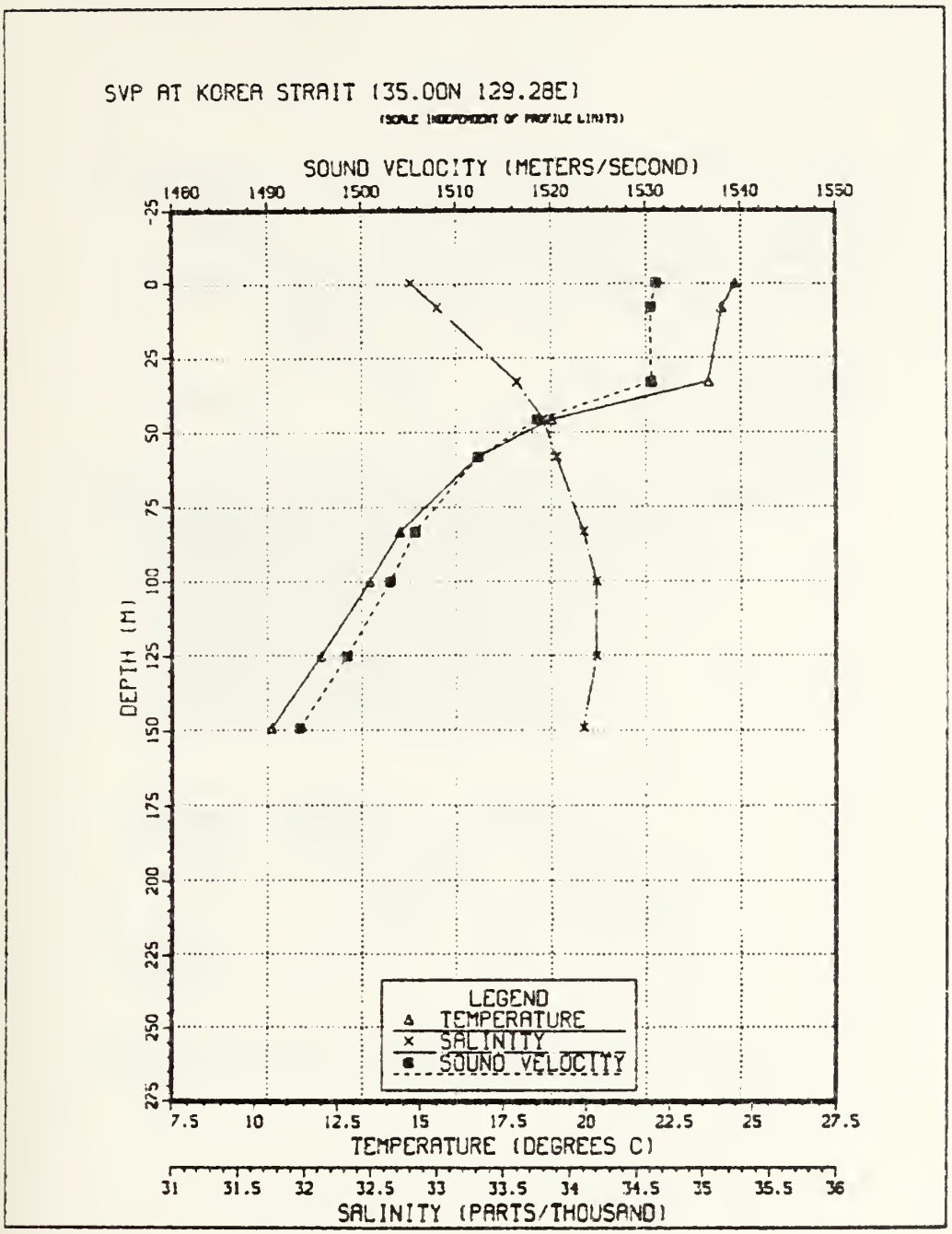

Figure 12. SVP at the Korea Trench in September. (From FNOC MOODS data)

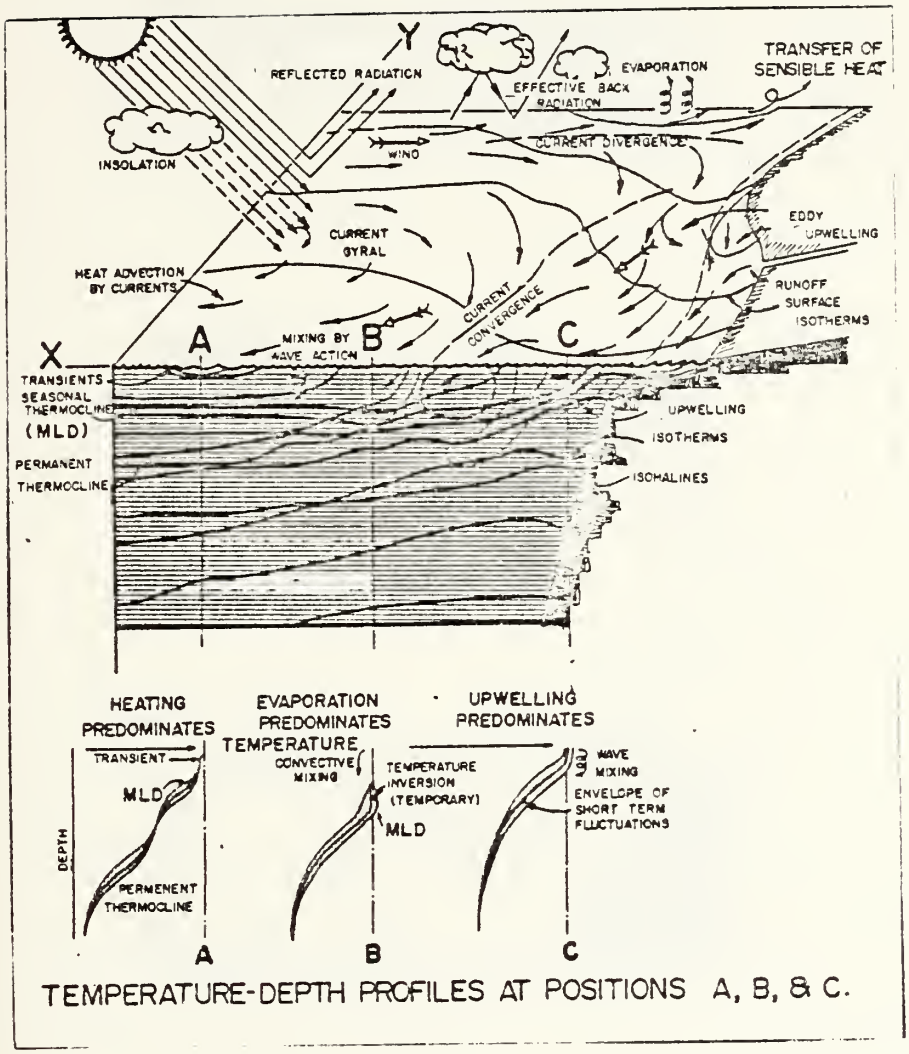

Figure 13. Schematic Picture of Factors Affecting Ocean Thermal Structure (From Laevastu, 1965)

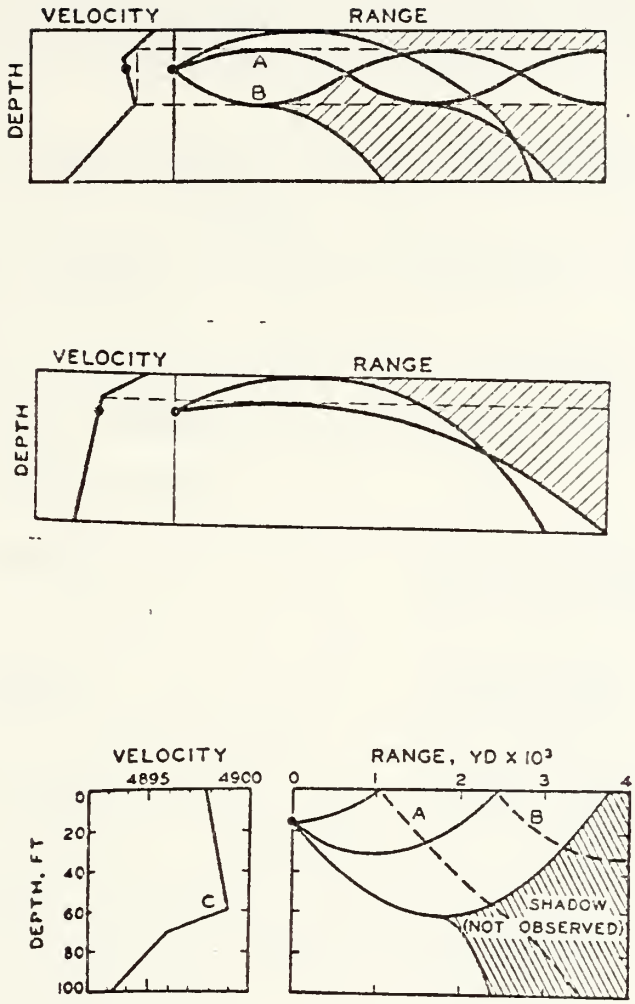

Figure 14. Limiting Ray Paths in Different SVP. (From Reference 21)

atmospheric conditions. The environmental factors influencing the sea-surface temperatures are:

1. Insolation which mainly depends on length of the day so that it varies with the date and geographical latitude. It also is a function of angle of incidence and the amount of cloud cover.

2. Evaporation which depends on the air-sea temperature gradient. The exchange at the interface is a function of windspeed. Evaporation is the most important source of heat loss at the sea surface.

3. Convective heat transfer driven by the air-sea temperature difference and wind speed.

4. Mixing by the wind or convective mixing due to instability in the water column.

5. Transport by current, upwelling or downwelling.

We can summarize above statements as follows:

General Process	Cause
Heating	Sun's radiation Back radiation Cool air temperature
Mixing	Wind, waves Instability, turbulence
Flowing	Internal wave Tide & current

These four general processes are closely interrelated and each has its own particular characteristic effect on the surface temperature gradient (Figure 15).

The monthly mean sea-surface temperatures in the Korea Strait vary, especially during the seasonal monsoon period. Generally the sea in the vicinity of Korea Strait is warmer than other Korean Peninsula coastal waters due to the effect of the northward flowing warm Kuroshio Current. The sea surface temperature in the Korea Strait is

coolest at the end of the winter period (in March) when it drops to 52 f due to the effect of cold northernly winter monsoons. It heats up gradually to 78 f by the end of summer season (in August and September) (Figure 16). The monthly mean sea-surface temperature distribution around the Korea Peninsula is listed in Appendix A.

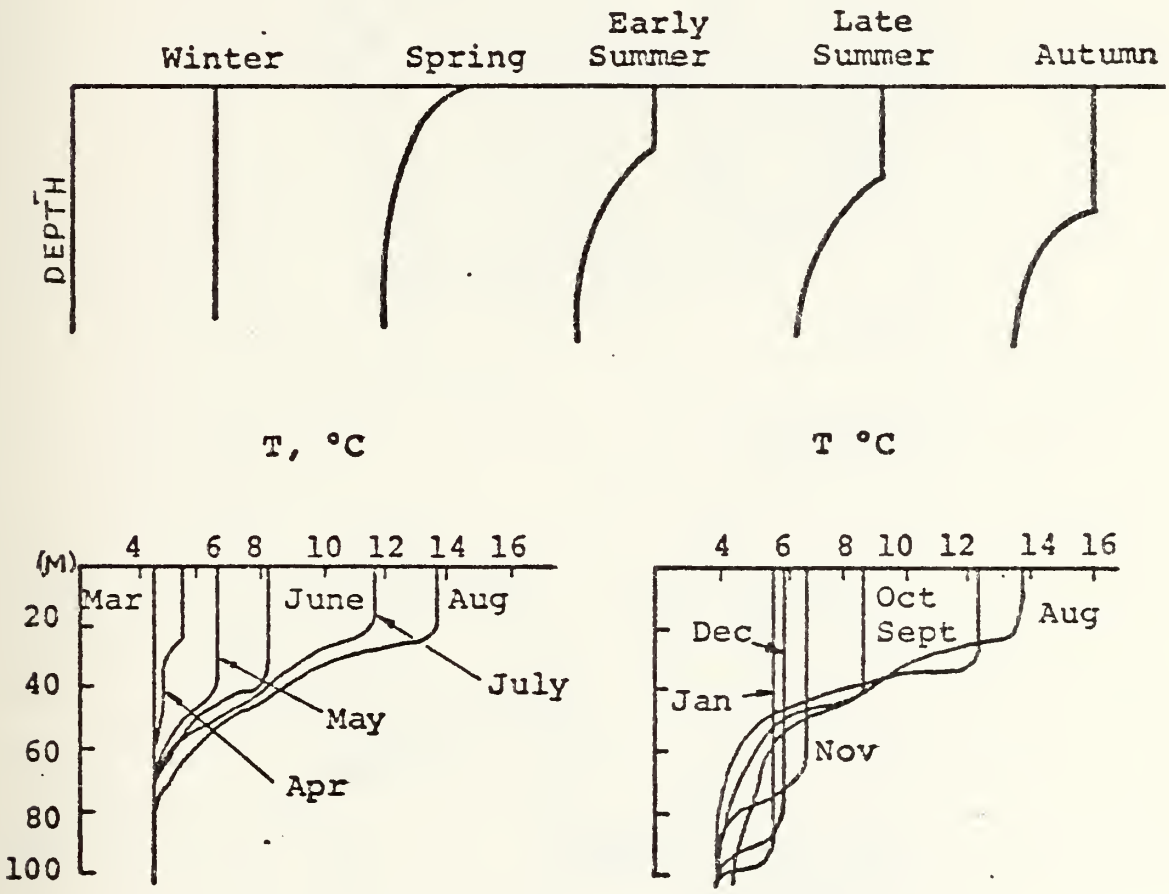

Figure 15. Generalized Seasonal, Monthly Change of Thermal Structure. (Urick, 1979)

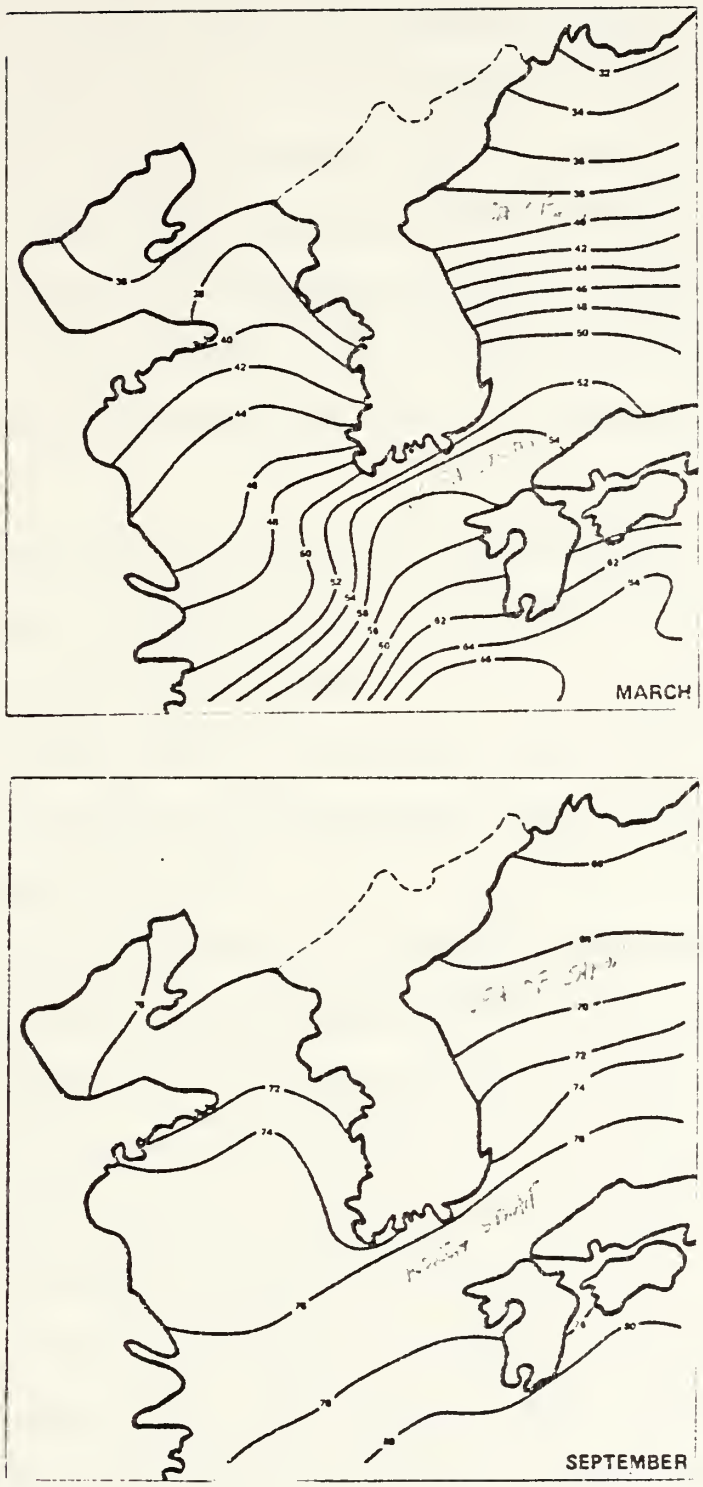

Figure 16. Mean Monthly Sea Surface Temperature distribution around the Korean Peninsula in March and September. (From Nestor, 1977)

b. Mixed Layer Depth (MLD)

In the summer period (June through August), mixed layer depths tend to be less than 100 ft. (30 m), primarily because of the large positive air-sea temperature differences. This is especially evident over cooler waters in the Yellow Sea and Sea of Japan. Cold arctic water and counter-currents near the Kuroshio Current are subject to long periods of heating, creating negative surface gradients and shallow mixed layers. The cool water has a relatively low velocity, so heating is not deterred by advection.

Through July, the shallow continental shelf water in the Yellow Sea displays very shallow MLD's (less than 50 ft or 15 m) because of the build-up from surface heating.

A second region of potentially shallow layer depth is the zone between cold Oyashio and warm Kuroshio water masses, hereafter called the "transition zone".

Along the boundaries of contrasting water masses, over-running warm water may create a negative gradient and shallow mixed layers.

During the fall regime (September through November), the cold seaward air flow provides a negative air-sea temperature difference that promotes convective mixing. As the northwest monsoon develops, wind mixing continues to deepen the mixed layers. By the end of the regime, MLD's in the seas around the peninsula are everywhere greater than when the season began. The transition zones continue to experience negative gradients and shallow mixed layers of 100 - 150 ft (30 45 m).

In contrast to summer, the winter regime has predominantly deep mixed layers in middle and high latitudes due to convection. The

cold arctic winter and counter-currents that were heated in the summer are now cooled and convection produces deep mixed layers. This is the result of the negative air-sea temperature difference normally present in winter.

Cold isothermal waters moving slowly from the arctic are not heated at the surface as the air temperature is usually as low as, or lower than, the sea surface temperature. The cold waters remain their deep mixed layer during advection.

The Kuroshio Current will also deepen due to convection as it moves north into mid-latitudes. The amount of cooling in the stream is limited by the rapid advection of warm water. Mechanical wind-mixing also increases, which contributes to deeper mixed layers. Again in winter, transition zones occur between the warm and cold water masses and are potential locations of shallow mixed layer depths.

In all the seas around the Korean Peninsula the mixed layer continues to increase to 200 - 300 ft. (60 - 90 m), especially in the Sea of Japan where 400 ft (122 m) MLD's are common in the winter period.

The spring transition season (March through May), fosters some unique mixed-layer characteristics. As the spring heating begins in the tropics and progresses northward, cool water begins to heat at the surface. The warming gradually moves north and the layer depths slowly decrease. For a short period in April, layer depth charts show both summer and winter conditions simultaneously. The seas around the Korean Peninsula reach their maximum mixed-layer depth at this time, and mixed layers in the shallow sea are then rapidly wiped out by surface heating. As advection of the major currents continues, mixed layer depths decrease until only scattered pockets of deep layers exist.

B. ACOUSTICS

1. Ambient Noise

The ocean is dynamic; it never stops moving. The waves splash each other and break at the beach. Various kinds of living organisms, shipping traffic, and industrial noise from near-shore plants contribute noise to the sea. All the above various noises associated with, or resident in, the sea itself are collectively called "ambient noise". The ambient noise is the residual noise background in the absence of individual identificable sources. The spectrum of ambient noise is broad band and fairly well defined in deep water but it is quite variable in shallow water.

The main sources of noise in the shallow coastal waters are: (1) wind-related noise, which are general locally generated noises. Other sources of noise are the rainfall on the sea surface and breaking waves. The variability of the noise level in shallow water is extremely high in space and time. The sources of ambient noise exhibit definite diurnal and seasonal variation. For all these reasons ambient noise cannot be specified as a definite, constant quality, but must be described in statistical terms; that is, an estimate can be made of the most probably or average amount of noise which is to be expected under given conditions.

The average ambient-noise spectrum levels measured in the Korea Strait are 8 - 20 dB higher when measured near shore than when measured far from shore. (Figure 17)

The prediction of ambient noise level in a particular area of the Korea Strait is very difficult, and rough approximations are frequently the only estimates available in the coastal waters.

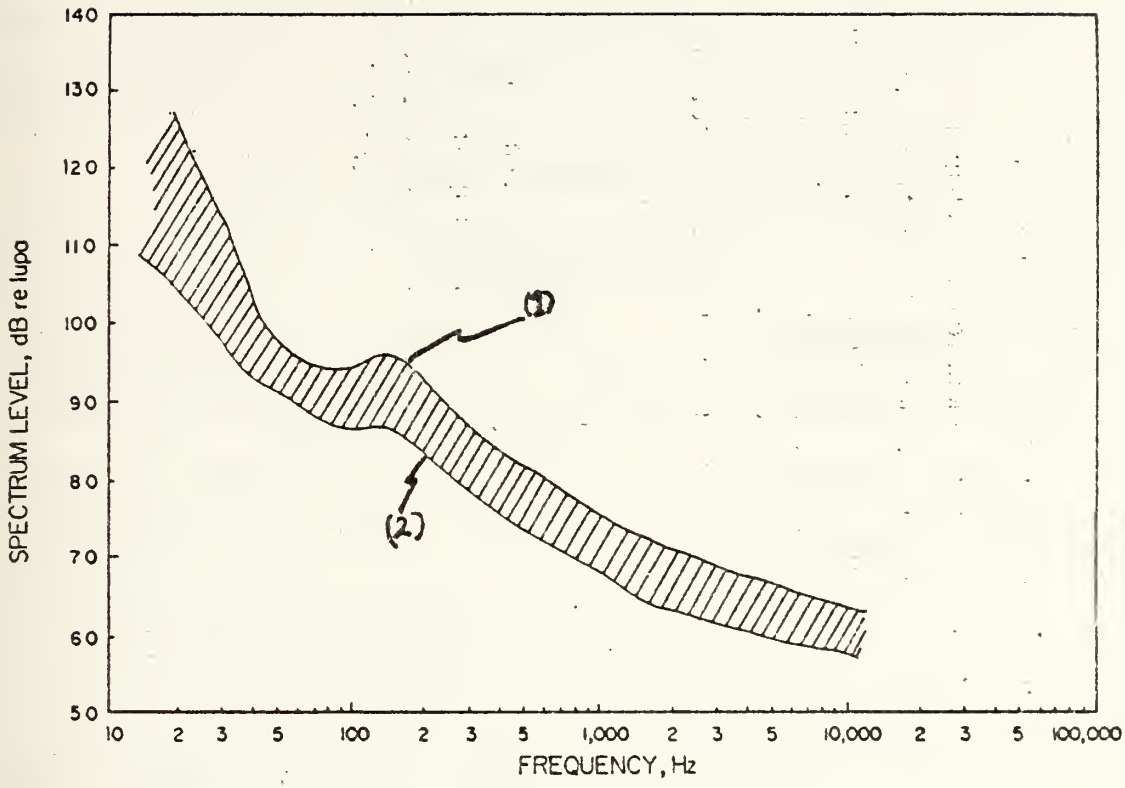

Figure 17. Average Ambient Noise Level in the Korea Strait (1) on shore location (34 47 N - 128 45 E) and (2) off-shore location (34 42 N - 128 00 E). (From Lee, 1980)

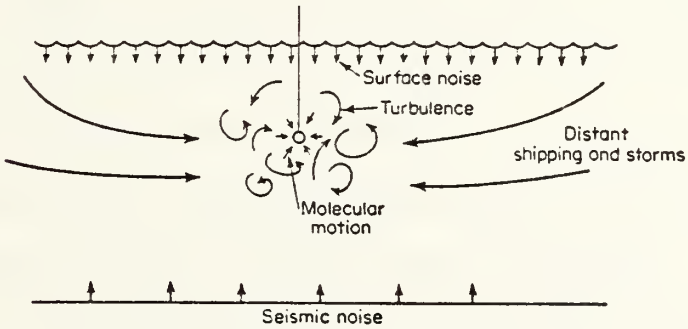

Figure 18. Conceptual Diagram of Sources of Deep Water Ambient Noise (From Urick, 1975)

The sources of noise in deep water are ocean tides, waves, seismic disturbances, ocean turbulence and distant shipping at low frequencies; and wind-generated wave noise, biological noise, and thermal noise which originated from the molecular motion of the water particles at high frequencies. (Figure 18)

TABLE 1. SUMMARY OF BACKGROUND NOISE AT SEA

Background Noise	
Self-Noise	Ambient-Noise
Platform motion Noise	Wind-related Noise
Circuit Noise	Biological Noise
Ship Noise	Shipping and Industrial

a. Wind-related Noise

Wind speed is an important parameter determining the Ambient Noise in shallow continental oceans as well as in the deep ocean. According to Piggot (1965) measurements made on the Scotian Shelf (water depths 150 ft) over a one-year period, for frequencies between 10 hz to 3 khz, showed the noise level increases 7.2 dB when the wind speed doubled; this dependence is slightly greater than the square of the wind speed.

In comparison with the Knudsen spectra for deep water, noise levels in shallow water are 5 to 10 dB greater than those in deep water at all frequencies. (Figure 19)

Urick (1975) summarizes that when the wind noise is the predominant source of noise in shallow water (negligible contributions from biological and shipping noise), the noise level agrees with the

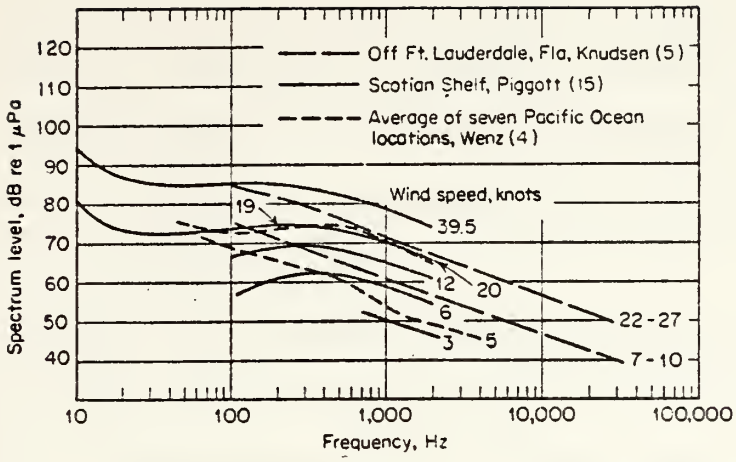

Figure 19. Wind-related Ambient Noise Spectra at Coastal Locations. (Urick, 1975)

deep water case at 1000 hz. (Figure 20) For wind speed greater than 5 kts, measured noise spectrum levels in shallow water increase 6 dB for each doubling of the wind speed. These spectrum levels are independent of hydrophone depth, water depth, and other geographical characteristics.

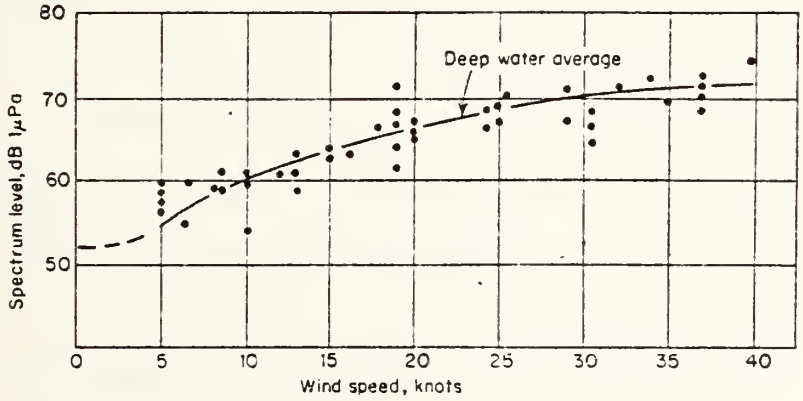

Figure 20. Wind Dominated Ambient Noise Level. (Urick, 1975)

Since directionality of wind noise is vertical, local wind speed and duration are important in estimating the noise level.

Wind-generated noise has a very small standard variation at all frequencies, especially at high speeds (20 kts) and above 100 kz (less than 0.1 dB). (Figure 21 e).

Bannister (1979) measured ambient noise in the basin south of Fiji and northeast of New Zealand where the major sources of ambient noise are from the contributions within the basin itself. He computed the deviation of the noise for frequencies between 10 to 500 hz. The effects of receiver depth, wind speed, and frequency were examined. He tried to relate the results to the wind speed and the local shipping. There were no marked dependence of standard deviation on receiver depth. The ambient noise level was dominated by the wind related noise with the wind blowing at 20 knots. The wind generated noise obscured most effects due to shipping. As the wind speed reduced the wind related noise reduced and shipping noise became noticeable with large variability. (Figure 21 a, d)

Other kinds of noise generated by wind are the hydrostatic effects of wind generated surface waves, and breaking white caps. In the absence of other noise sources, at low frequencies and low wind speeds, shallow water can be appreciably quieter than deep water.

On the other hand, when shipping noise or other man-made noises exist, or when biological sources contribute to the noise background, shallow water can be a noisy and exceedingly variable environment for most SONAR operations. The noise levels in shallow coastal waters are usually 5 to 10 dB higher than in deep water.

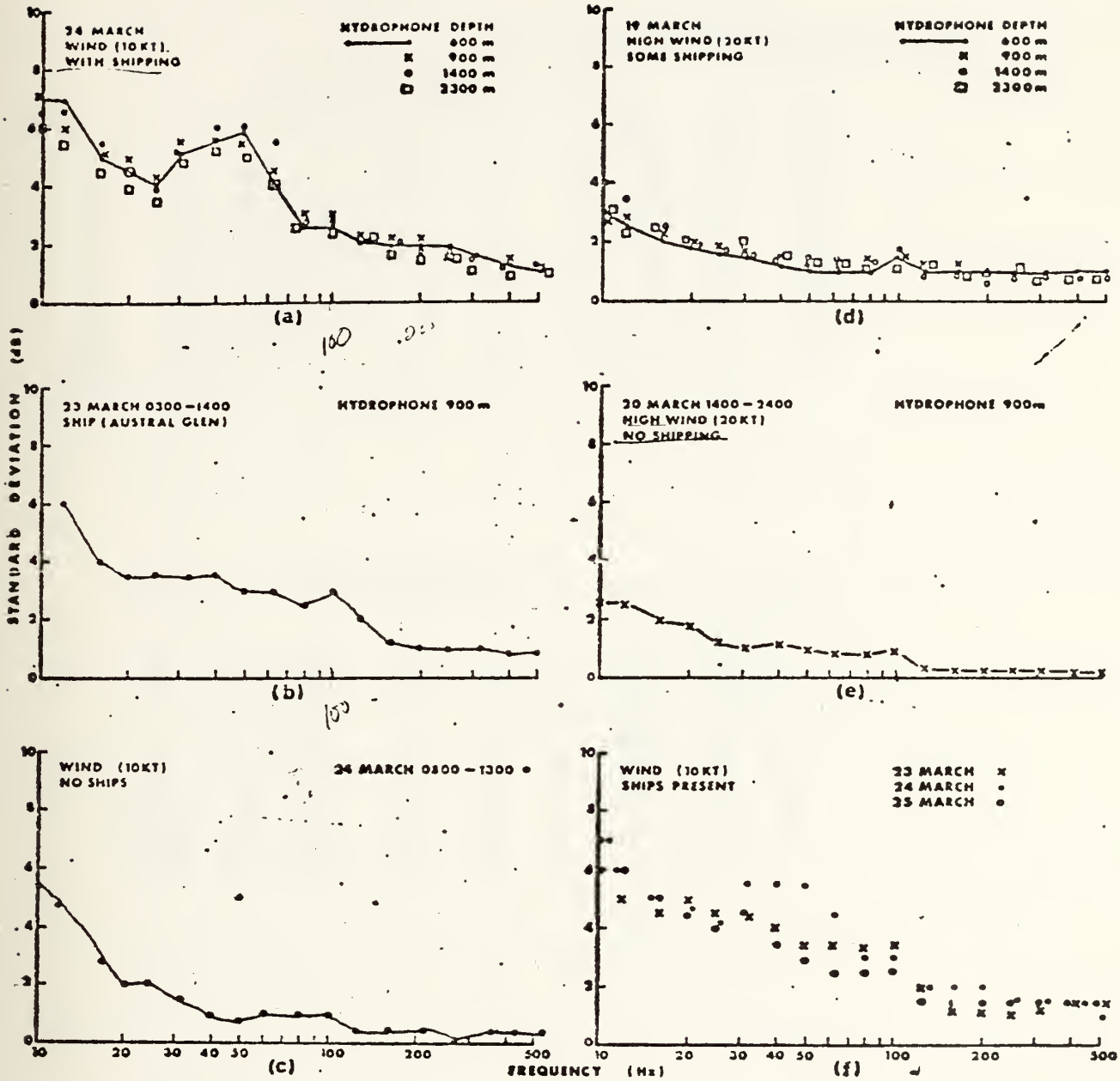

Figure 21. Standard Deviation of Ambient Noise with Winds, Shipping Contribution (From Bannister et al., 1979)

SEPTEMBER

TABLE 3

PERCENTAGE FREQUENCY OF WIND DIRECTION BY SPEED

WND DIR	WIND SPEED (KNOTS) 0-3	4-10	11-21	22-33	34-47	48+	TOTAL OBS	PCT FREQ	MEAN SPD
N	1.2	6.4	4.9	1.7	.4	*	320	14.6	12.3
NE	1.4	14.3	14.0	4.8	.6	.1	771	35.2	13.5
E	1.3	5.6	3.9	.8	.0	.0	252	11.5	10.4
SE	1.3	3.0	1.4	.3	.0	*	133	6.1	8.7
S	.6	3.0	1.5	.4	*	.0	121	5.5	9.9
SW	1.6	5.3	1.7	.5	*	.0	198	9.1	8.4
W	1.0	5.4	2.3	.2	.0	.0	195	8.9	8.8
NW	1.0	4.6	1.5	.1	*	.0	157	7.2	8.2
VAR	.0	.0	.0	.0	.0	.0	0	.0	.0
CALM	1.9						41	1.9	.0
TOT OBS	248	1040	684	192	25	3	2192		11.0
TOT PCT	11.3	47.4	31.2	8.8	1.1	.1		100.0	

WND DIR	WIND SPEED (KNOTS) 0-6	7-16	17-27	28-40	41+	TOTAL OBS	PCT FREQ	MEAN SPD
N	4.4	6.3	3.2	.7	.2	320	14.6	12.3
NE	6.4	17.2	9.3	2.1	.2	771	35.2	13.5
E	3.3	6.4	1.8	.1	.0	252	11.5	10.4
SE	2.9	2.6	.5	*	*	133	6.1	8.7
S	2.3	2.4	.7	.2	.0	121	5.5	9.9
SW	4.2	4.1	.6	.2	.0	198	9.1	8.4
W	3.4	4.7	.7	*	.0	195	8.9	8.8
NW	3.0	3.8	.3	*	*	157	7.2	8.2
VAR	.0	.0	.0	.0	.0	0	.0	.0
CALM	1.9					41	1.9	.0
TOT OBS	698	1039	373	73	9	2192		11.0
TOT PCT	31.8	47.4	17.0	3.3	.4		100.0	

Table 2. Monthly Mean Wind Speed and Direction in September in the Korea Strait. (From SSMO Vol. 9)

ANNUAL

TABLE 3

PERCENTAGE FREQUENCY OF WIND DIRECTION BY SPEED

WND DIR	WIND SPEED (KNOTS) 0-3	4-10	11-21	22-33	34-47	48+	TOTAL OBS	PCT FREQ	MEAN SPD
N	1.0	6.6	4.8	1.2	.1	*	4445	13.7	11.3
NE	1.1	8.9	8.0	2.2	.2	*	6458	20.4	12.2
E	1.0	4.5	2.5	.4	*	*	2722	8.5	9.8
SE	.9	2.7	.9	.1	*	*	1490	4.7	8.0
S	1.0	3.7	1.9	.5	*	*	2276	7.1	9.7
SW	1.4	7.0	4.1	.7	*	*	4192	13.2	10.0
W	1.0	6.7	4.5	1.1	.1	*	4360	13.3	10.5
NW	1.0	7.1	6.3	1.4	.1	*	5233	15.9	10.0
VAR	.0	.0	.0	.0	.0	.0	0	.0	.0
CALM	3.2						1053	3.2	.0
TOT OBS	3736	15091	10728	2503	163	11	32232		10.6
TOT PCT	11.6	47.1	33.1	7.7	.5	*		100.0	

TABLE 3A

WND DIR	WIND SPEED (KNOTS) 0-6	7-16	17-27	28-40	41+	TOTAL OBS	PCT FREQ	MEAN SPD
N	3.9	6.8	2.6	.4	*	4445	13.7	11.3
NE	4.7	10.1	4.8	.7	.1	6458	20.4	12.2
E	3.1	4.2	1.1	.1	*	2722	8.5	9.8
SE	2.4	1.9	.3	*	*	1490	4.7	8.0
S	2.8	3.2	.9	.2	*	2276	7.1	9.7
SW	4.6	6.5	1.8	.2	*	4192	13.2	10.0
W	4.0	6.6	2.4	.3	*	4360	13.3	10.5
NW	3.9	8.1	3.6	.4	*	5233	15.9	10.0
VAR	.0	.0	.0	.0	.0	0	.0	.0
CALM	3.2					1053	3.2	.0
TOT OBS	10447	15274	5723	740	48	32232		10.6
TOT PCT	32.6	47.3	17.6	2.3	.2		100.0	

Table 3. Annual Mean Wind Speed and Direction in the Korea Strait. (From SSMO Vol. 9)

In the Korea Strait, the annual mean wind speed is 12.2 kts; in September it is 13.5 kts with the dominant direction from northeast. (Tables 2 and 3)

b. Biological Noise

The sound from the organisms in the sea are extremely variable in time and in space. There are three categories of marine life that are well known as noise sources in the Korea Strait; some species of shellfish (Crustacea), some species of true fish, and the marine mammals (Cetacea).

The Korea Strait and the Sea of Japan are areas in which sound generating fish are active all year round. Nestor (1977) studied the distribution of sound producing fish and other biological contributions to the ambient noise in the Korea Strait. (Figure 22 and Figure 23) The greatest activity occurs during the spawning months of April through October. Schools of anchovy in the Korea Strait produce a high level of noise. At this same time, squid and sardines contribute a large portion of noise in the Korea Strait. The migration routes are not the same from year to year, but general migration routes and periods of activity for the major species in the Korea Strait are shown in Figure 24 and Figure 25.

Nestor (1977) reported that most fish emit sounds with frequencies below 100 hz; however, triggerfish emit sounds in the range of 2400 to 4800 hz. It is believed that warm water fish produce more attenuation than cold water species.

Snapping shrimp and spiny lobsters are the main noise generating crustaceans in the Korea Strait. Snapping shrimp make loud

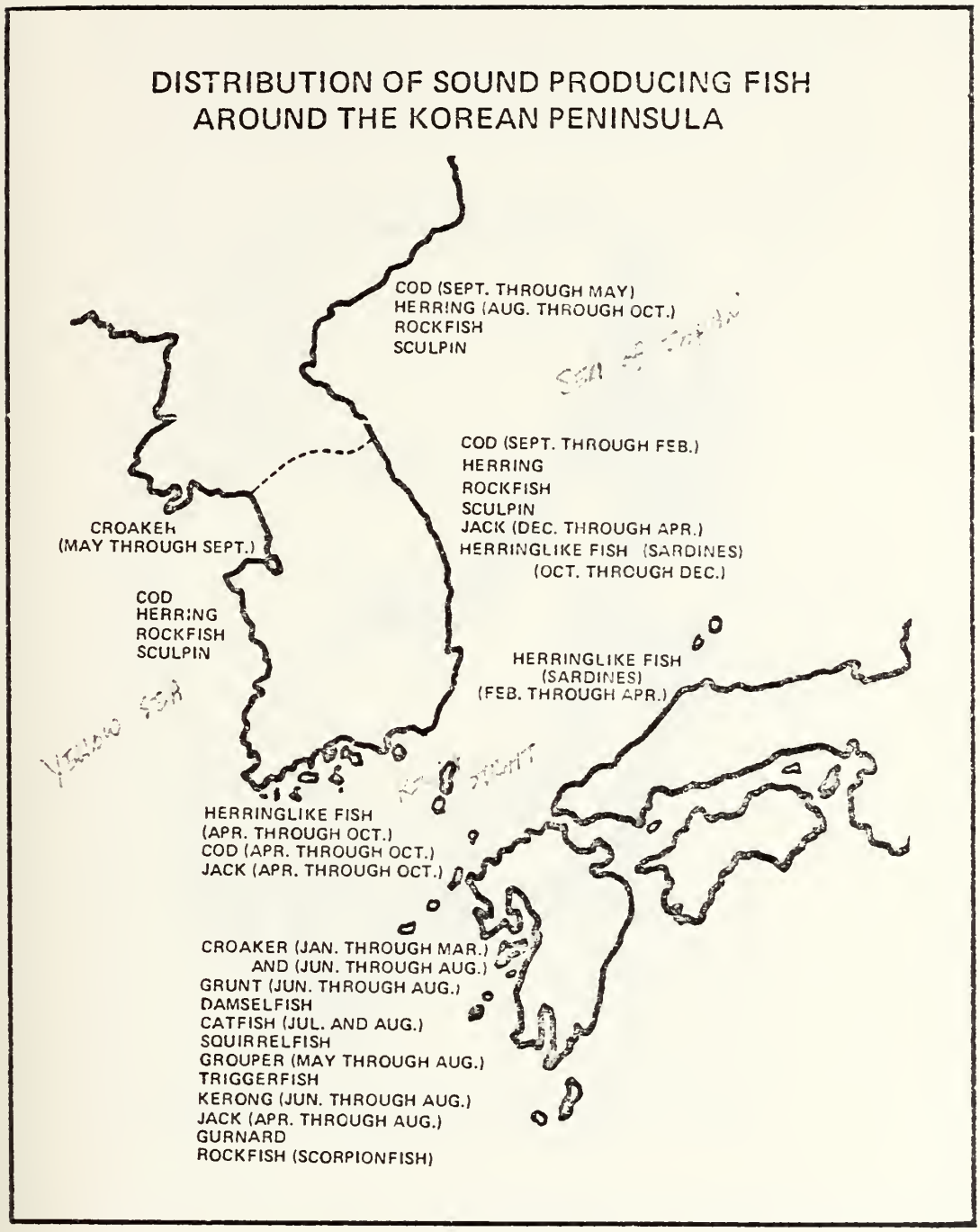

Figure 22. Distribution of Sound-Producing Fish around the Korean Peninsula. (From Nestor, 1977)

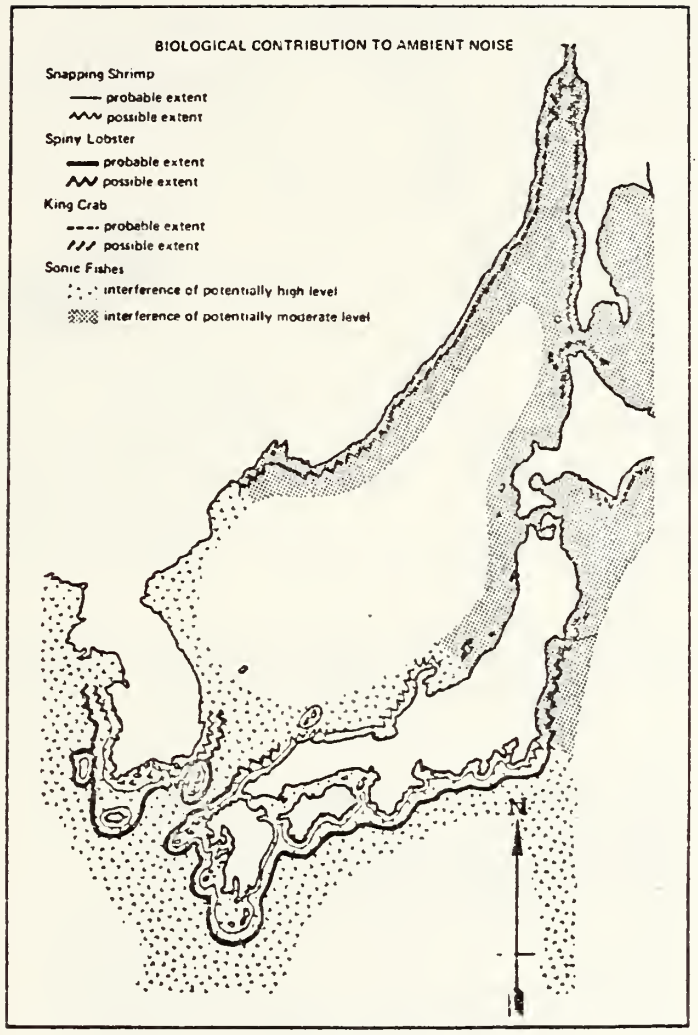

Figure 23. Biological Distribution around the Korean Peninsula. (From Nestor, 1977)

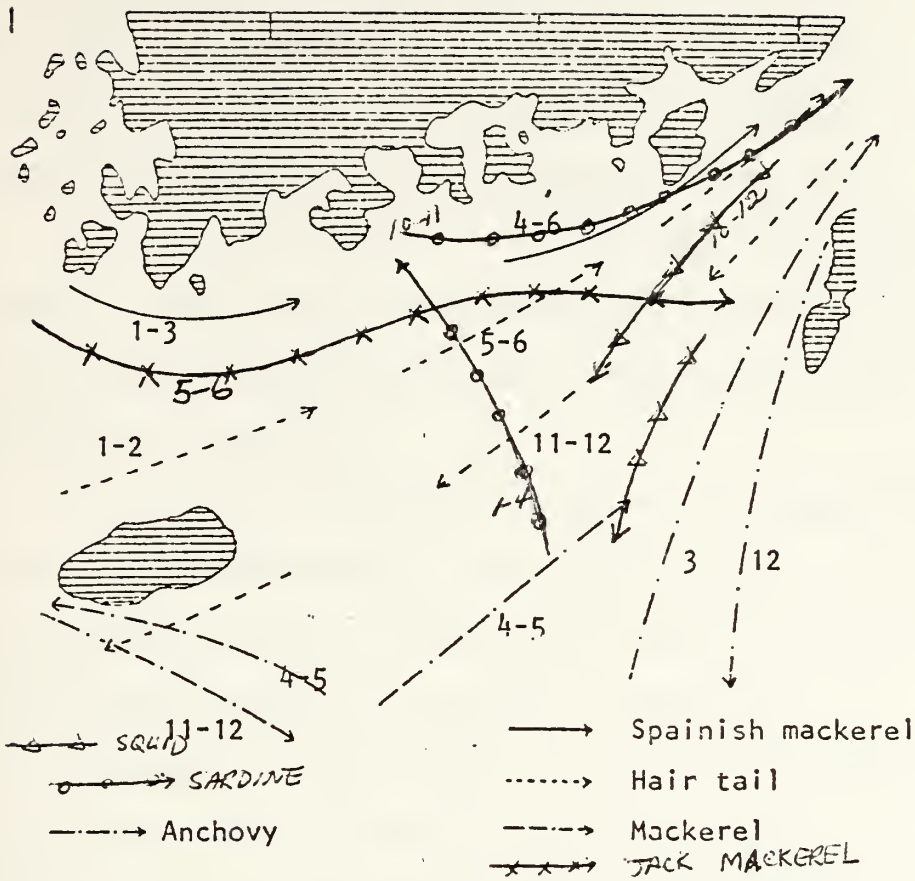

Figure 24. Migration Months and Route of Common Fish in the Korea Strait. (From Lee, 1980)

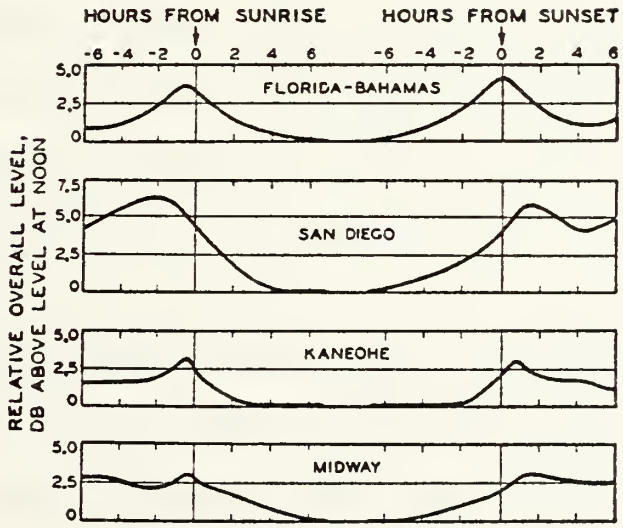

Figure 25. Overall Diurnal variation of shrimp noise level at various locations. (From Reference 21)

sounds with their claws with frequencies ranging from 500 hz to 20 khz (Nestor, 1977). It is also known that sounds in the frequency range from 1.5 khz to 45 khz are caused by shrimp found throughout most of the shallow areas around the Korean Peninsula (Nestor, 1977).

Seasonal variations in biological noise have not been observed. It is suspected that there may be a slight diurnal variation with small maxima occurring near sunset and sunrise; and night levels are higher than day levels. (Figure 25)

In general, a significant increase in biological noise will be noticed in the shallow waters. Thr shrimp beds are located mainly along the southwestern coast of Japan in the Sea of Japan and southeastern coast of the Korean Peninsula in the Korea Strait area.

The spiny lobster makes a rasping or rattling sound by rubbing its antennae against its shells emitting sound in the frequency range from 40 to 900 hz, with maximum intensity occurring at 600 and 800 hz. These Crustaceans congregate in groups and can be a major factor in the overall ambient noise level of an area.

Whales and seals are principal sound-generating marine mammals in the Korea Strait. The areas of concentration vary with the season and migratory patterns of the species. Major species of whales are the Fin, Killer, Grey, White and Mink-Bryde. The Harbor Seal is the only species of the seal in the Korea Strait. (Figure 26 and Figure 27)

Marine mammals produce sounds with frequencies ranging from about 0.1 to 0.2 khz which are generated by their swimming motion through the water. They also produce squeals and groans containing frequcies between 1.5 - 2.5 khz, with a maximum sound pressure level of about 60 to 74 dB re uPa.

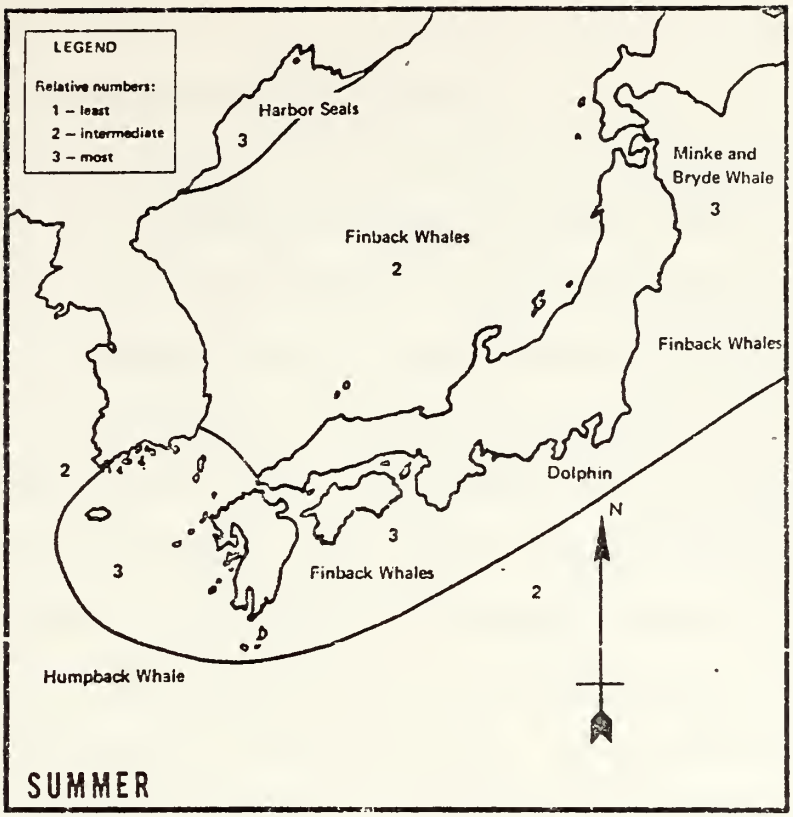

Figure 26. Distribution of Marine Mammals around the Korean Peninsula in Summer. (Nestor, 1977)

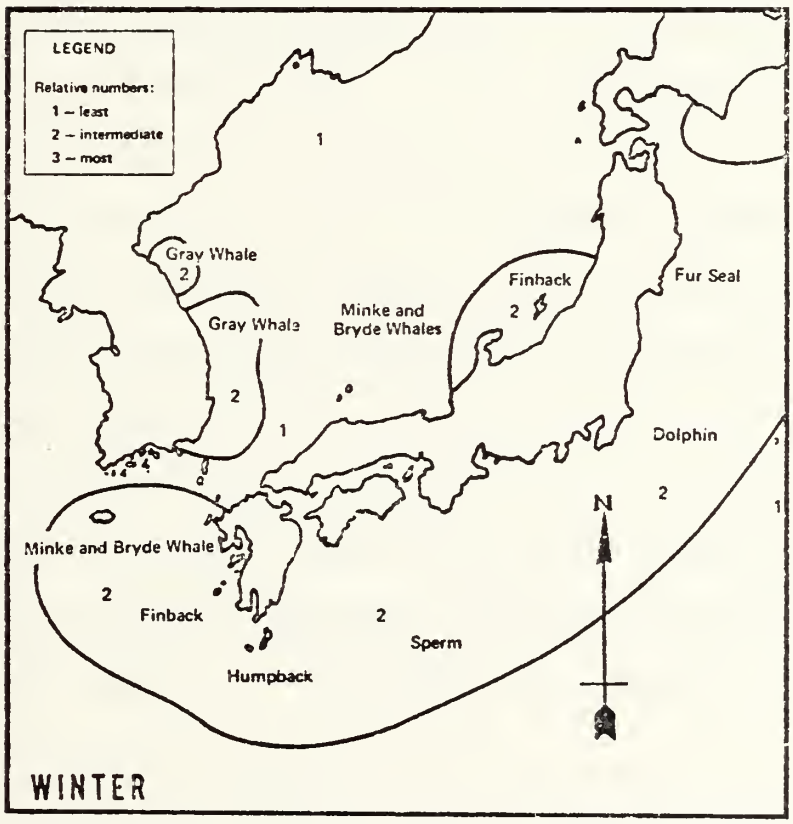

Figure 27.- Distribution of Marine Mammals around the Korean Peninsula in Winter. (Nestor, 1977)

c. Shipping and Industrial Noise

Shipping noses in the Korea Strait are mainly from small fishing boats active during the migration period of anchovy and sardines; big commercial tankers and container-cargo ships traveling through the Korea Strait to the major ports of Pusan, and Musan; and naval vessels moving in and out of Chinhae. Shipping noise commonly has a high standard deviation below 100 Hz. The magnitude of the standard deviation is related to the different source spectra involved and the number of ships contributing at a given time. In areas dominated by distant multiple ships the standard deviation increases with frequency due to the differential attenuation of line structure. If the ships are local, the standard deviation is almost independent of frequency.

Perron (1974) studied ambient noise statistics for the Grand Banks region where the major sources of noise is shipping; and the major shipping was local fishing vessels. Peron's measurements had greater standard deviation above 100 hz than Bannister's (1979) data which had a greater wind noise contribution at the higher frequencies. (Figure 28)

Noise from industrial sources is highly dependent on the level of activity. Ship building facilities and automobile plants on the southeastern coast of Korea are the major source of industrial noise in the Korea Strait. Industrial activity on Tsushima Island also contributes noise to the sea. Figures 28 and 29 show the average ambient noise level at Pusan and Ulsan Harbor, respectively, measured every two hours. We can summarize the characteristics of shipping noise and wind noise:

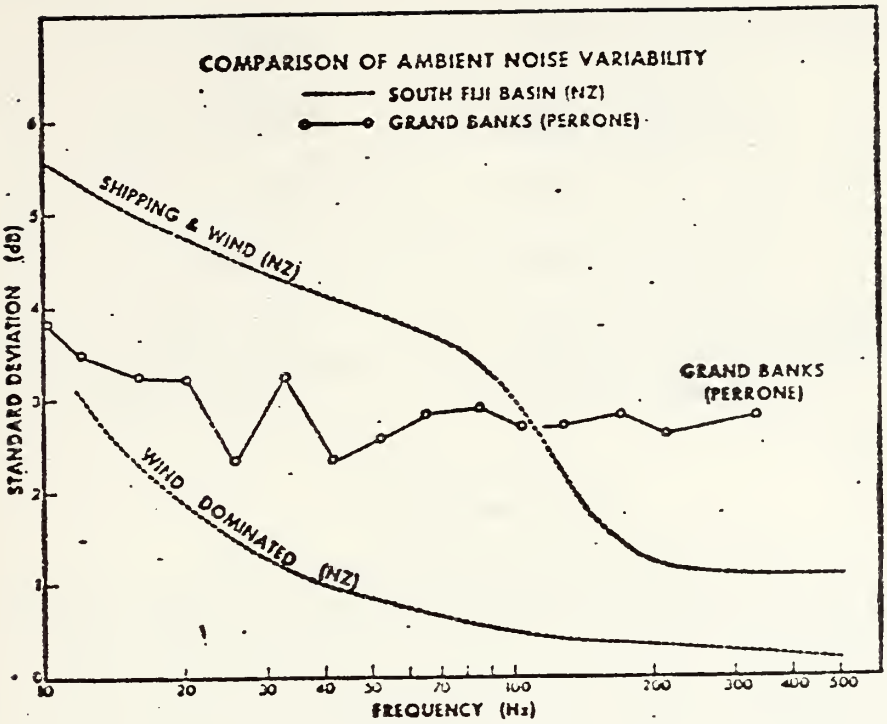

Figure 28. Comparison of Ambient Noise Standard Deviation Dominated by Shipping and Wind at Different Locations. (Bannister, 1979)

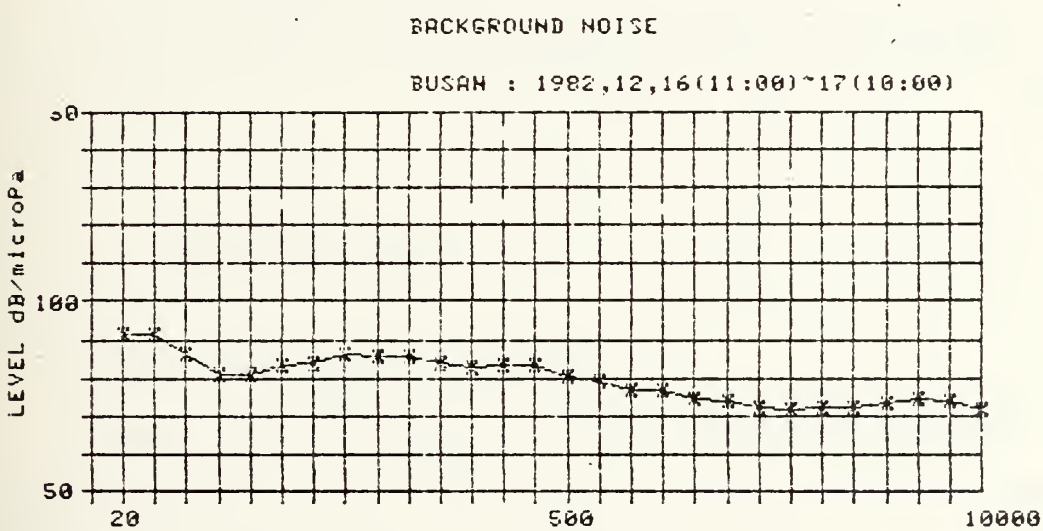

Figure 29. Average Ambient Noise Level at the Entrance of Pusan. (ADD Report, 1982)

Shipping Noise	Wind Noise
Origin: Distand Shipping	Local wind on sea surface
Frequency: Low Frequency (below 100 hz)	High Frequency (above 1000 hz)
Path: Refracted and reflected	Direct Path
Angle: From low angles	From high angles
Contribution: Relatively unimportant except for nearby source in shallow water.	Tends to dominate spectrum when shipping and biological noises are negligible.

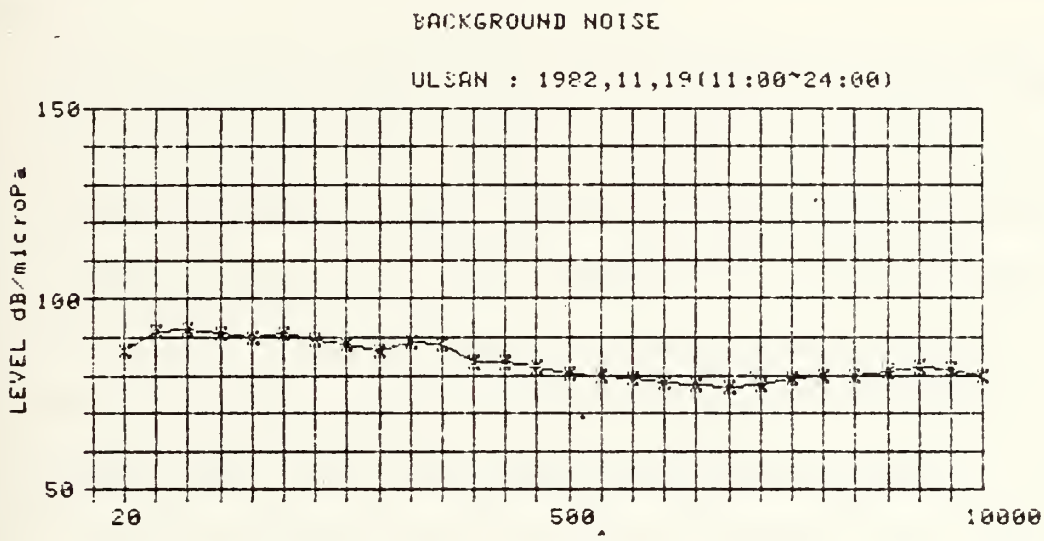

Figure 30. Average Ambient Noise Level at the Entrance of Ulsan Harbor. (ADD Report, 1982)

2. Acoustic Effects of the Bottom

Because the Korea Strait is shallow, the bottom topography plays an important role in sound transmission. As sound propagates through the water, the acoustic energy will be reduced by interaction with the bottom. When the sound impinges on the sea floor, some of the incominc

energy will be reflected and some of it will be absorbed due to the difference between the acoustic impedances at the interface. The interaction with the sea floor is much more complex than with the sea surface because of the complex effects of such properties as bottom roughness, layering, bottom composition, sediment thickness, bottom slope and porosity.

Bedford et al. (1982) examined typical velocity gradient and attenuation values in natural sediments and concluded that the properties of sediments at 200 - 500 m depth are important to sound transmission at 50 hz.

In shallow water, interaction with the bottom is a more dominant factor than it is in deep water. This is because, except in isothermal water such as in the Arctic, sound traveling in shallow water repeatedly interacts with the bottom. The work of Mitchell and Focke shows that in shallow water the bottom properties to a depth of 50 m are important at 50 Hz, while properties at depths of only a few meters are important at several hundred hertz. Thus, the sediment properties important to low-frequency acoustic propagation may be directly determined from coring sampling.

The affect of the bottom also depends upon the grazing angle of the incoming sound. In general, bottom loww increases with grazing angle up to 30 degrees and is almost constant between 30 and 60 degrees. In coastal waters, bottom loss tends to increase with grazing angles greater than 60 degrees. (Figure 31)

A rough approximation of bottom loss can be obtained from plots of bottom loss vs. grazing angle for various bottom types and frequencies (Figure 32). Sand and rock bottoms have less bottom loss than muddy

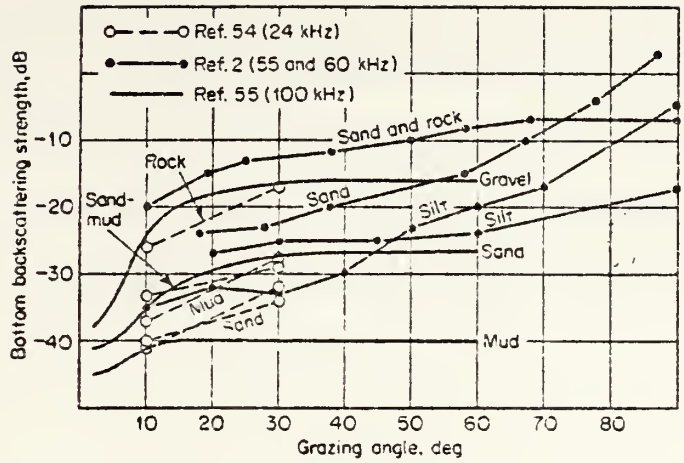

Figure 31. Measured Bottom Backscattering Strength of Various Bottom Materials (Urick, 1975)

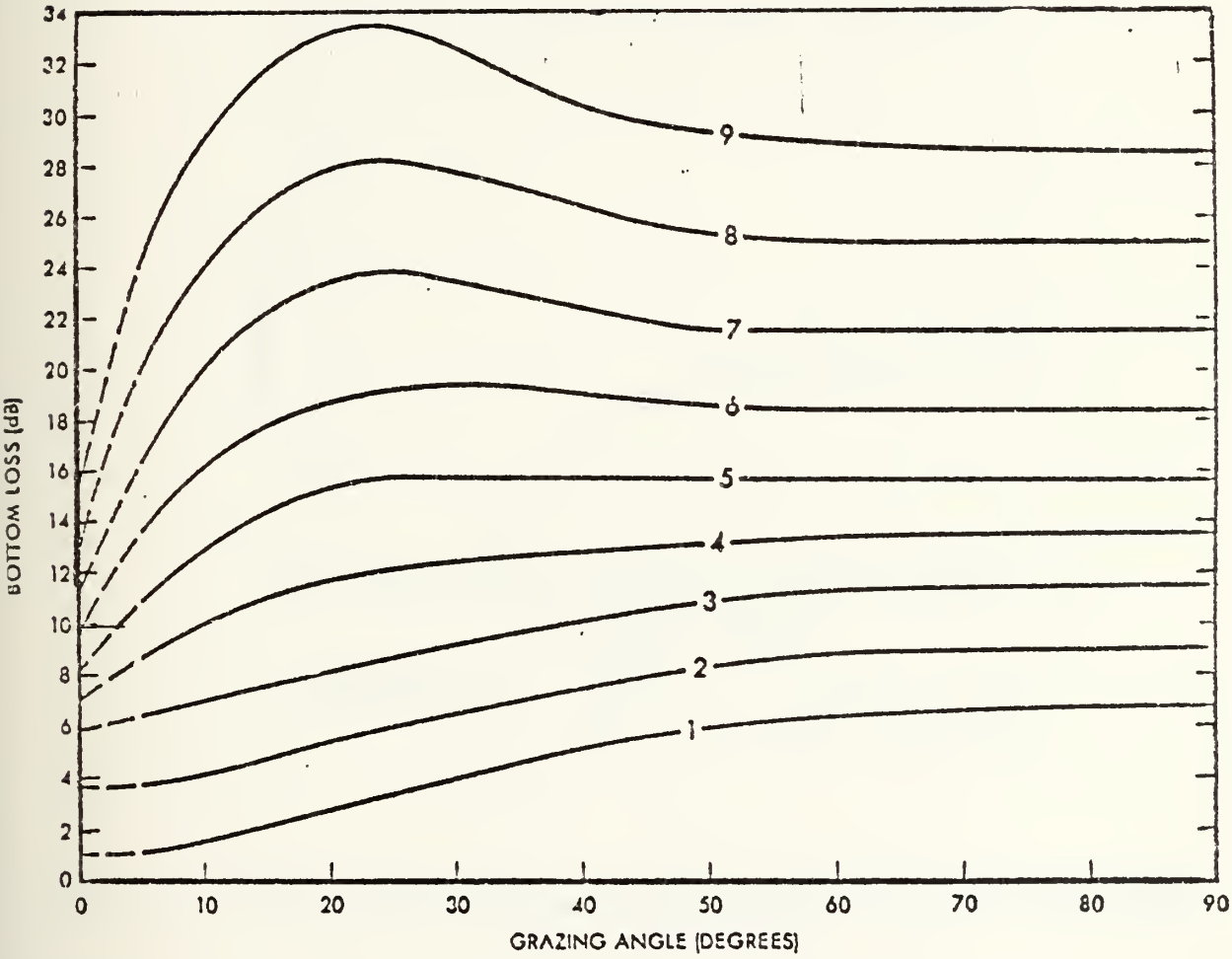

Figure 32. Bottom Loss Classification for Frequency 1 - 4 khz. (Urick, 1979)

bottoms. By examining the BLUG data of FNOC, the bottom loss at different grazing angles in different frequencies does not show much variation at different locations in the Korea Strait. The bottom loss steadily increased with increased grazing angles in all frequency bands from 50 hz to 1000 hz (Figure 33). We expect high bottom loss in the Korea Strait.

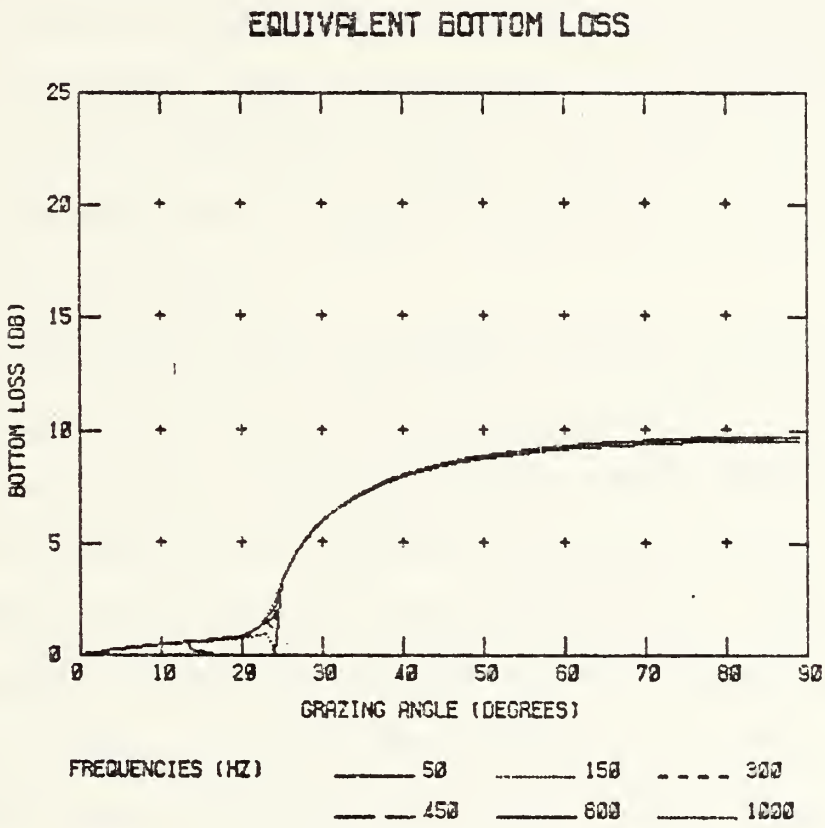

Figure 33. Typical Bottom Loss in Korea Strait. (From FNOC BLUG Data)

3. Signal Fluctuation

When sound energy propagates through sea water, it encounters many mechanisms that distort it. The sea is not stationary in time and it is not uniform. In addition, transmitting and receiving platforms move in irregular manners. All this contributes to changes in signal amplitude and phase.

Storms, variations of sound velocity structure due to the temperature change, internal waves, and tidal variations produce signal variability. The relative contributions of these various mechanisms differ with different locations, times, and equipment. It is difficult to determine the relative importance of these various effects, but generally the effects associated with the biological scattering layers are the most common cause of fluctuations.

Experiments reveal that the maximum variations caused by the deep scattering layer occur near mid-latitude (54 N,S) and minimum variations occur near 20 N,S of the equator. Sound energy attenuation resulting from marine life usually is not important in the deep open ocean, but it is important in shallow coastal waters (Urick, 1975). Large changes in received-signal levels may often be noticed at sunrise and sunset (Weston et al., 1969). Since fish and plankton are sensitive to light intensity, they migrate vertically in the water column. They go deep during the day and move toward the surface at night. The average depth varies with geographical location. The amount of scattering and absorption of sound by the fish depends upon their degree of aggregation; this is particularly important for pelagic fish which have swim bladders.

Fish tend to swim individually at night, producing high overall attenuation, and then form groups during the day with less resulting attenuation. There is large diurnal change at sunset and sunrise (Figure 34). The size of a fish swim bladder depends on the size of the fish and its depth. The different sizes of swim bladder resonate over a wide frequency range, especially at low frequencies.

Storms increase ambient sea noise levels and also raise the surface reverberation due to increased sea state. Changing wind speed and duration changes the sea surface wave height and period. The storms also produce air bubbles which cause the fluctuation of acoustic signals by scattering and absorption. Fish no longer school in groups during storms thereby enhancing reverberation level and attenuation. It is also known that after a storm the fish may be quite slow to re-form into shoals. The effects of fish in storms might not be important in the winter and at night. Waves and wind change the structure of the water column by the turbulent mixing process. These changes in the mixed layer can either improve or worsen the sound transmission.

Changes in water depth accompanying tides are important in changing the modal interference patter in shallow water because propagation in shallow water is limited to a small number of normal modes. For transmission between fixed transducers, the interference patter is swept past the receiver by the change in water depth, and the spatial variation is converted to a temporal variation. This produced fluctuations in the amplitude and phase of the signal. The period of the acoustic fluctuation would then be the same as that of the water depth changes; i.e. the period of the semi-diurnal tide in the Korea Strait.

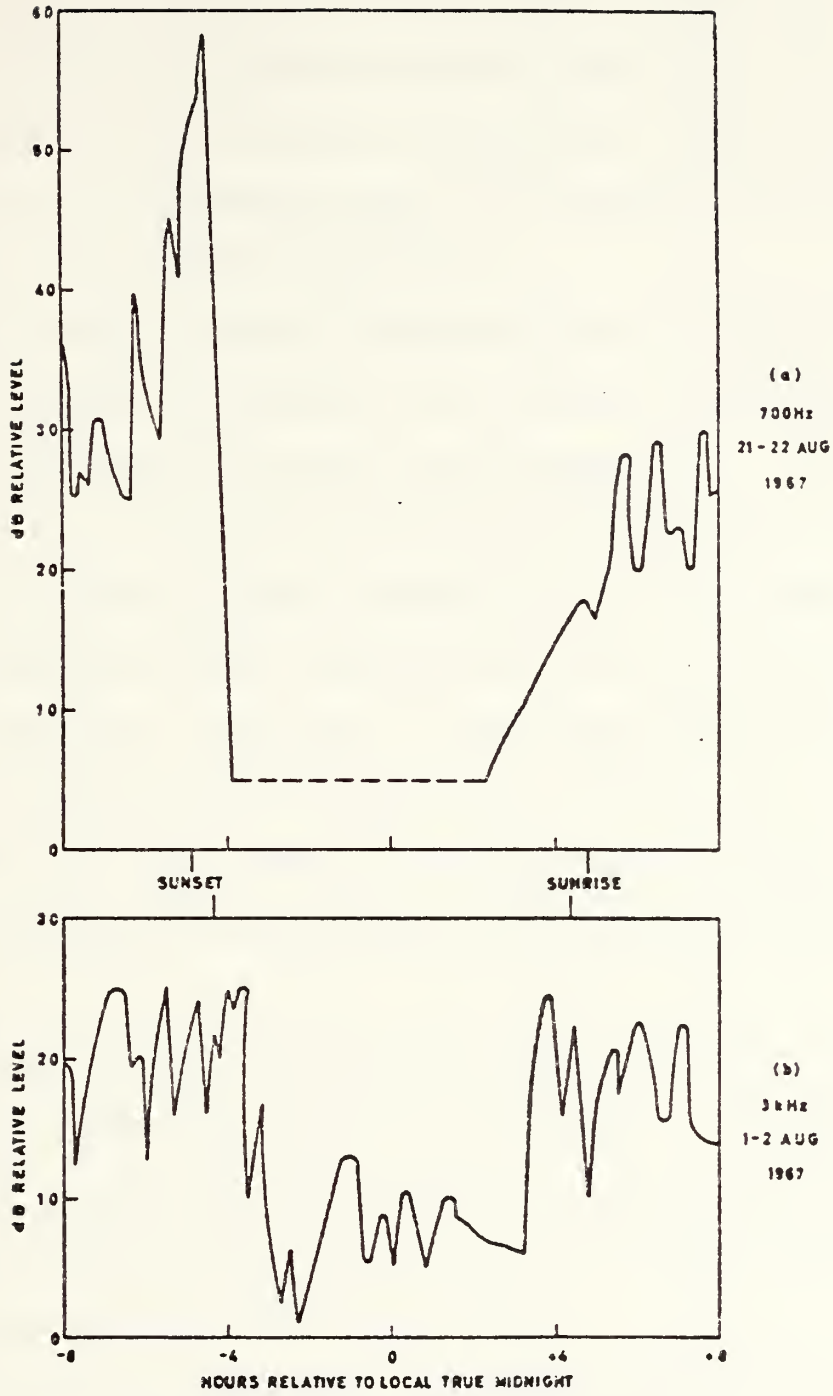

Figure 34. Diurnal Variation of Fish Attenuation. (From Weston et al., 1970)

The variation of sound velocity structure in the water column also gives signal attenuation in shallow water especially when strong negative sound velocity gradients cause the sound rays to refract downward creating a strong interaction with sea floor. Both the sea surface and the sea floor makes energy scatter or be absorbed. This behavior is obviously a shallow water phenomenon.

The erratic or periodic pitching motions of a SONAR platform causes the axis of the transmitter of receiver beam patter to wobble, thereby causing amplitude changes in sound signals.

The water column is not stationary in its properties. Since sound travels different paths in different types of water masses, when the sound propagates through different water masses it can encounter different interfaces. This effect is strong when sound travels through cold or warm eddies or across ocean fronts. The size of the water mass is important but at short ranges the most important physical process producing fluctuations is considered to be focusing and defocusing of the sound.

Along with fish, internal waves are the most common phenomenon contributing to signal variations in shallow water. In practice, it is difficult to separate the acoustic effects of internal waves from similar effects caused by other sources, such as the thermal and density microstructure (Arthur D. Little Inc., 1966).

Internal waves may occur in the region marked by vertical density difference in the water column. The density of the sea is controlled by the temperature and salinity. The sea surface temperature in the Korea Strait reaches up to 24C in September. The temperature profile

shows a sharp negative thermocline below a 40 m thick isothermal layer and then drops to nearly 10 C at the sea floor. The salinity variation of the water column shows a gradual increase with depth. The upper fresh water is due to river run-off. Below the sharp negative thermocline, we can expect strong internal waves in the Korea Strait. Since temperature gradients are the primary cause of refraction of sound waves, the motion of the thermocline (caused by internal waves) will cause corresponding large effects in the acoustic propagation. Generally, internal waves have a wide spectrum of frequencies and amplitudes; short period oscillations with periods of 1 to 2 minutes have wavelengths of centimeters, while long period waves (with periods of days or weeks) have wave lengths of tens of miles and amplitudes of hundreds of feet. In the Korea Strait, in September, internal waves have a maximum period of 10 min and a minimum period of 4 minutes.

The Brunt-Vaisala period for internal waves ($N^2 = -\frac{gap}{paZ}$) varies from as short as 1 - 2 minutes for amplitudes of centimeters to as long as days or weeks with wavelengths of tens of miles and amplitudes of hundreds of feet. Diurnal and Semi-diurnal tidal waves are common along the Continental Shelf and may have amplitudes of tens of feet and short periods (1 min to 1 hour); such waves occur frequently close to the coast.

Fluctuations in acoustic intensity have been directly related to the passage of internal waves. In isothermal water, fluctuations of 4 dB were observed (Arthur D. Little Inc., 1966). The fluctuations in the acoustic signals caused by ocean turbulence is about $\pm$ 6 dB. The

acoustic signal fluctuations caused by the strong surface interference and fish are the order of 10 dB in the shallow water.

The distribution of sound energy for a case of a thermocline of constant depth follows a regular pattern of decreasing magnitude with range. On the other hand, the spatial distribution of sound energy for a horizontally-sisusoidal thermocline is irregular with broad partial-shadow zones.

When the depth of the thermocline spatially varies, internal waves may cause signal fluctuations as much as 22 dB at short range.

Ocean fronts are the boundaries between water masses having different physical, chemical, or biological properties. Ocean fronts have greater variety than in the atmosphere. The gradient of temperature and salinity can either be very sharp or undistinguishable. Some fronts are stable in space and time, but some move considerably and change their intensity. The exact position of an ocean front and its intensity can be detected by utilizing remote sensing devices. The front can be recognized by the instrument as well as by visual observation in many cases. The usual indications of fronts are rapid sea-surface temperature changes, water color changes, accumulation of debris, and sea smoke.

There are a few oceanic fronts around the Korean Peninsula. The South Korean Coastal Front occurs in the Korea Strait where the branch of the Kuroshio Current meets with West Korean Coastal waters which are relatively fresh due to the coastal river run-off in fall and winter. This front is moderate to strong in its intensity and is mostly stable.

Another important front is formed when northernly winds driven by the winter monsoon force the warm waters of the Yellow Sea into contact with the Tsushima Current in the western channel of the Korea Strait.

The influence of fronts on the transmission of sound energy is mainly in changing the depth of the ray turning point and focusing or defocusing of rays, depending on the relative position of the source and receiver.

III. MEASUREMENT OF TRANSMISSION LOSS IN THE KOREA STRAIT

1) Date: September 17, 1980

2) Time: 1030 to 1130 Local

3) Location: Korea Trench (35 00 N 129 28 E)

4) Platform: S-2E aircraft

5) Source depth: 60 ft.

6) Receiver depth: 60 ft.

7) Sponsor: NADC and ADD

8) Purpose: To acquire an initial set of acoustic data useful for predicting LOFAR and SONAR performance

9) General procedures:

To determine propagation loss as a function of range, the aircraft planted a pair of shallow-setting (60 ft.) calibrated SSQ-57A sonobuoys to serve as receivers and then proceed to drop shallow-setting Mk-64 SUS charges every 35 seconds in 140 KIAS and drop altitude 600 ft. above MSL.

10) Operations:

a) Once the S-2E aircraft was on station and prior to the start of the drop sequence, the receiver channels were tuned for recording sonobuoy channels. The sequence of drops was controlled by timing the interval between drops while maintaining a constant indicated airspeed (140 KIAS), altitude (600 ft. MSL), and heading (true).

b) The measurement started with the release of a Mk-25 smoke flare at the origin (35 00 N-129 28 E). The first run was in the direction 032 True from the marker. The aircraft dropped a sonobuoy at the origin and proceeded with preassigned airspeed and altitude. 2.5 minutes after dropping the first sonobuoy a second sonobuoy was released. After the second sonobuoy was launched, a SUS charge was dropped every 35 s while maintaining constant aircraft heading, altitude, and airspeed for the entire run. (Figure 35) A total of 13 SUS charges were dropped in each direction.

c) A log of the drop sequences was carefully kept for later analysis. The acoustic signal was recorded on a B&K tape recorder along with a signal from a time code-generator.

The pilot monitored the explosions of the SUS charges in order to back up the sensor operator and to expedite prompt replacement of bad SUS charges.

d) After recording all the SUS explosions, the aircraft returned to the first sonobuoy and started the second run perpendicular to the first on heading 122 (T) and repeated same sequence of drops. (Figure 35)

11) The recorded acoustic data were analyzed by NADC, U.S. and ADD, ROK scientists for 5 frequencies (50, 100, 200, 400, 800 hz).

12) The bottom contours along the directions of the two runs are shown in Figures 36 and 37.

The measured data were analyzed by NADC, U.S. and the transmission loss values were provided by ADD, Korea. Figures 38 and 39 show the measured transmission loss at each frequency and in each direction.

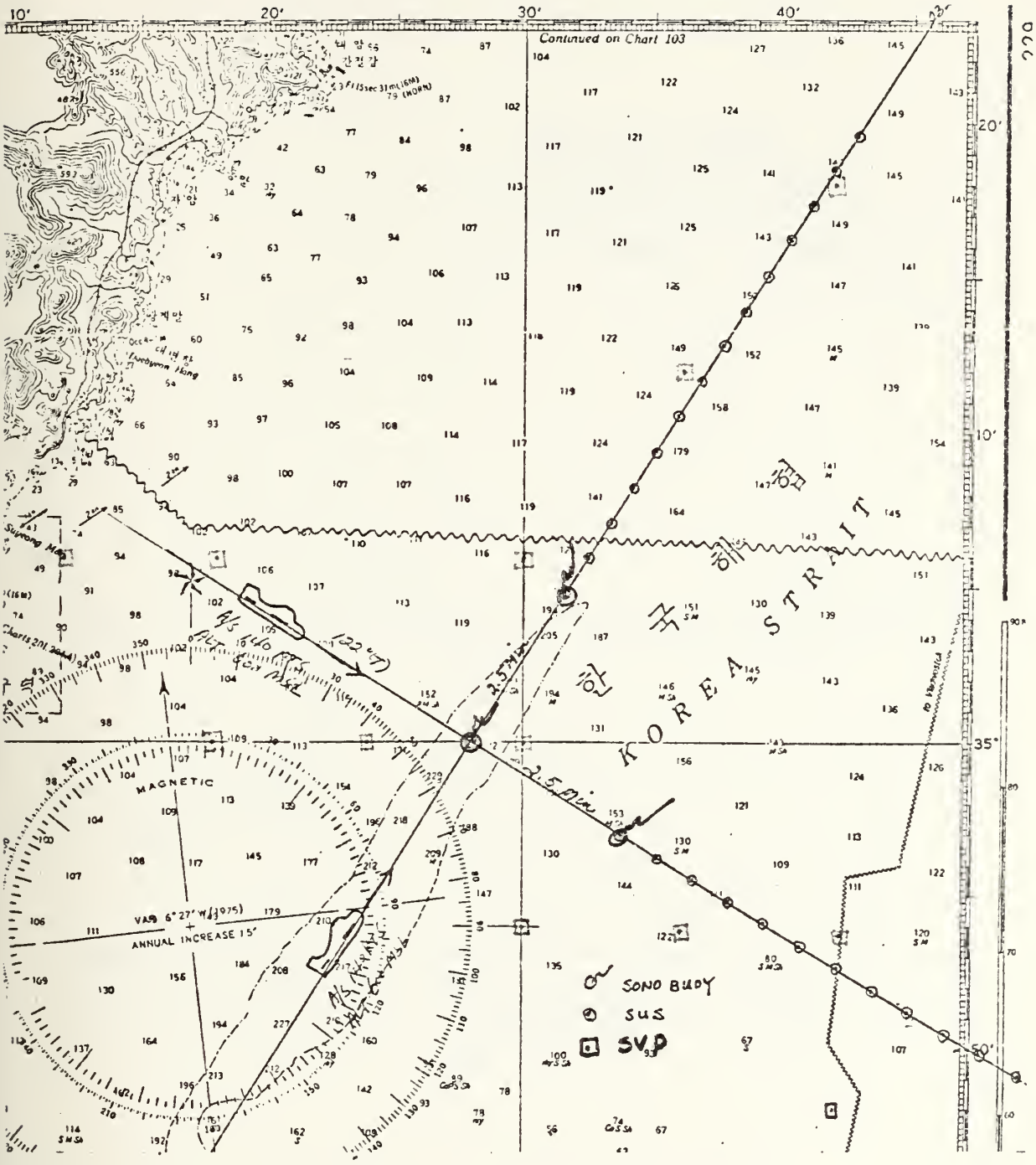

Figure 35. Drop Pattern Diagram for Transmission Loss Measurement in the Korea Strait.

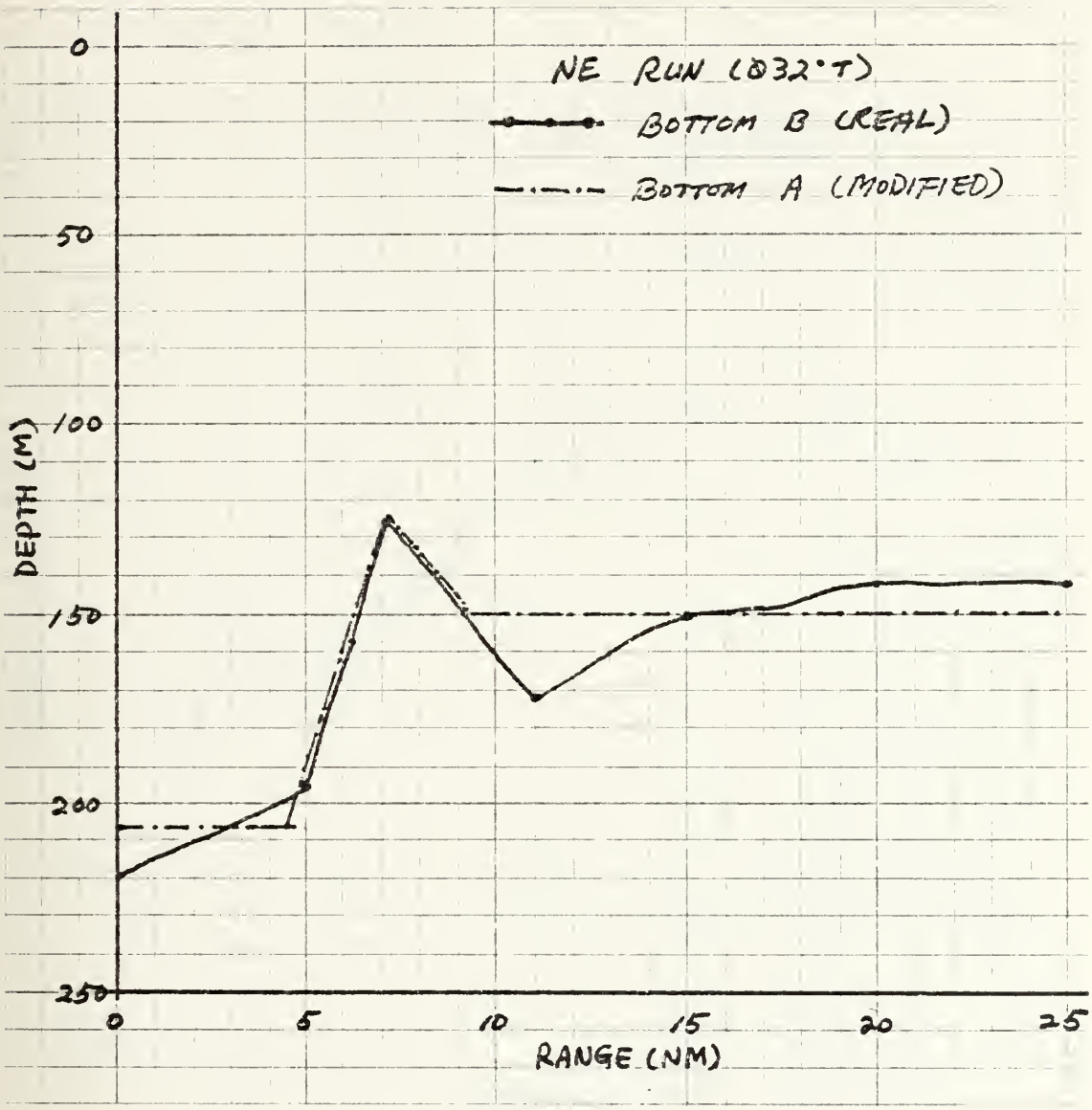

Figure 36. Bottom Contour in NE Direction.

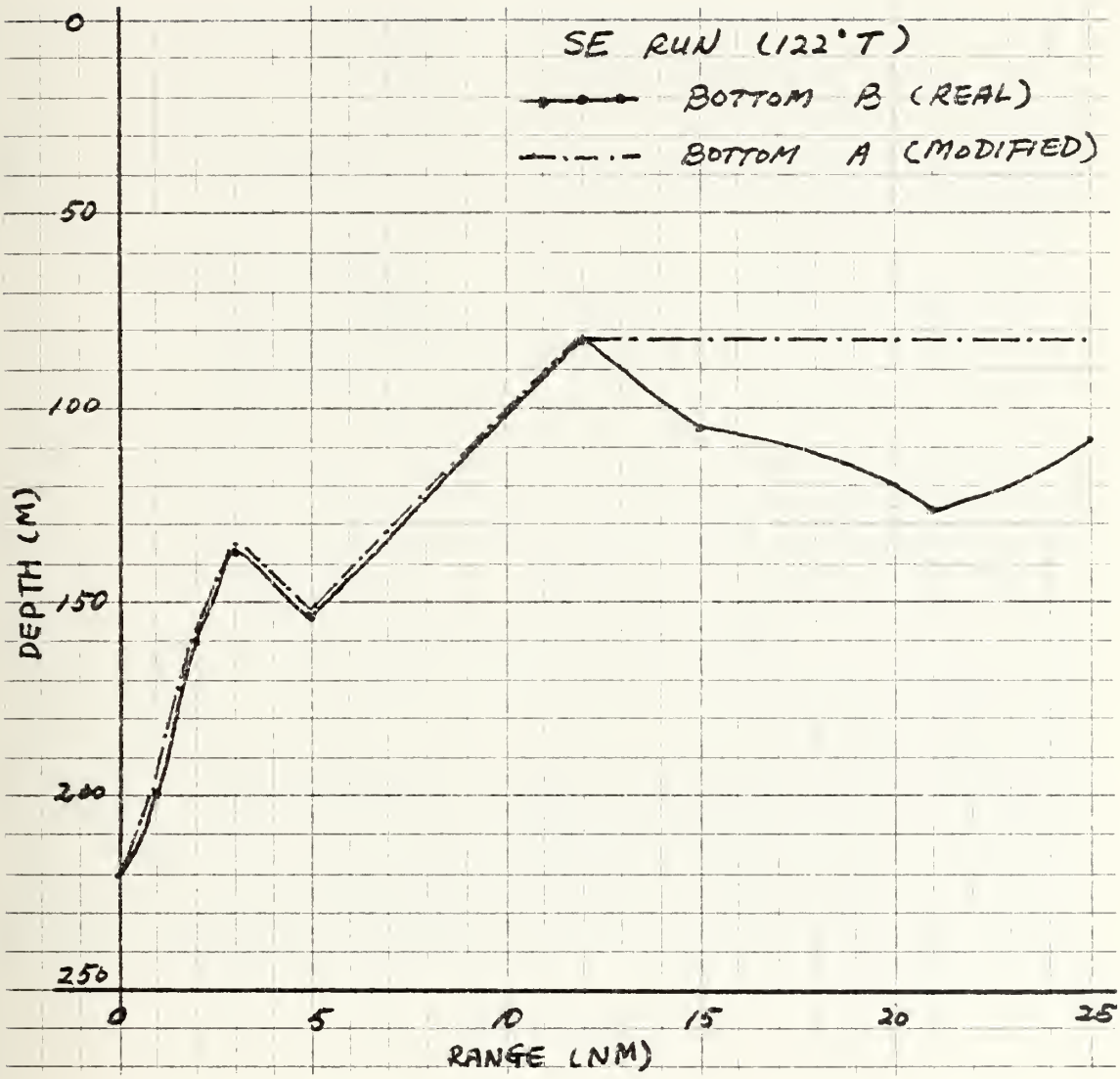

Figure 37. Bottom Contour in SE Direction.

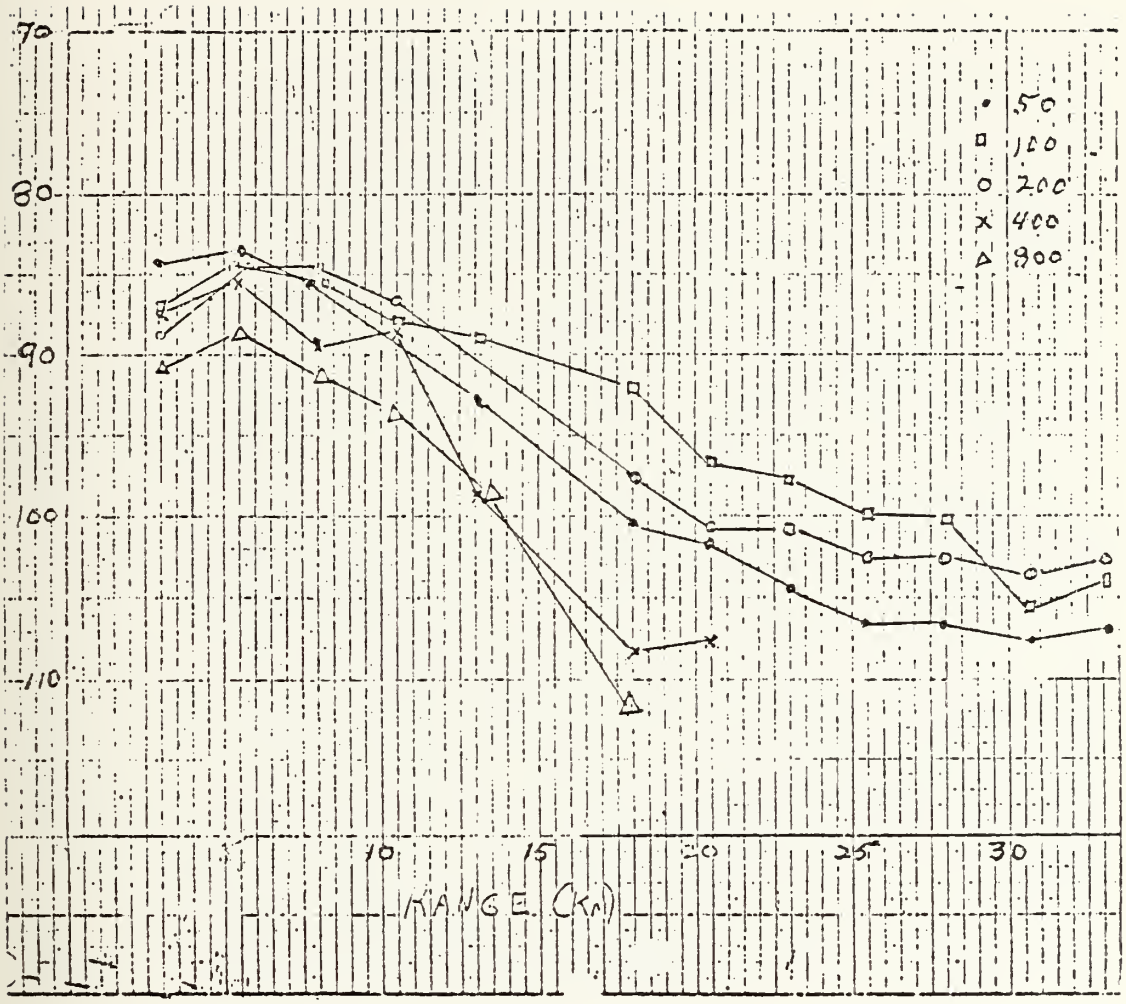

Figure 38. Measured Transmission Loss in NE Direction.

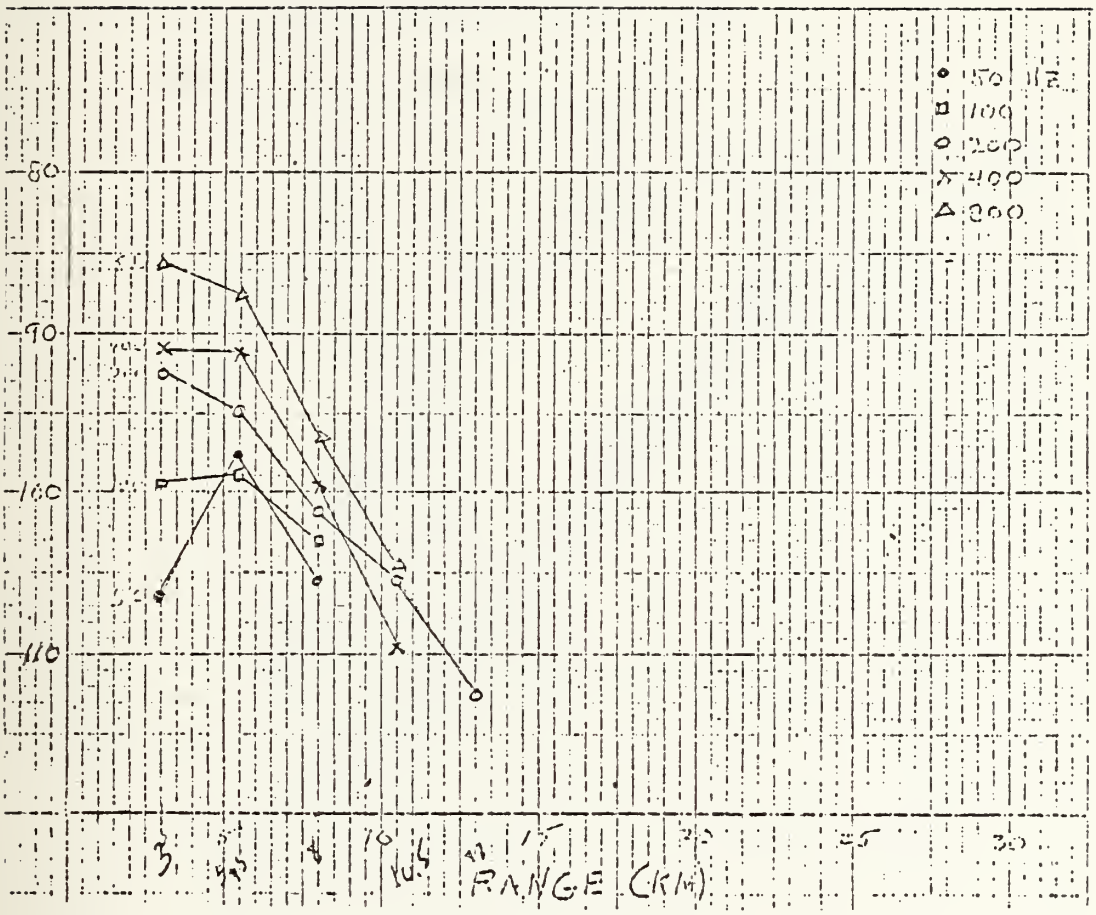

Figure 39. Measured Transmission Loss in SE Direction.

3) Source and receiver depths were fixed at 60 ft. because the existing water depths required using the shallow setting on the SSQ-57A sonobuoy and Mk-64 SUS.

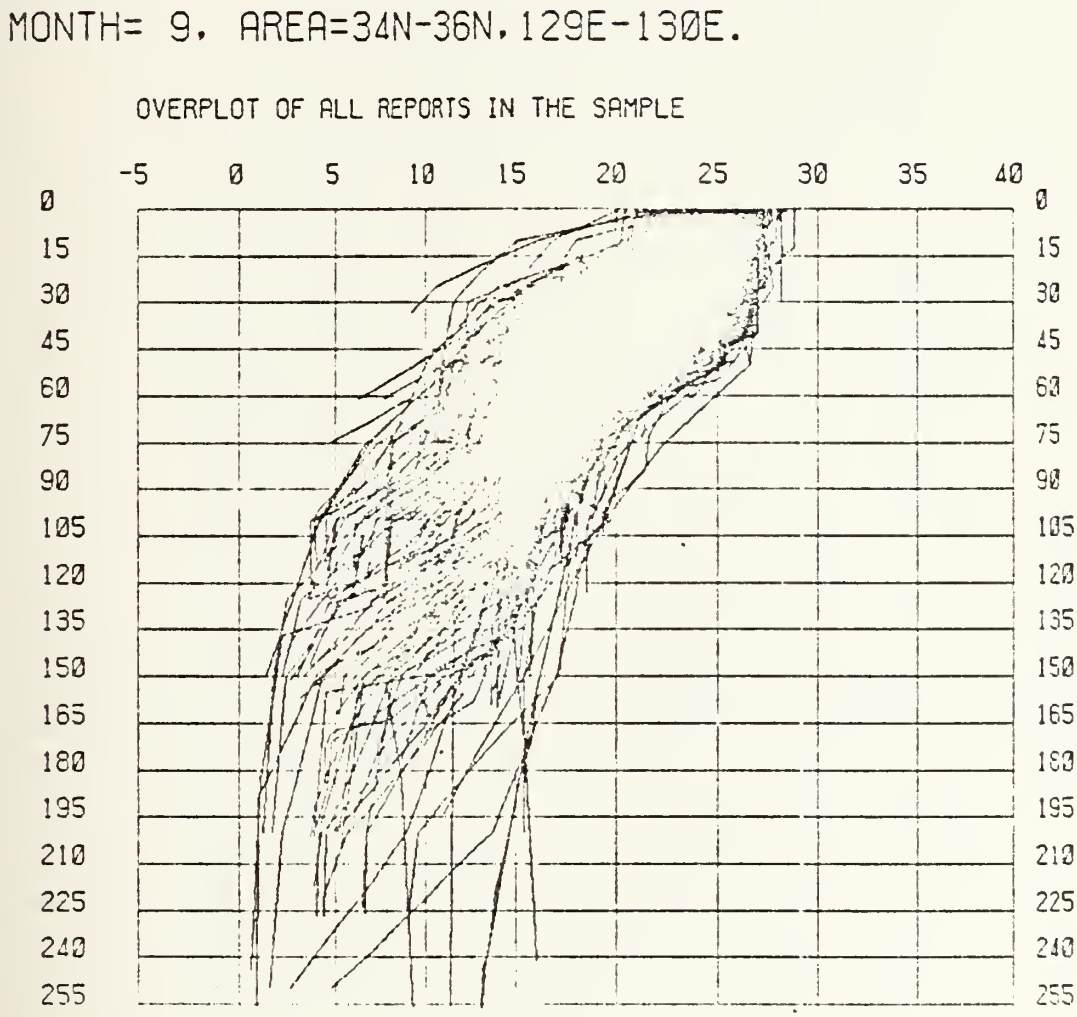

Figure 40. Historical September BT Plot in the Korea Strait (From FNOC MOODS).

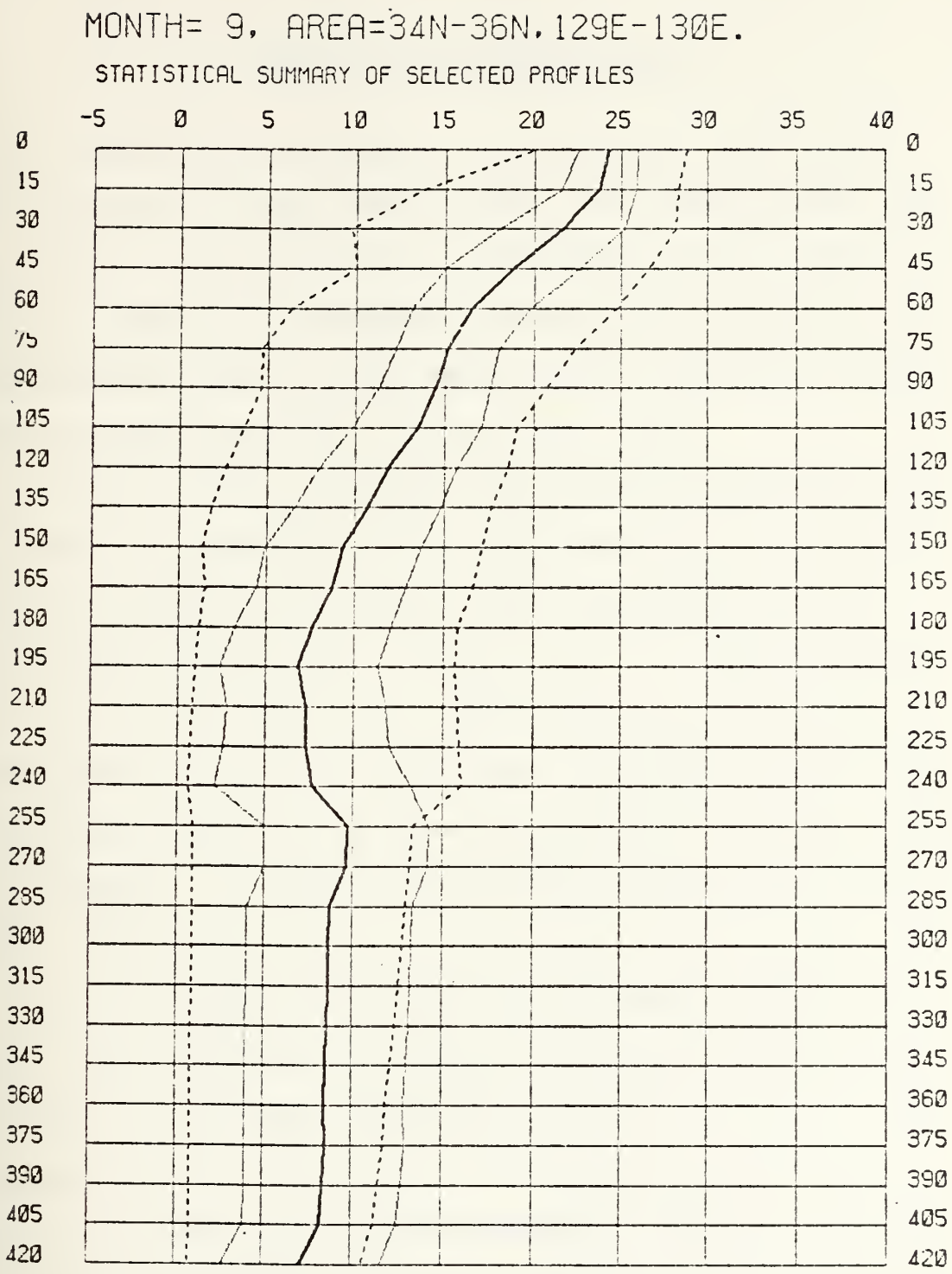

Figure 41. Maximum and Minimum Temperature Profile in the Korea Strait (From FNOC MOODS).

IV. COMPARISON WITH COMPUTER MODELS

The results of the transmission loss measurements were compared with the products of three computer models. The computer models used were chosen not only because of their applicability to the conditions of the experiment but also because of the availability and willingness of knowledgeable people gracious enough to give of their time to advise on the strengths and weakness of each computer model.

As much as possible each computer model was given identical inputs:

1) Historical temperature profiles for September at twelve locations of the Korea Strait in the vicinity of the experiment (Figure 40) were obtained from FNOC MOODS. Average maximum and minimum profiles were then calculated (Figure 41). The average SVP at all twelve locations were vary similar to each other. The profile nearest to the receiver body was selected as the SVP representative along each direction of measurements. All computer runs used this SVP truncated at the local bottom. (Figure 12)

2) Sounding information was obtained from NAVOCEANO, NSTL Station, Bay St. Louis, Mississippi (Hydrographic Survey smooth data plot by USNS KELLAR, 1970), DMAHTC, Washington, D.C., and chart No. 229 ROK Hydrographic Office, 1975. (Figure 36 and 37) The only available information on bottom properties were sediment distribution (Figure 5). No information was available about the properties of the sediments below the surface. Bottom loss Vs grazing angle was determined from FNOC BLUG. (Figure 33)

A. FNOC MODEL

1. Reference: ARL-TR-82-64, 1982

2. Transmission Loss Model: MEDUSA (Range dependent ray model)

3. Ray Trace Model: RP-70

4. General Features:

   a) Developed at ARL University of Texas at Austin, October, 1982.

   b) It is a Range-Dependent Ray Model.

   c) Multiple range-dependent SVP and bottom bathymetry can be entered.

   d) Eliminates false caustics and false shadow zones by representing the sound speed and bathymetry with smooth function and solving the various ray equations numerically.

   d) New interpolation procedures are introduced to compute accurately ray paths with range-dependent environments.

5. Inputs used:

   a) Frequency: 200, 400, and 800 hz.

   b) Bottom type: FNOC Bottom Classification.

6. Outputs obtained:

   a) Ray paths from -5 degree to 5 degree in 0.5 degree increments. (Figure 42 and 43) The properties of the rays are generally similar in the two directions. At long ranges most of the sound energy arrives by refracted paths that do not interact with either the top or bottom. At close ranges rays reflected from the bottom are very important. In the NE direction (032 degrees) bottom-reflected rays do not contribute beyond 12 nm. In the SE direction (122 degrees), bottom-reflected rays suddenly diminish beyond 10 nm.

   b) For 200 hz the transmission loss was obtained as a function of range. The transmission loss was calculated three ways: Coherent Summation of the rays, Incoherent Summation, and no bottom loss. The results of the Incoherent Summation are shown in Figures 44 and 45.

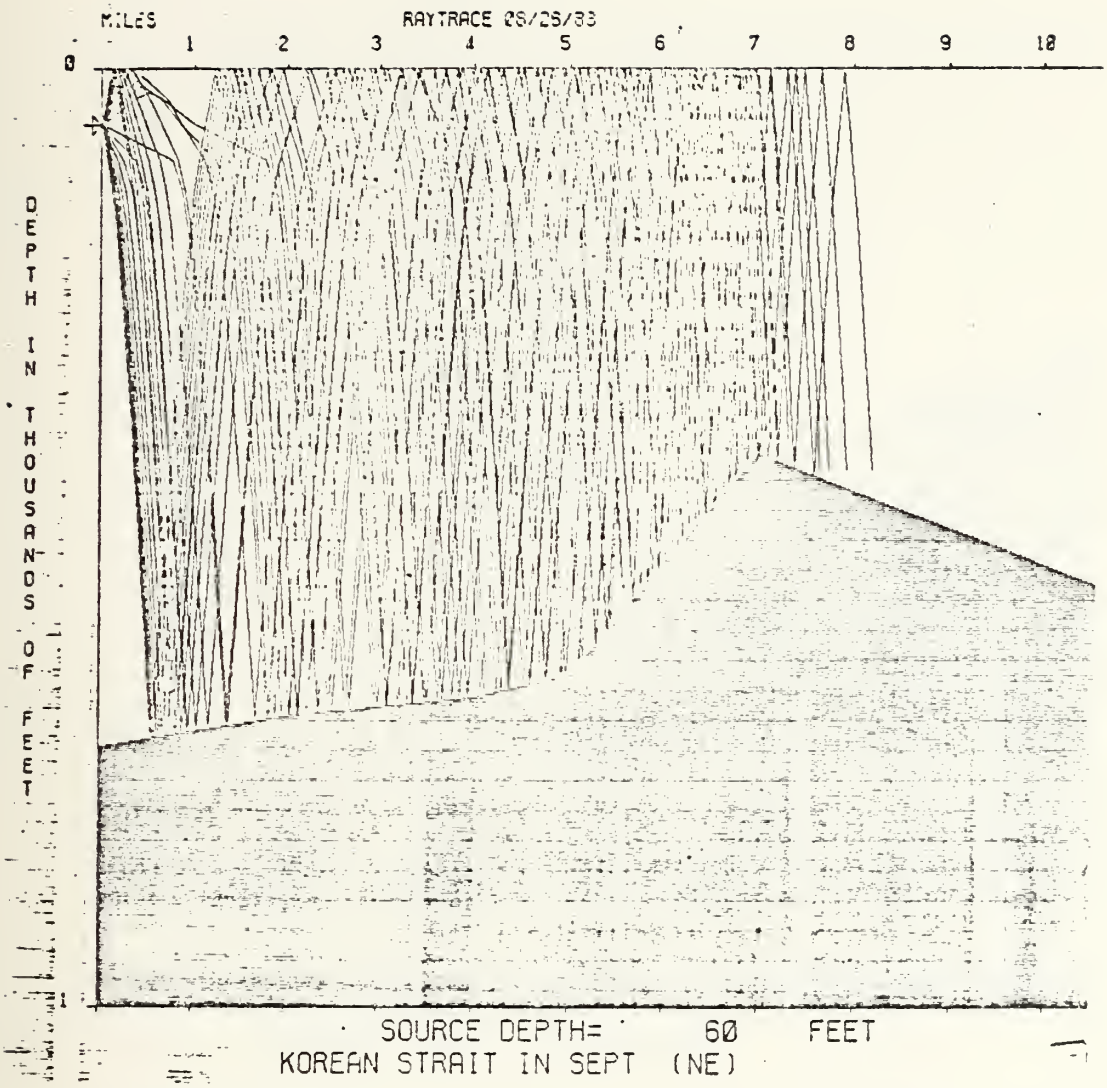

Figure 42. Ray Path in the NE Direction with Single SVP (From RP-70).

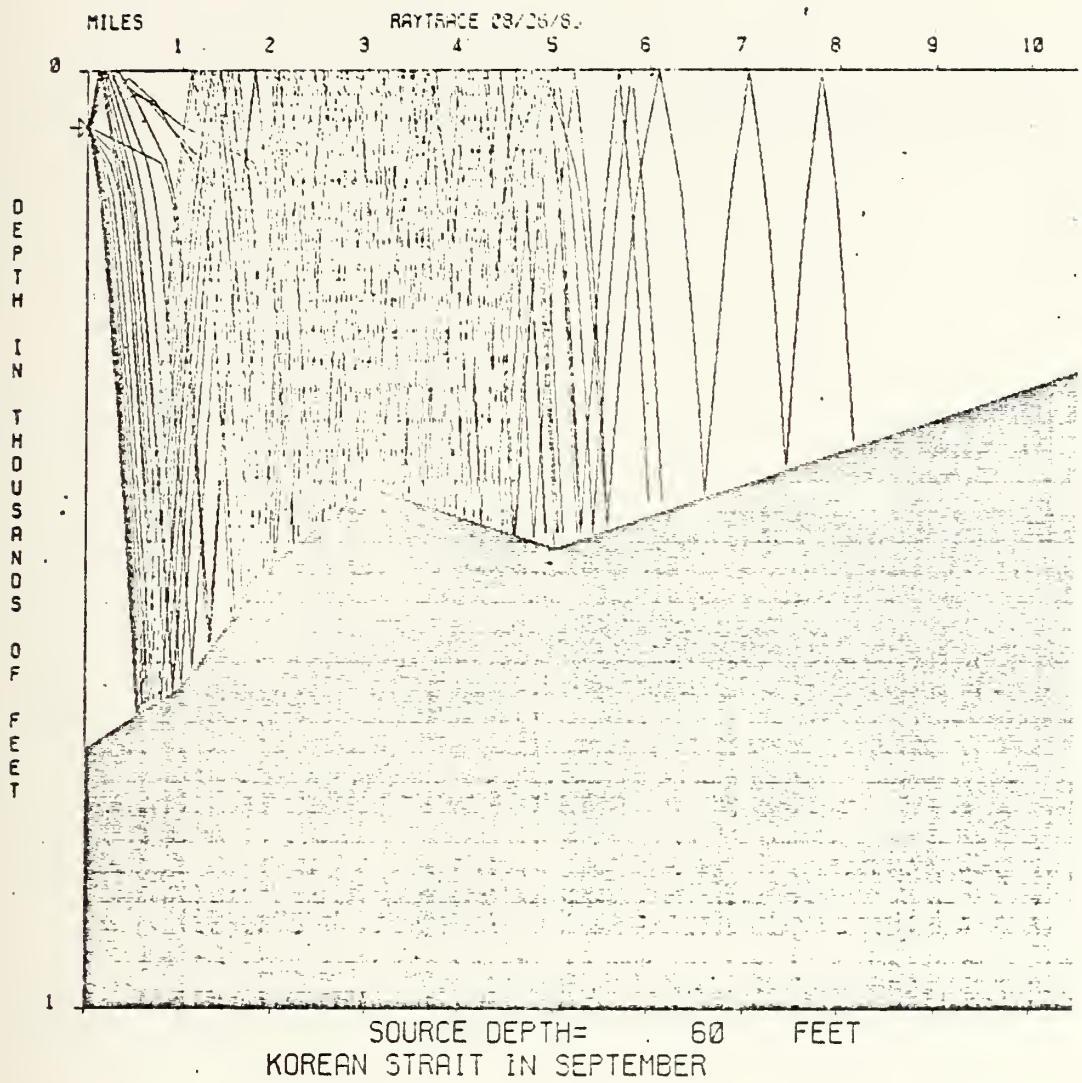

Figure 43. Ray Path in the SE Direction with Single SVP (From RP-70).

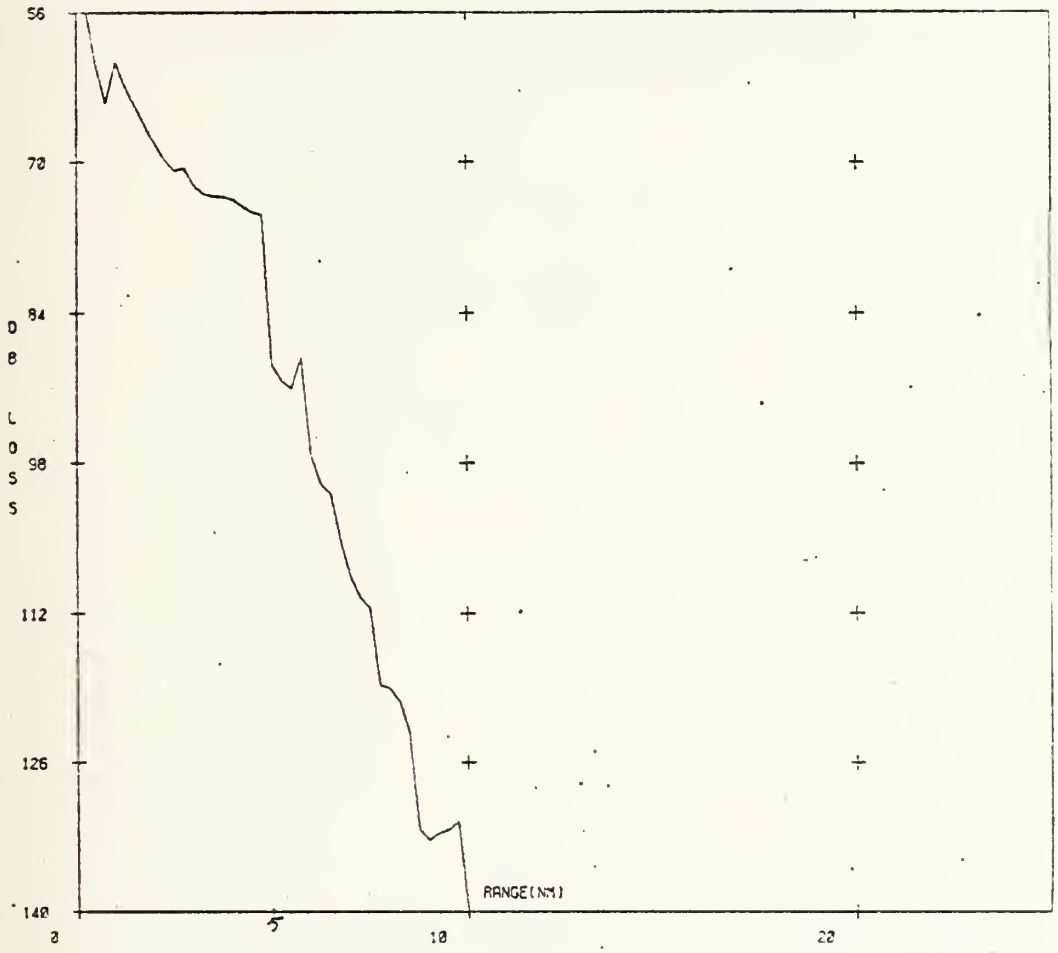

Figure 44. Incoherent TL in NE Direction, 200 hz (From MEDUSA).

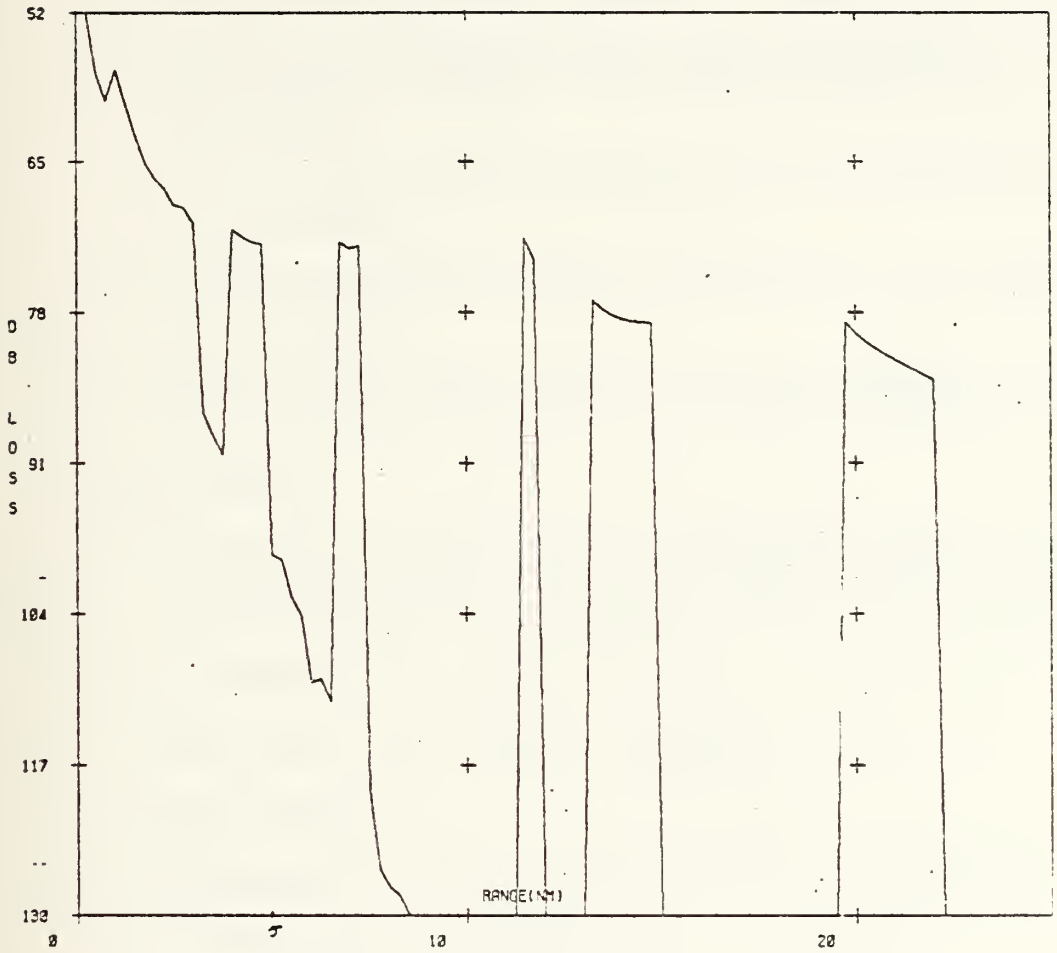

Figure 45. Incoherent TL in SE Direction, 200 hz (From MEDUSA).

B. NAVOCEANO MODEL

1. Model Name: NEWPE

2. General Features:

a) Range-dependent; multiple SVP can be entered.

b) Volume attentuation may be varied.

c) Range-dependent bottom bathymetry and type can be handled.

d) Bottom loss information can be either bottom loss vs, grazing angle or sediment sound speed gradient and attenuation.

e) Single source depth and multiples up to 20 receiver depths may be entered.

f) The model required continuous sound speed at the water-bottom interface.

g) Maximum grazing angle allowed is about 33 degrees. Beyond that the bottom is assumed to be fully attenuating.

3. Inputs used:

a) Bottom loss as a step function with grazing angle; 0 to 25 degrees (no bottom loss) and infinite loss at steeper grazing angles.

b) Frequencies: 50, 100, and 200 hz.

c) Half-beam width: 20 and 60 degrees.

4. Outputs Obtained:

a) Transmission loss as a function of range (Figure 46).

b) Transmission loss contour.

C. JAEGER MODEL

1. Reference: NPGS MS thesis September 1983.

2. General Features:

a) Solves parabolic equation in range-dependent shallow water.

b) High flexiability and reliability for various environmental parameters.

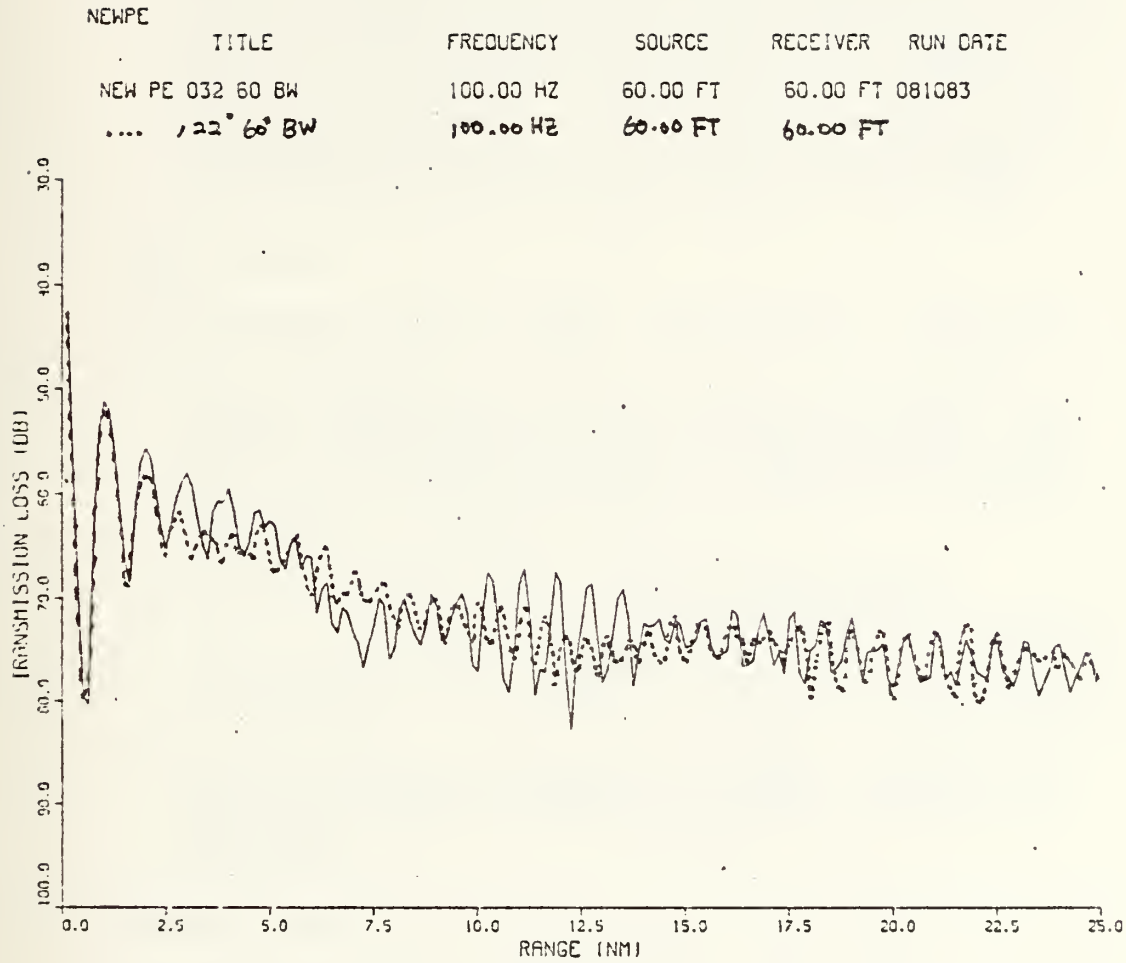

Figure 46. TL Comparison in 100 hz, Half-beam Width 60 Degree, in both Directions by NEWPE Model.

c) Bottom is homogeneous with no depth dependence in the speed of sound, density, or attenuation.

d) Use single SVP.

e) Maximum vertical number of grid points are 5000.

f) Where the bottom is level, horizontal step is chosen so that it is less than one wavelength of the sound. On a sloping bottom, the horizontal step is determined by the intersection of the bottom with the vertical grid and it can get very long for a shallow slope. For example, if the vertical step is 1 m and the slop is 1 degree, the horizontal range step is 57.3 m; the frequency for the wavelength is 57.3 m in 26 hz so that for freqencies greater than 26 hz, the range step may be too large.

3. Inputs used:

a) Frequencies: 50, 100, 200, 400 and 800 hz. (Table 4)

b) Because of possible difficulties with gently sloping bottoms, two different bottom profiles were used: one was the same as used for input the other two computer models; the other was modified to eliminate all slopes less than 0.1 degrees.

c) Number of vertical grid points: 4000 and 5000.

d) The density of the sea water was taken to be 1 gm/cm^3 and its attenuation was internally calculated by the model.

e) The properties of the bottom were taken to be those for fine sand as given by Hamilton (1980): density 1.94 gm/cm^3, sound speed 1749 m/s, and attenuation 0.87 dB/ wavelength.

4. Outputs Obtained:

a) Transmission loss as a function of range (Figure 47,48)

E. RESULTS

The transmission loss given by both JAEGER PE and NEWPE is about 60 dB at 5.0 km. Because the experimentally-measured transmission losses at this range are 30 dB less than this at all frequencies, it is suspected there may be a constant error in the measurements.

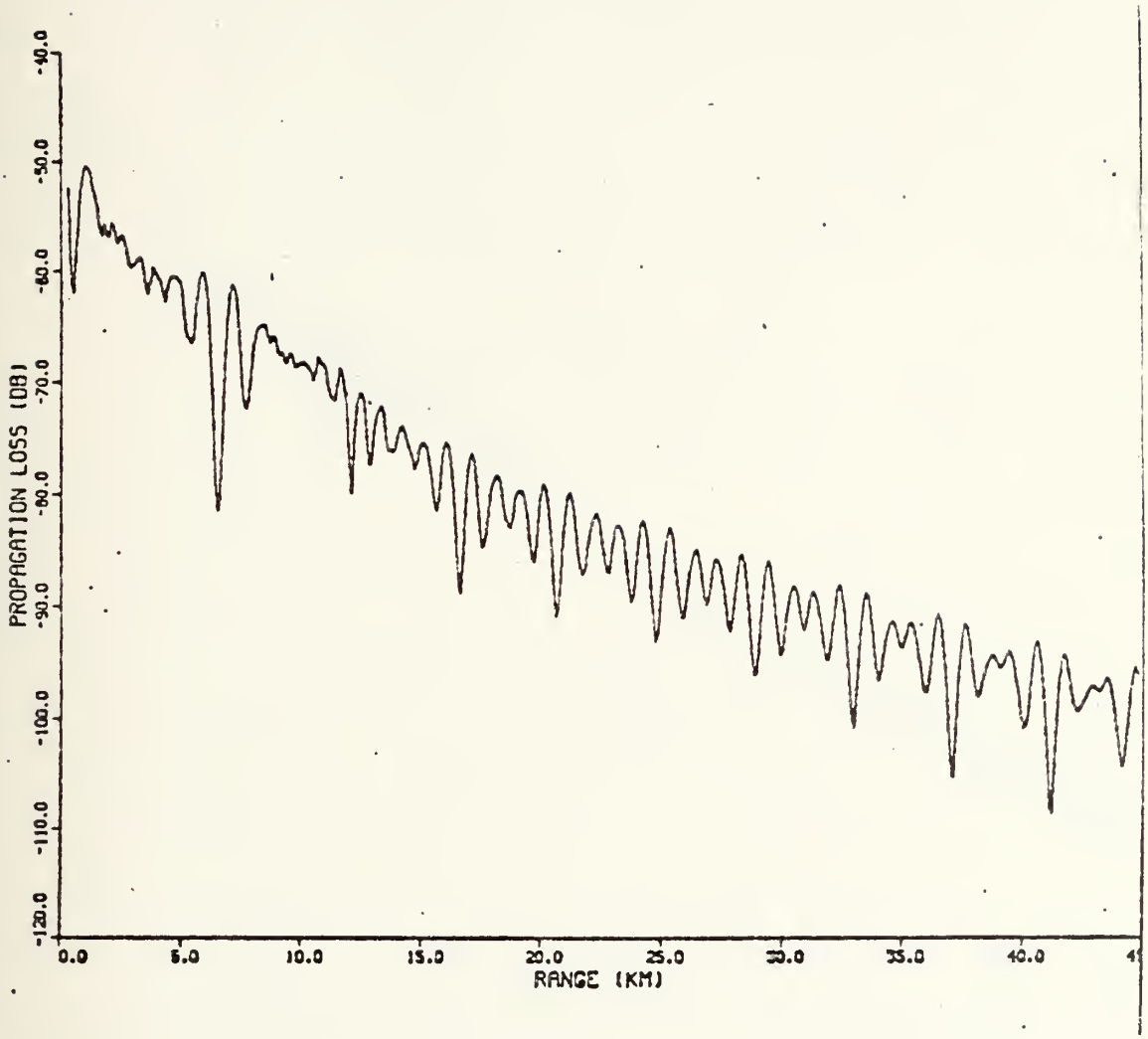

Figure 47. TL in the NE Direction, 50 hz, N=4000, smooth =5. KSI

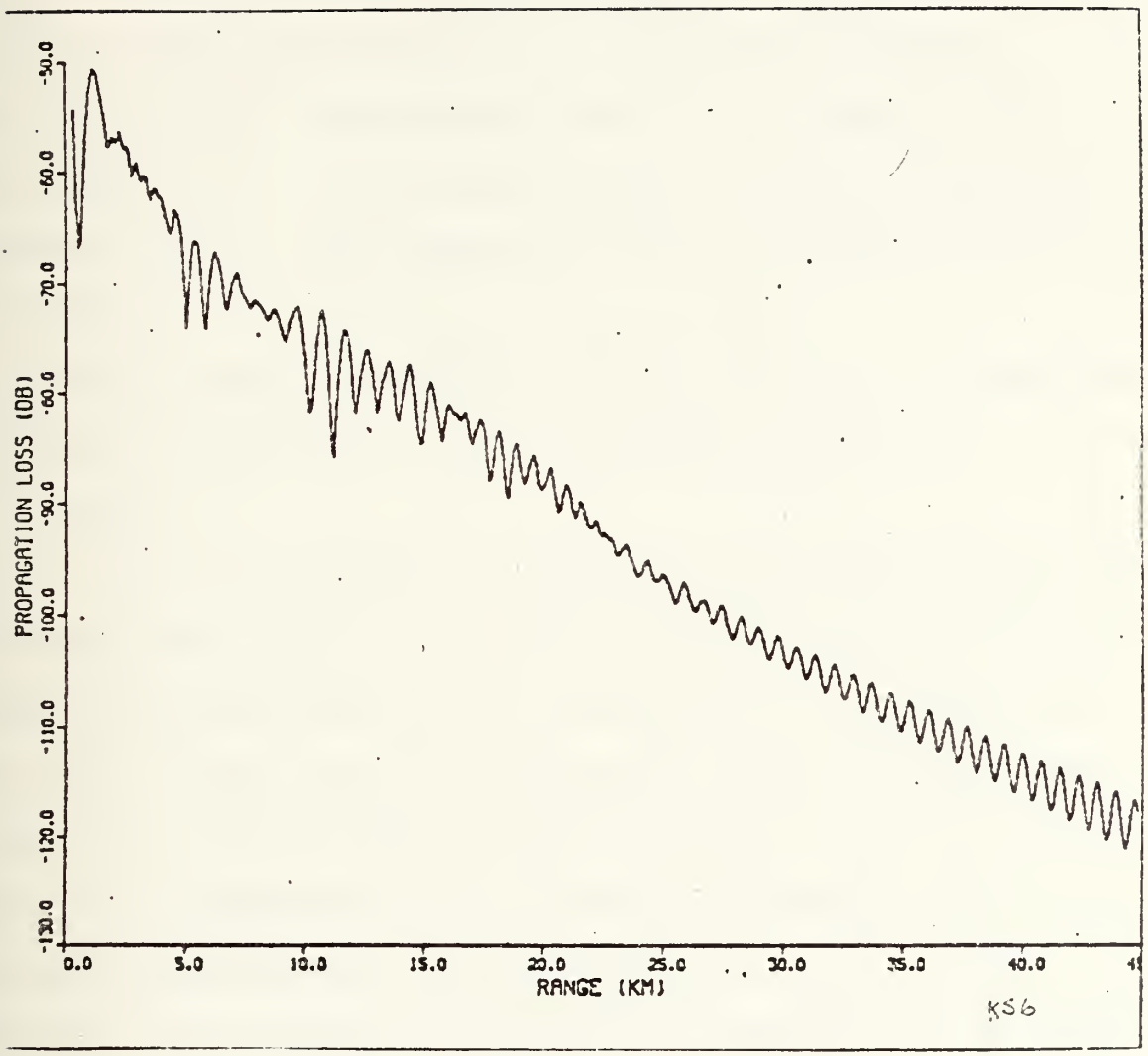

Figure 48. TL in the SE Direction, 50 hz, N=4000, smooth =5.

For this reason, all values of the measured transmission loss were increased by 30 dB before comparing with the predictions of any of the computer models.

NEWPE Model

The smoothed predictions of NEWPE compared with the experimental results are shown (Figure 49, 50, 51). At all three frequencies (50, 100, and 200 hz) the agreement between the prediction and the experiment is poor: for the bottom parameters used, the dependence of transmission loss on range predicted by the computer model is less than was observed.

More importantly, the computer model does not predict the significant difference between the two different propagation directions.

FNOC Model

Ray paths for propagation in both directions are shown (Figure 42, 43). At ranges greater than a couple of nautical miles, the sound field is entirely dominated by rays which have bounced off the top and bottom many times. Beyond 5 nm in the SE direction, there is much less sound energy than at similar ranges in the NE direction. This is in qualitative agreement with experimental results where the transmission loss in the SE directions increases much faster with range than it does in the NE direction. The comparison of the predicted transmission loss by MEDUSA model and experimental results are shown. (Figure 52)

In the NE direction the predicted transmission losses drop off much too fast with range, being some 55 dB lower than the experiment at 10 km. The model does predict a difference for transmission in the two directions, with the transmission loss at 5nm being roughly 10 dB greater in the SE

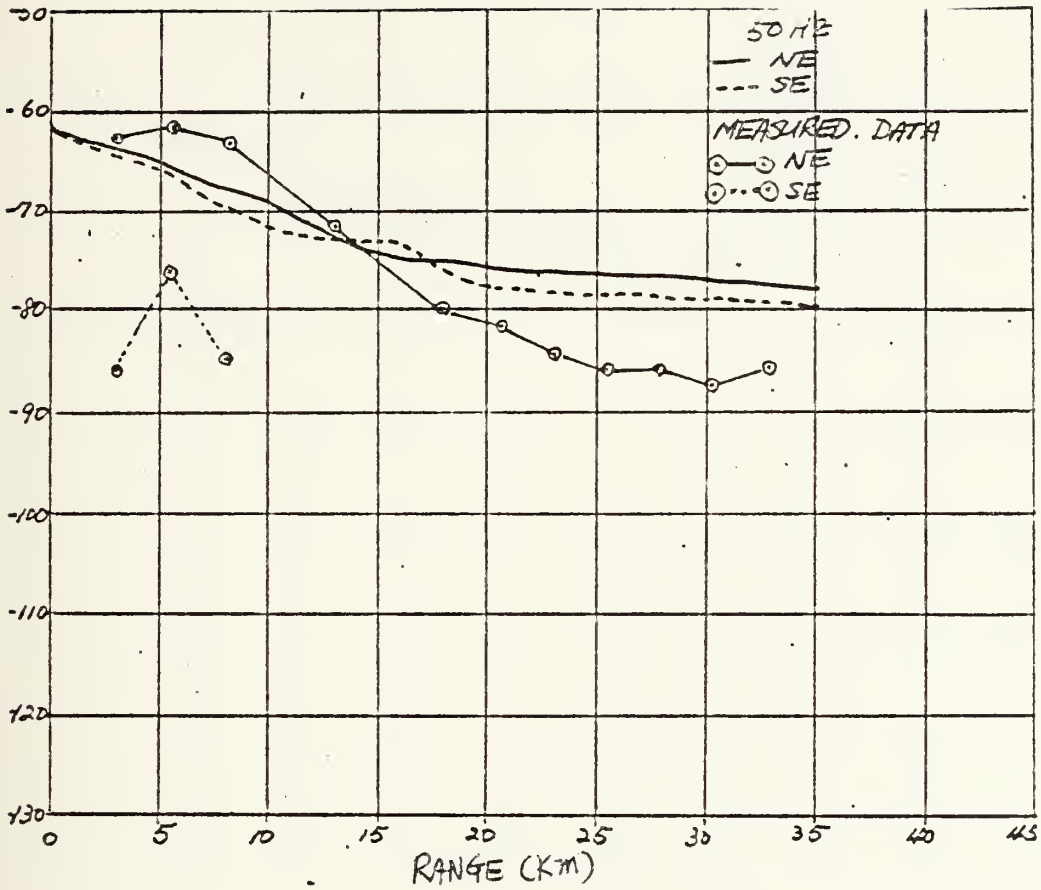

Figure 49. Comparison of Smoothed NEWPE Prediction with Measurements 50 hz, 60 degrees half-beam width.

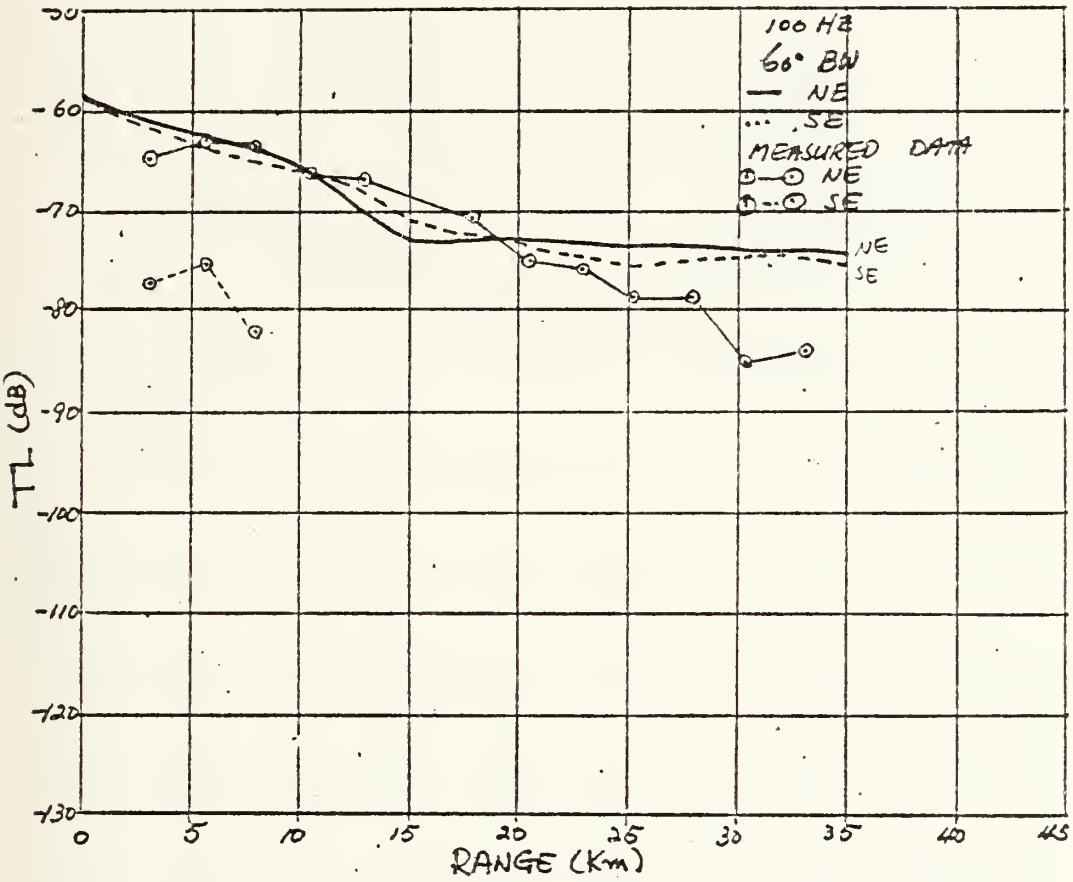

Figure 50. Comparison of Smoothed NEWPE Prediction with Measurements 100 hz, 60 degrees Half-Beam Width.

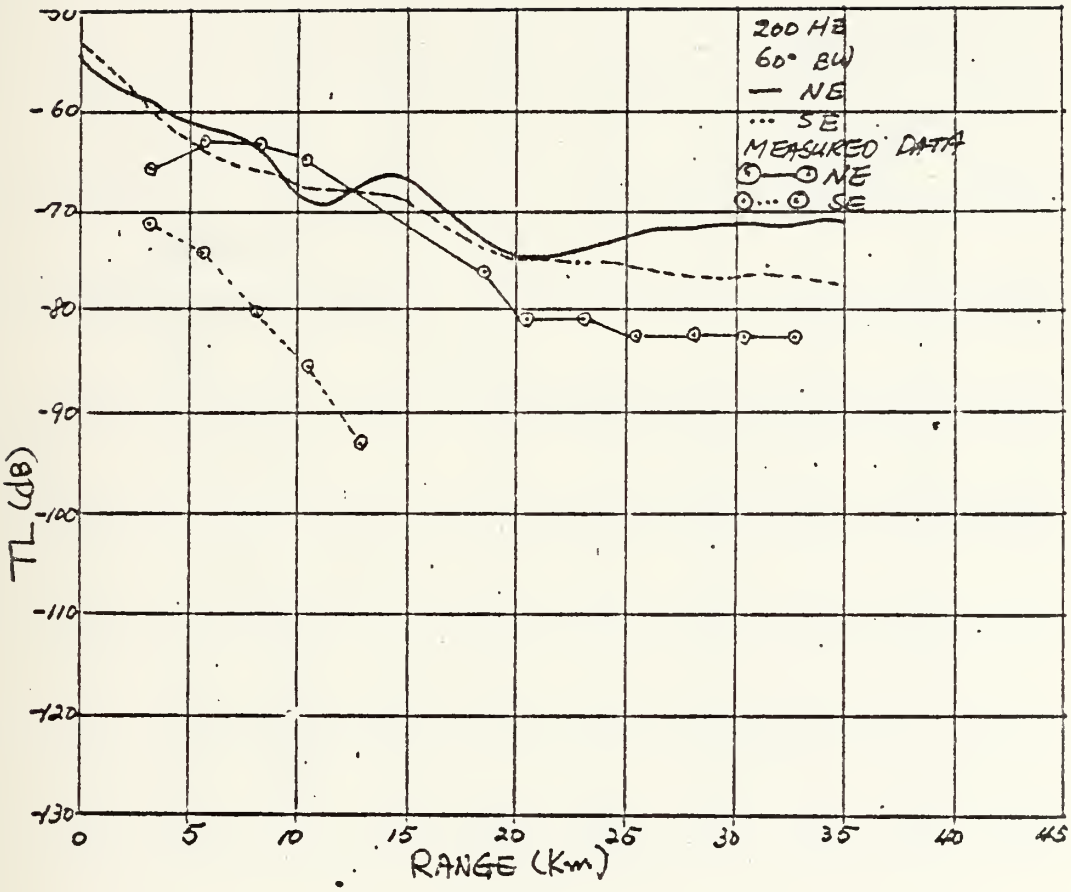

Figure 51. Comparison of Smoothed NEWPE Prediction with Measurements 200 hz, 60 degrees Half-Beam Width.

than at same distance in the NE direction, while the experiment shows a 20 dB difference. (The peaks shown on the transmission loss curve for the SE direction are very suspect. There is no other evidence from any other model or the experiment for such behavior. These are most probably mistakes in the model.)

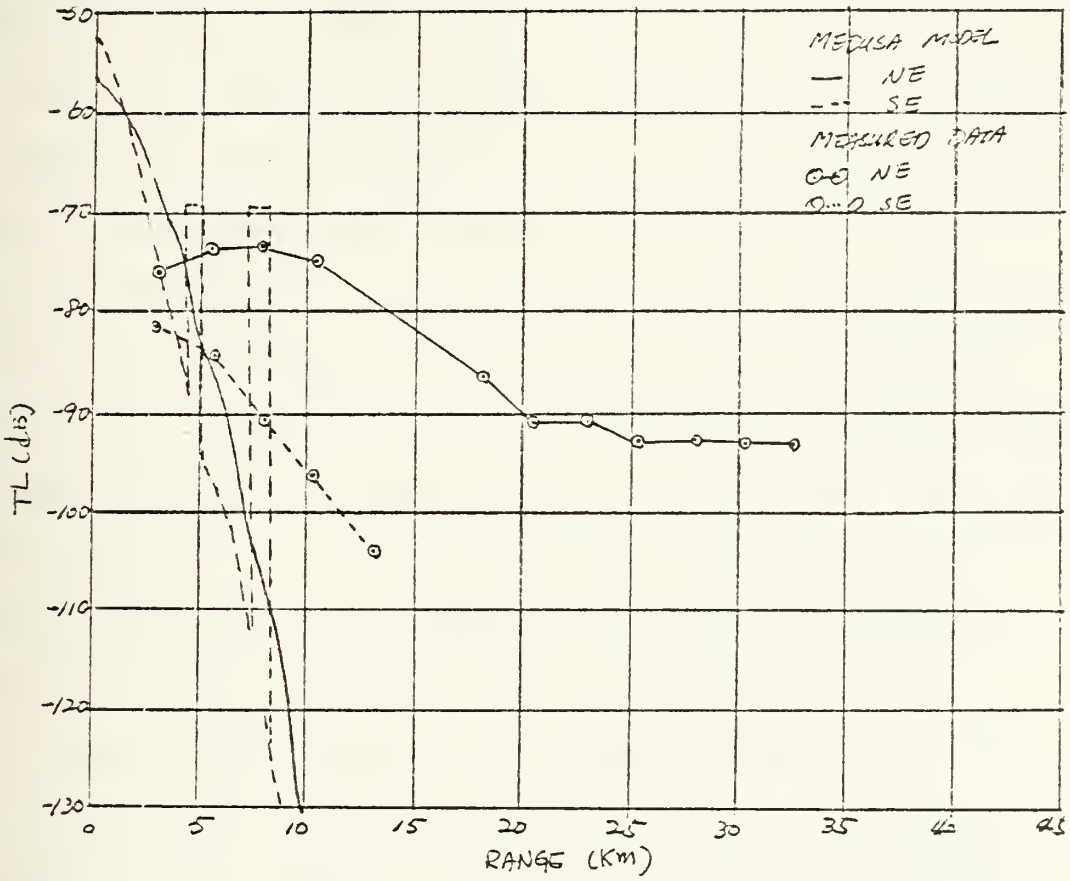

Figure 52. Comparison of TL with MEDUSA Model and Measurements.

JAEGER Model

Because it was available on the NPGS computer, the JAEGER PE model was tested for its sensitivity to some of the more important input parameters (Table 4).

a) Figure 53 shows the effect of changing the number of vertical grid points at 200 hz. Since there is very little difference between the results using 4000 or 5000 grid points, it was felt that for frequencies at and below 200 hz and for the bottom profiles used, 5000 grid points were sufficient for accurate results. Figure 54 shows the same comparison at 800 hz since the number of grid points effect the results, no comparisons were attempted at 400 and 800 hz.

b) Two models for the bottom profile were used. One was a straight forward fit to the bathymetry without regard to the resulting slop (Figure 36, 37). The greatest slop of these profiles was about 1 degree with some segments having slopes as small as 0.15 degrees. Since the smallest vertical grid spacing used was 0.2 m (1000m/5000), the horizontal range steps on the segments with the small slope would be much greater than a wavelength even at the lowest frequency.

For example: For a slope of 0.15 degrees the range step is 76 m, which is greater than the wavelength at 50 hz (30 m). To test the importance of this, a modified bottom profile was constructed with no slopes less than 0.32 degrees (Figure 36, 37). Figure 55 shows the comparison of runs made with these two bottoms: the differences in the results are significant.

c) As another check of the sensitivity of the model to bottom profile, a run was made with a flat bottom and the same sediment properties. The

RUN ID	FREQ (HZ)	DIRECTION	N	BOTTOM
KS 1	50	NE	4000	A
2	100	NE	4000	A
3	200	NE	4000	A
4	400	NE	4000	A
5	800	NE	4000	A
51	800	NE	5000	A
6	50	SE	4000	A
7	100	SE	4000	A
8	200	SE	4000	A
9	400	SE	4000	A
10	800	SE	4000	A
11	800	SE	5000	A
12	400	SE	5000	A
13	50	NE	5000	B
14	50	NE	4000	B
15	100	NE	4000	B
16	50	NE	5000	A
17	100	NE	5000	A
18	200	NE	5000	A
19	400	NE	5000	A
20	50	SE	5000	A
21	50	NE/SE	5000	FLAT (150m)

Table 4. Summary of Sensitivity Check of JAEGER Model.

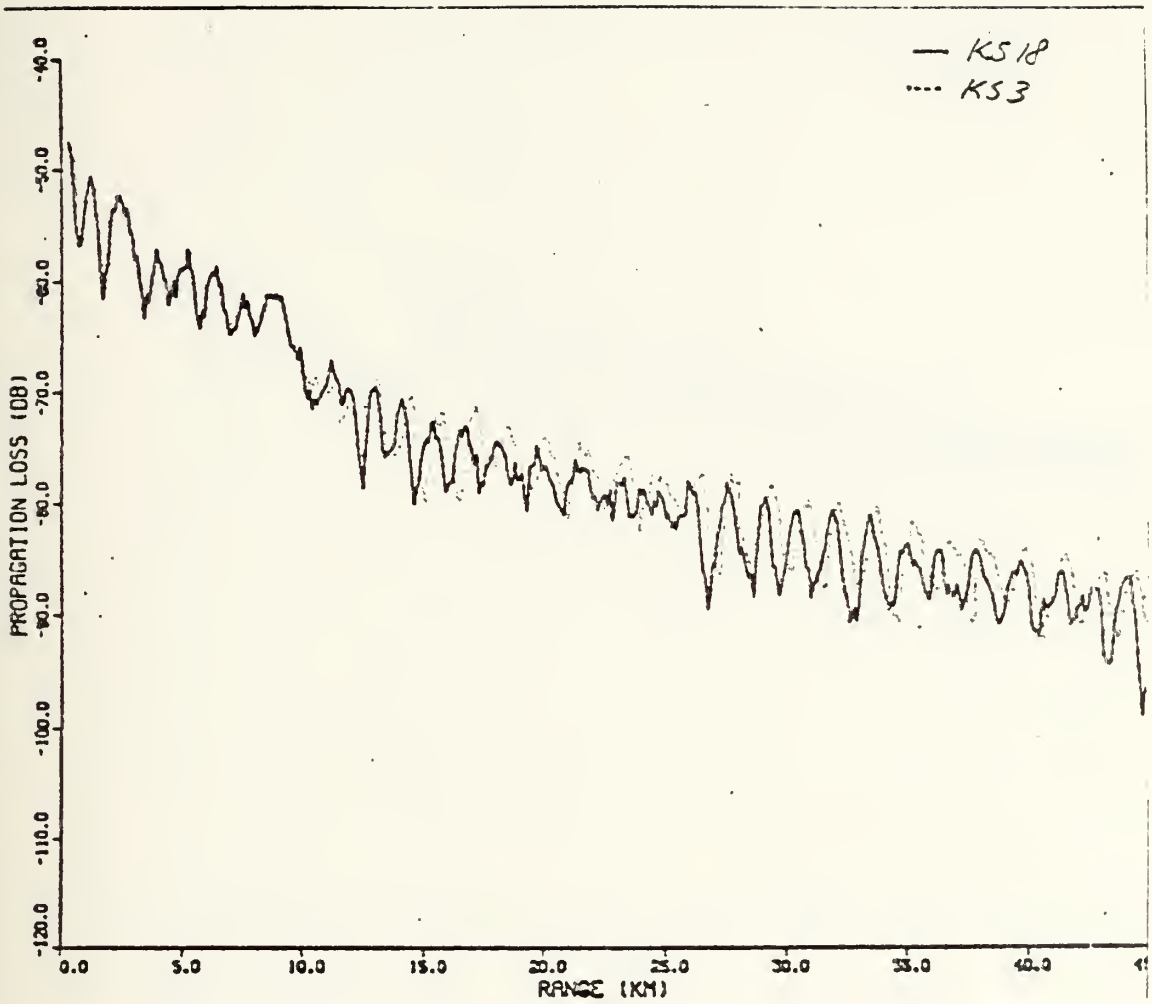

Figure 53. The Effect of the Number of Vertical Grid Points, 200 hz.

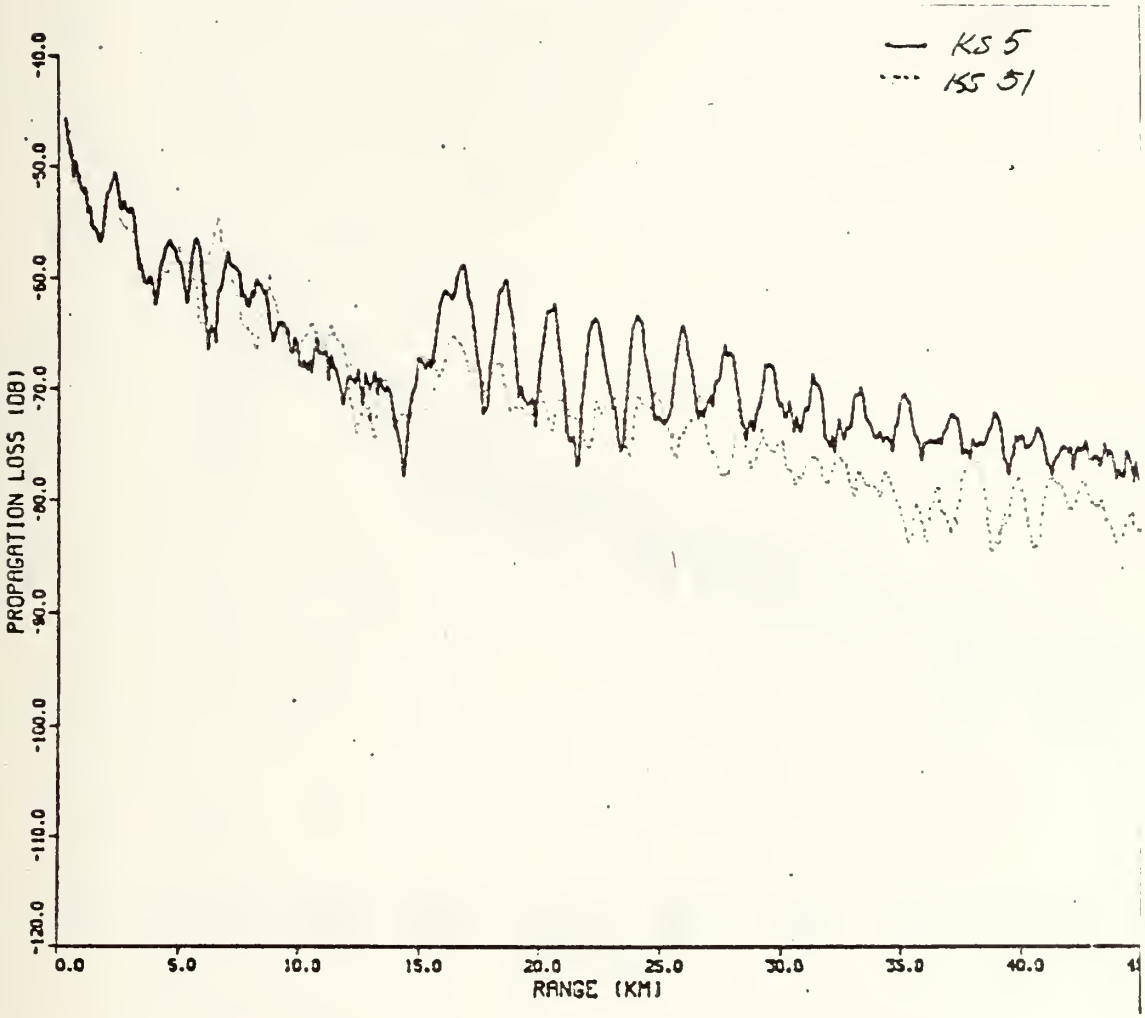

Figure 54. The Effect of the Number of Vertical Grid Points, 800 hz.

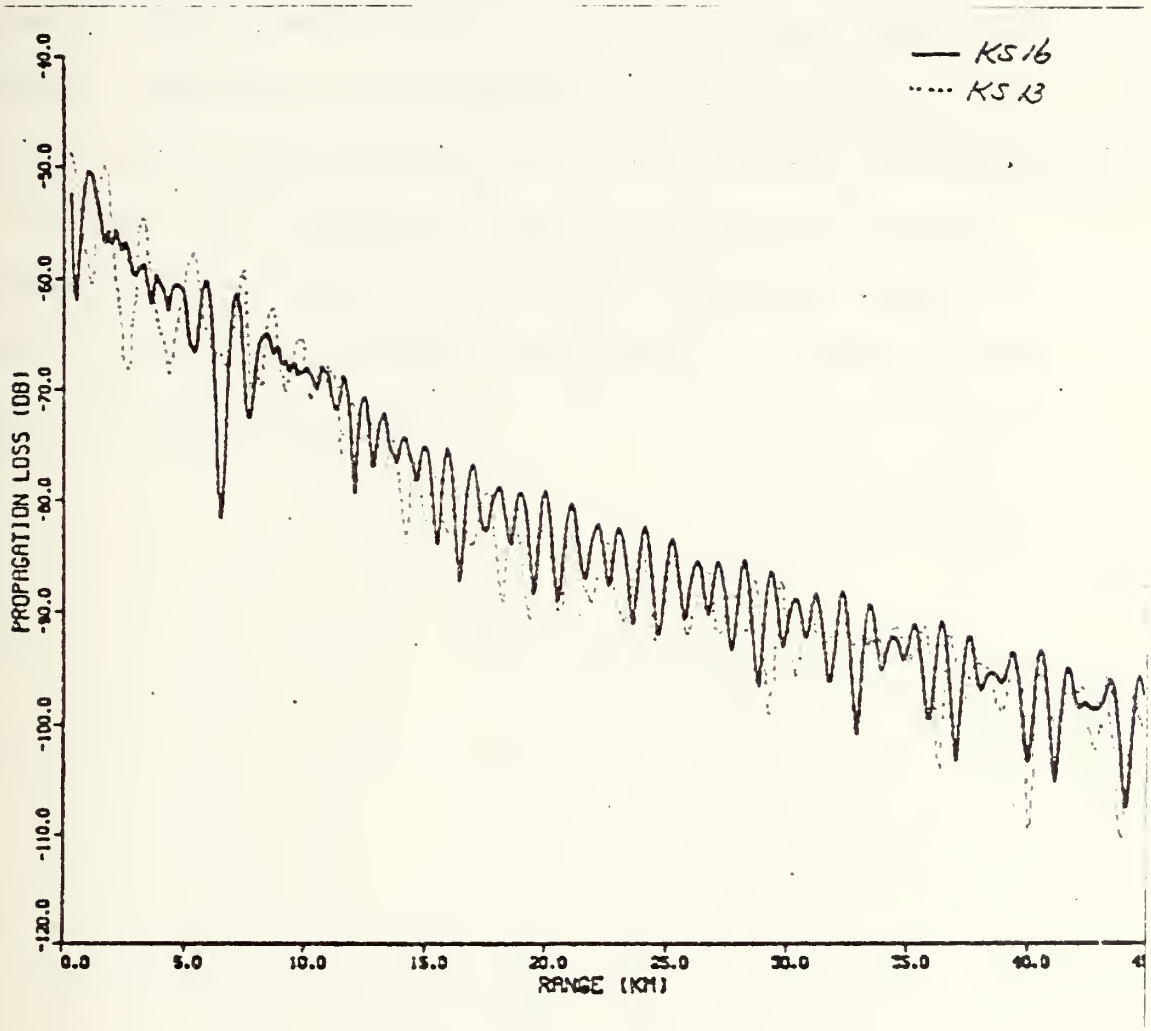

Figure 55. TL Comparison of the Effect with Different Bottom Profile.

water depth was chosen to be approximately the average depth in the area. The results are intermediate between those for the two propagation directions. (Figure 56).

The comparison between the predictions of the JAEGER PE and the measured transmission losses is shown (Figure 57, 58, 59). At all frequencies the agreement is good in the NE direction. While the model does predict that the transmission loss in SE direction will be significantly greater than that in the NE direction, agreement with the data for the SE direction is not as good as that for the NE direction. The experimentally-determined transmission losses in the SE direction are much greater than predicted and drop off much faster with range than predicted.

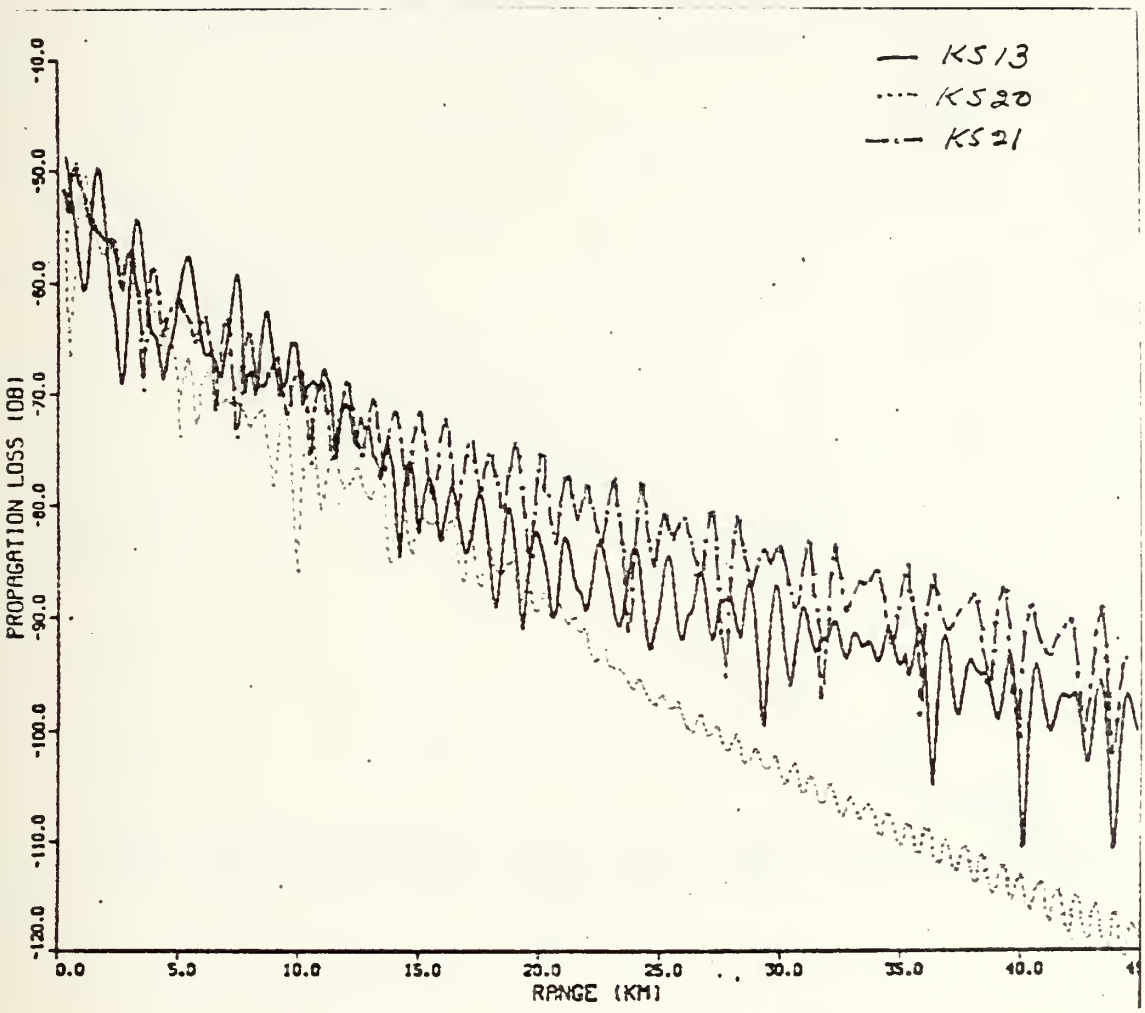

Figure 56. TL Comparison with Flat Bottom, in Both Directions, 50 hz.

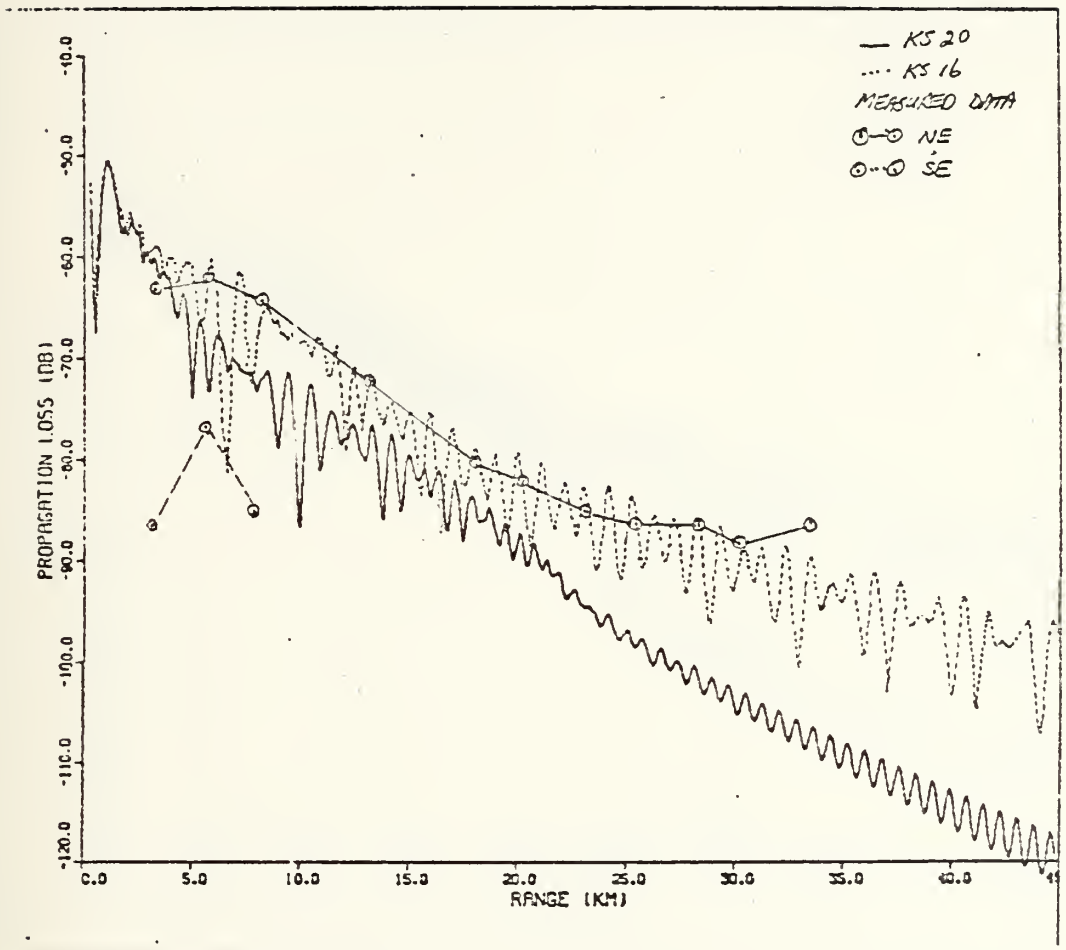

Figure 57. TL Comparison with JAEGER Model and Measurements, 50 hz.

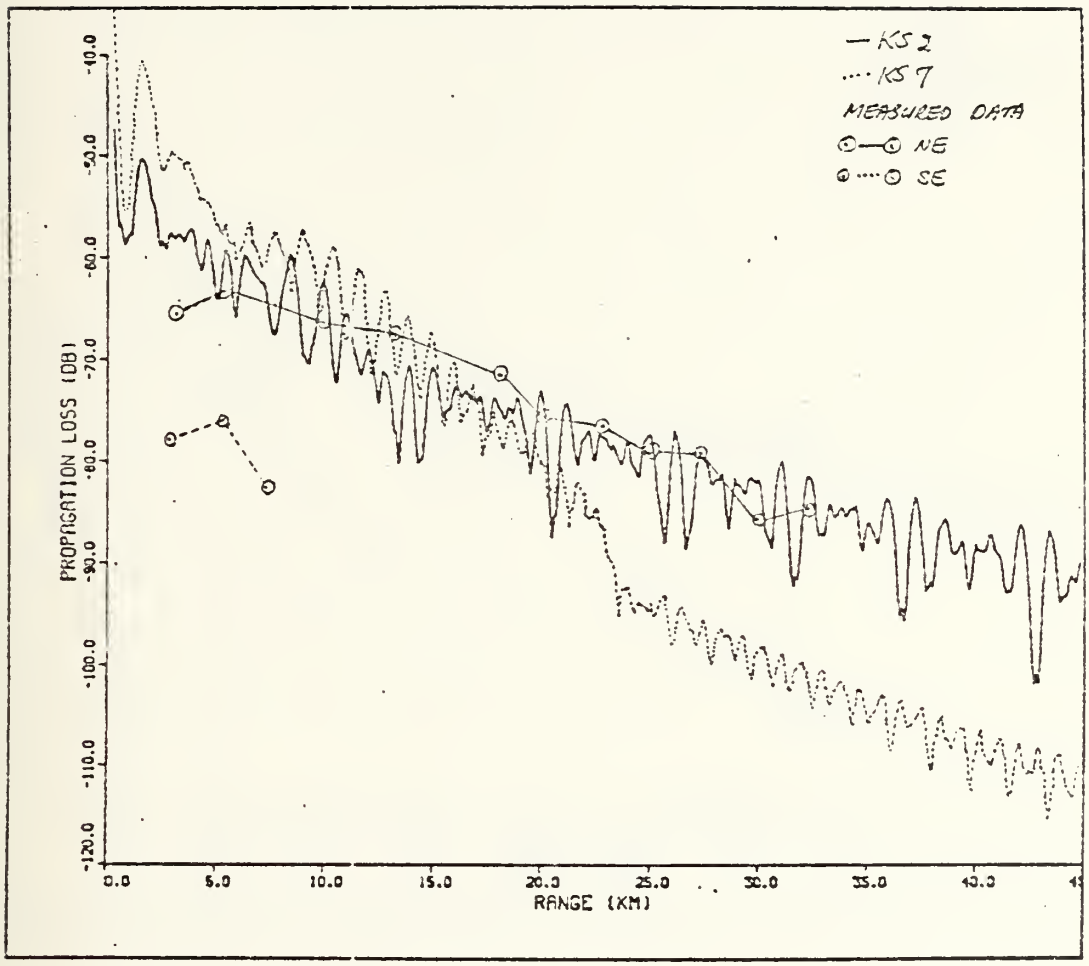

Figure 58. TL Comparison with JAEGER Model and Measurements, 100 hz.

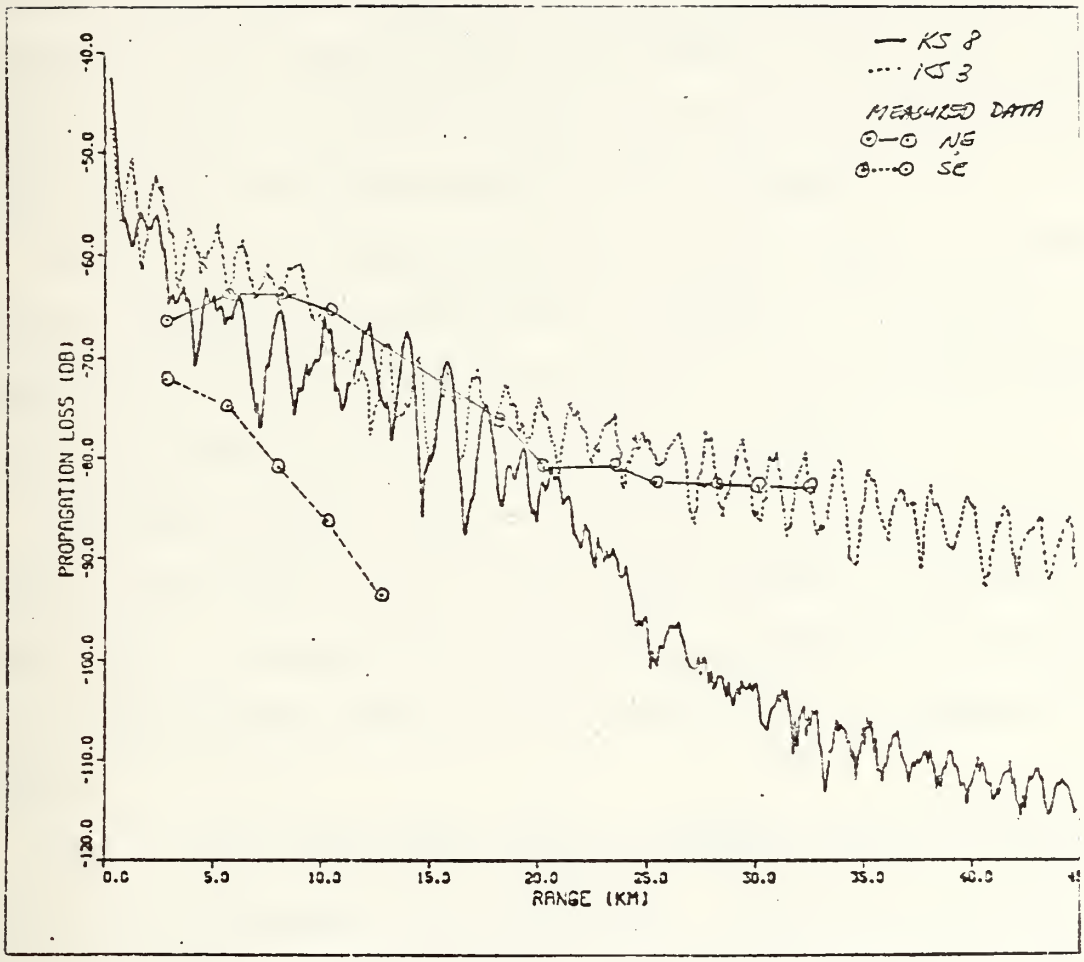

Figure 59. TL Comparison with JAEGER Model and Measurements, 200 hz.

V. CONCLUSIONS AND RECOMMENDATIONS

A. CONCLUSIONS

The prediction of underwater acoustic propagation in shallow water is extremely complicated. However, the demand for accurate forecasts of propagation loss in shallow water is increasing as naval weapon systems for air, surface, and subsurface platforms advance in sophistication and find more application in the shallow water environment.

Various kinds of computer models have been developed for prediction of acoustic propagation in shallow water. Comparison of the results of an experiment carried out in the shallow waters of the Korea Strait with several applicable models gives insufficient agreement.

The JAEGER PE model, developed at the Naval Postgraduate School, seems to agree quite well for gently sloping bottoms for frequencies below 200 hz. Agreement between experiment and prediction was not good for a steeply sloping bottom and, for both bottoms, for frequencies above 200 hz.

None of the computer models studied adequately predict transmission loss for all conditions in the Korea Strait. However, the implicit finite difference parabolic equation model, can be improved to provide better transmission-loss predictions for low frequencies over the types of bottom found in the Korea Strait.

B. RECOMMENDATIONS

During this study, many lessons were learned that will influence future investigations of underwater acoustic propagation in the Korea Strait.

1) In the data collection and measurements phase, more detailed atmospheric and oceanic data were needed. In particular, BTs, (or preferably SVP) should be obtained over the acoustic path during all measurements, and more complete knowledge of the bottom and sub-bottom is needed.

To efficiently test computer models, we suggest that two measurement sites be selected: one should remain centered over the trench and the other should be in an area of similar bottom type but with little or no slope.

2) Concurrently, work should be carried out to investigate the sensitivities of the JAEGER model to the various input parameters and to compare the existing measurements to predictions obtained by changing the bottom density, attenuation, and sound speed and the SVP in the water column to see if better agreement can be obtained.

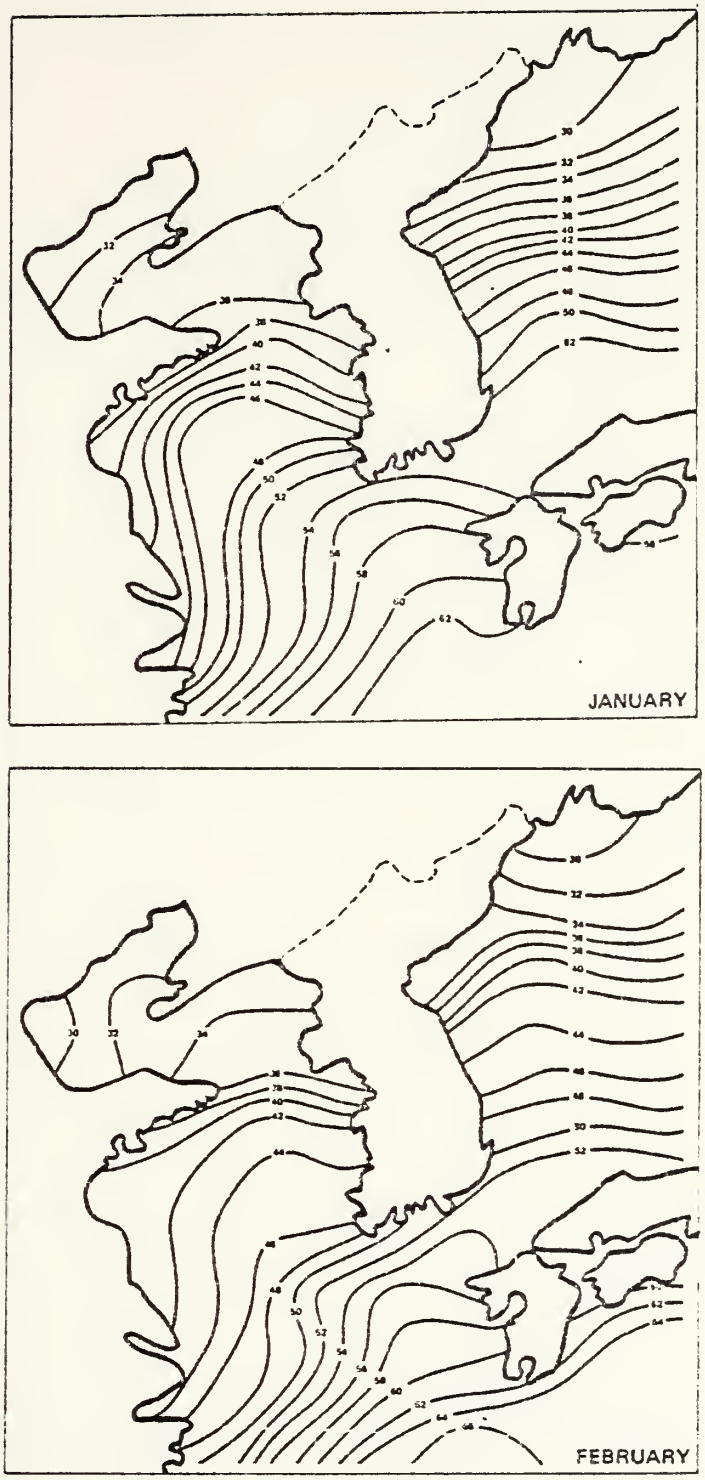

Figure A-1. Monthly Mean SST in January and February.

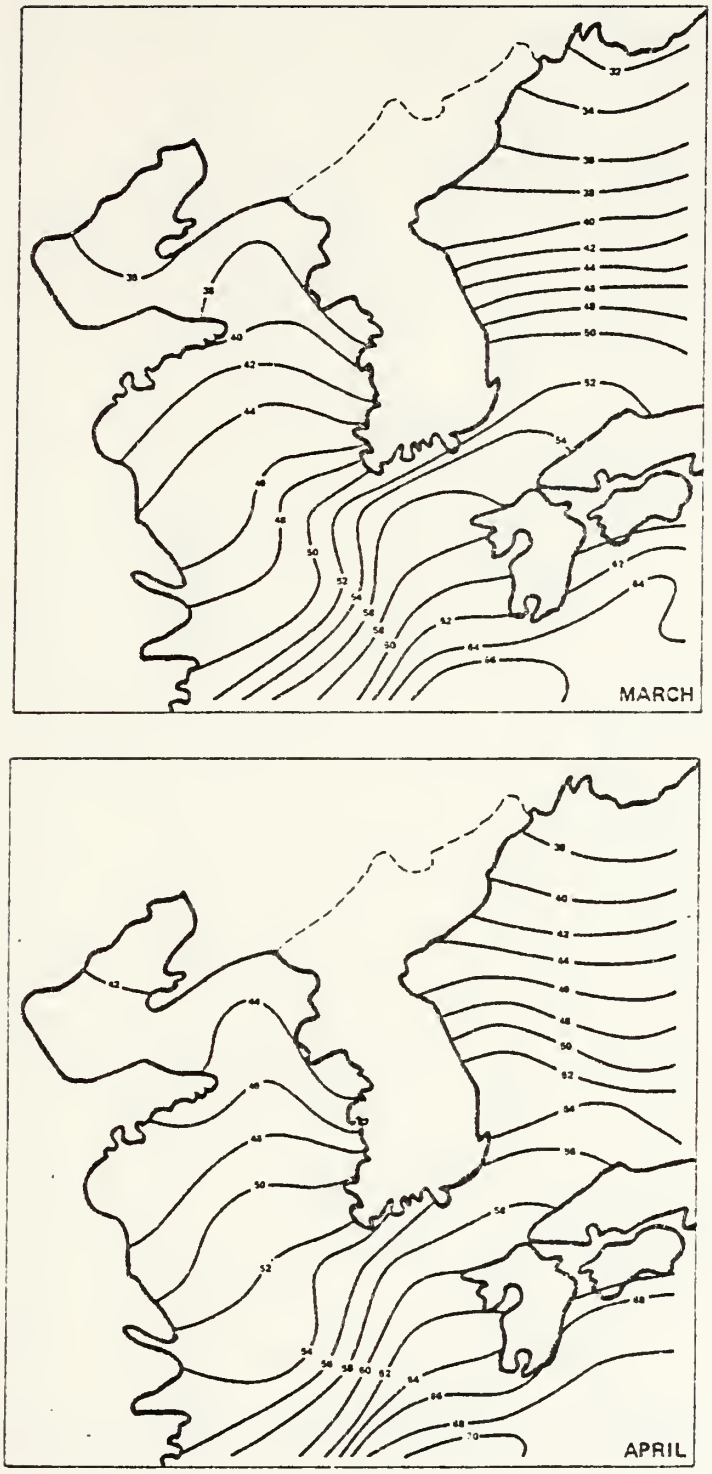

Figure A-2. Monthly Mean SST in March and April.

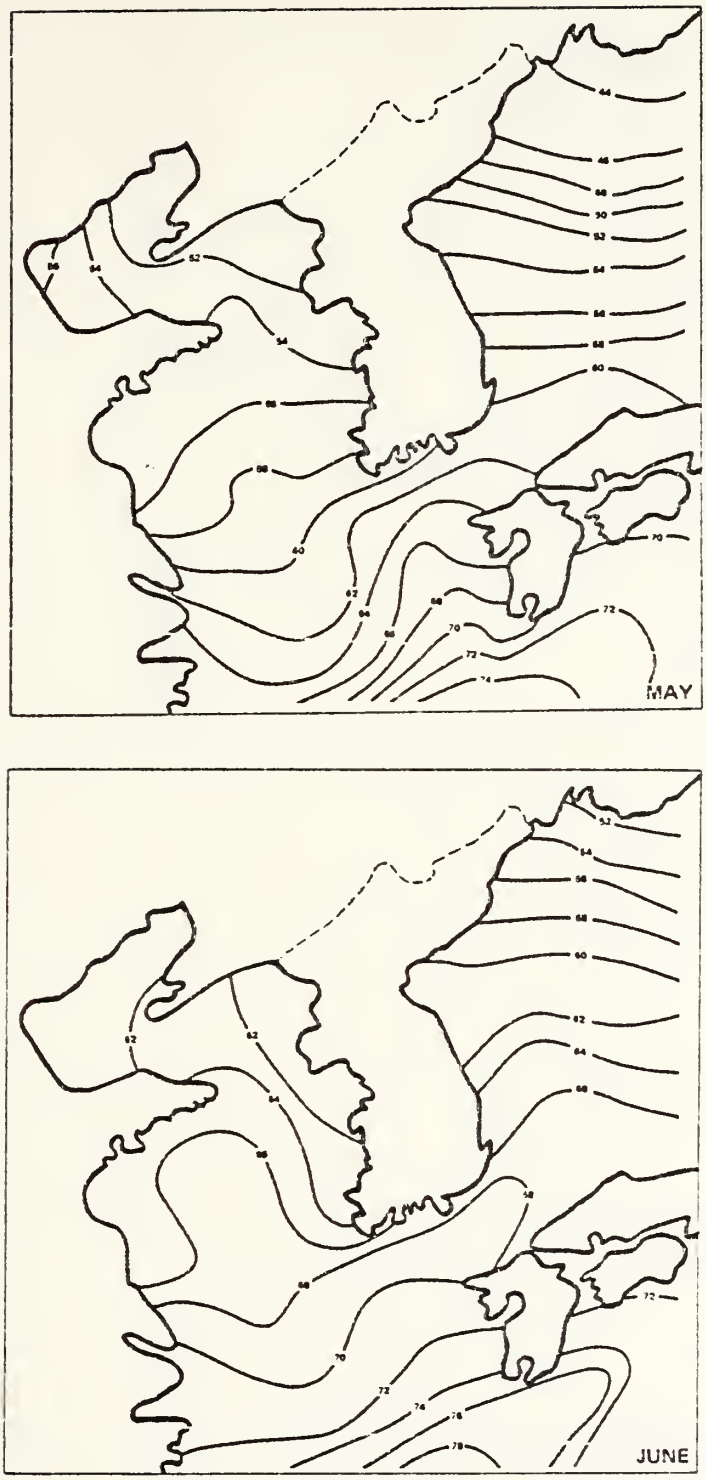

Figure A-3. Monthly Mean SST in May and June.

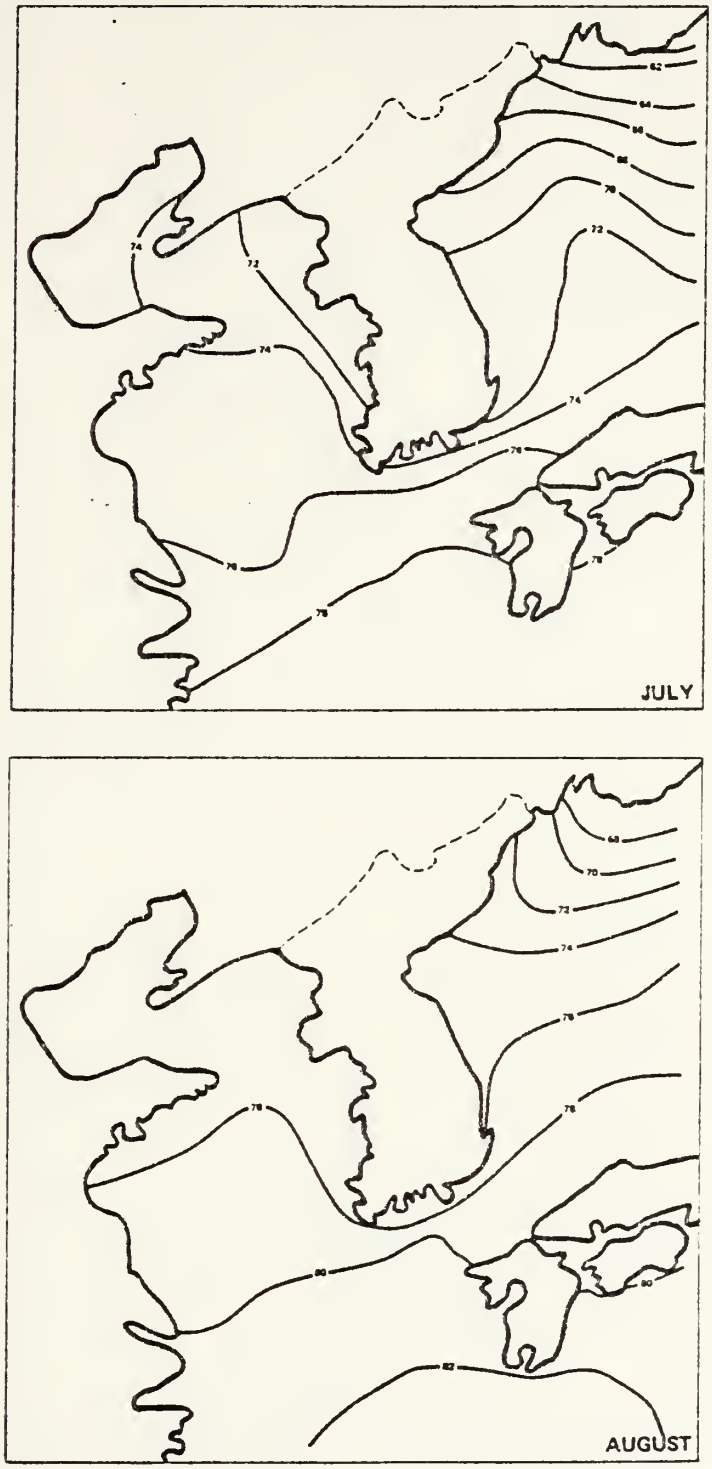

Figure A-4. Monthly Mean SST in July and August.

Figure A-5. Monthly Mean SST in September and October.

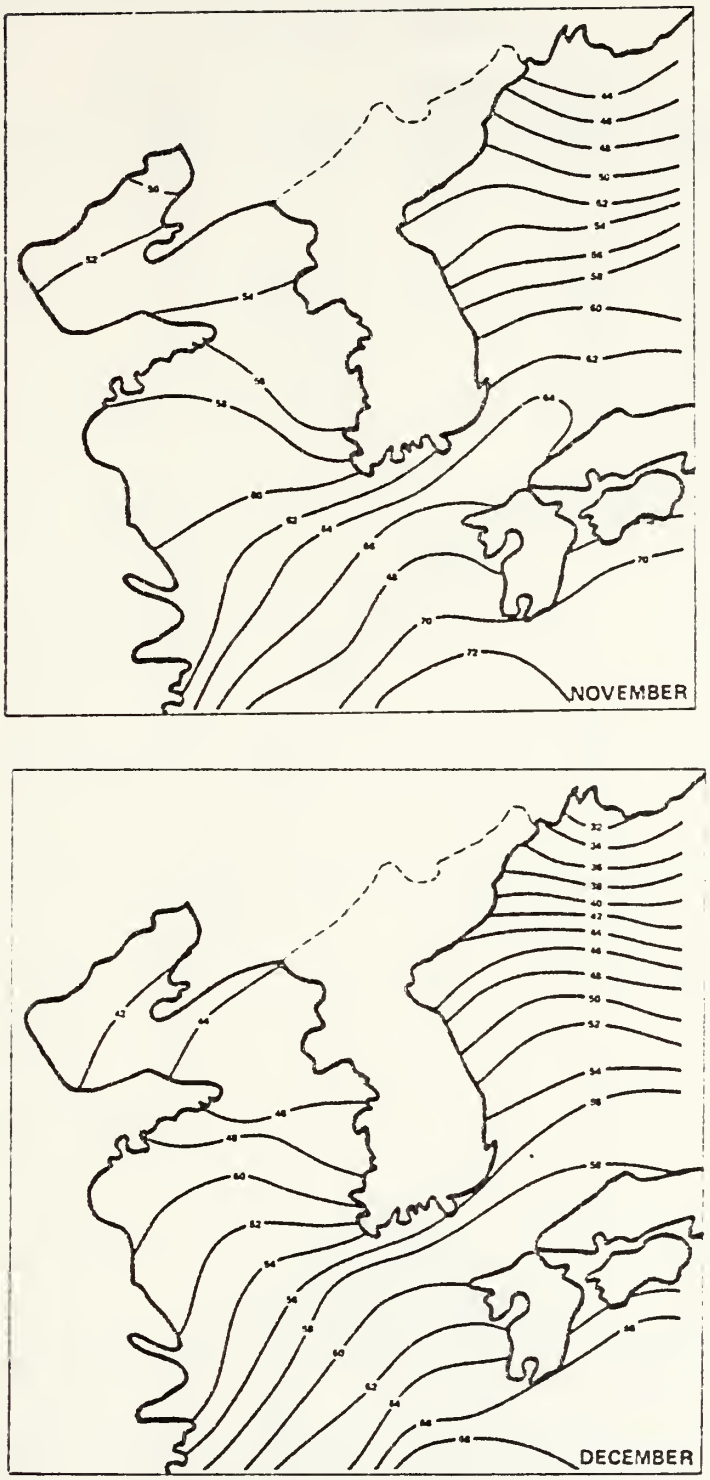

Figure A-6. Monthly Mean SST in November and December.

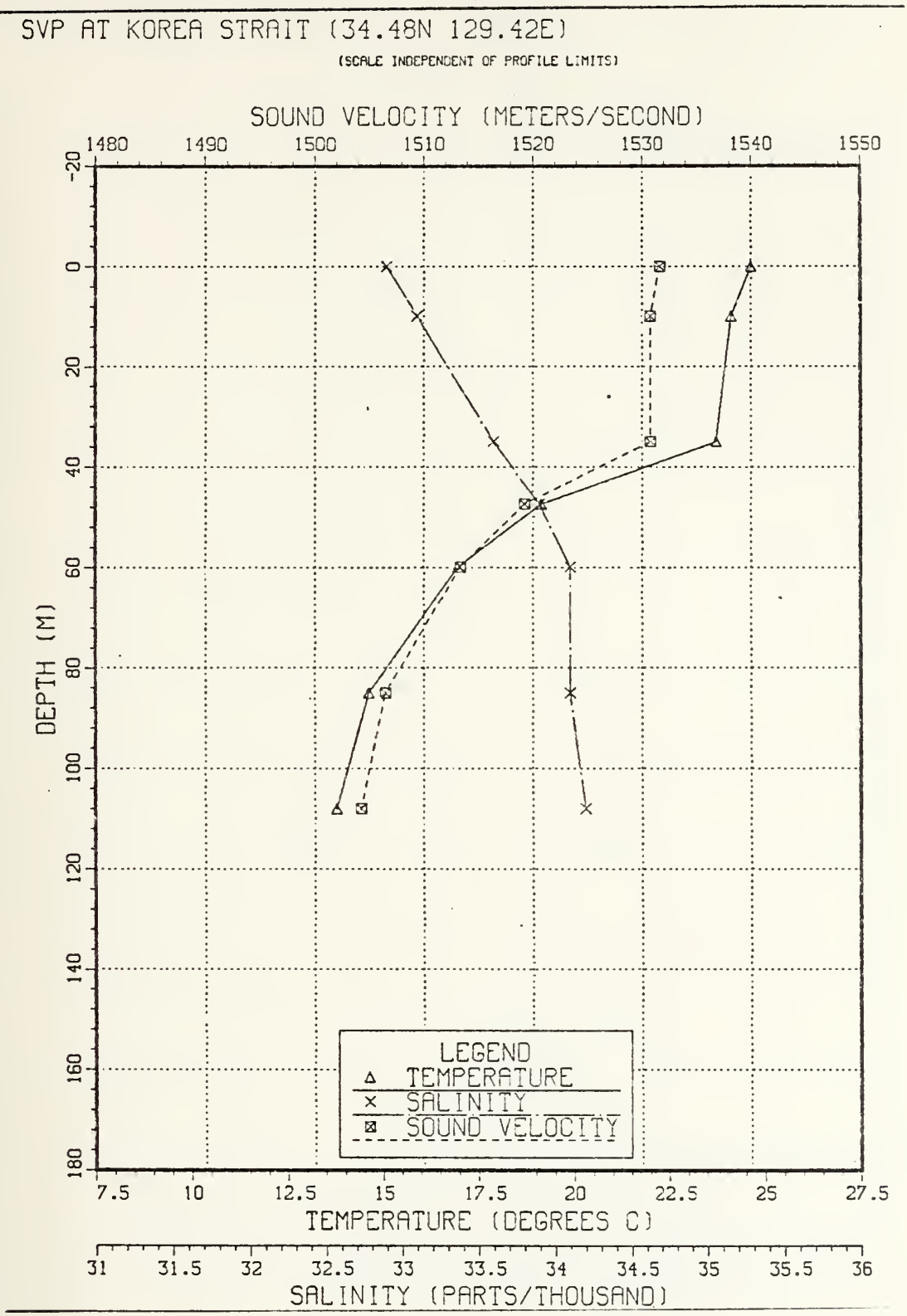

Figure B-1. Historical SVP in September (34.8N-129.7E).

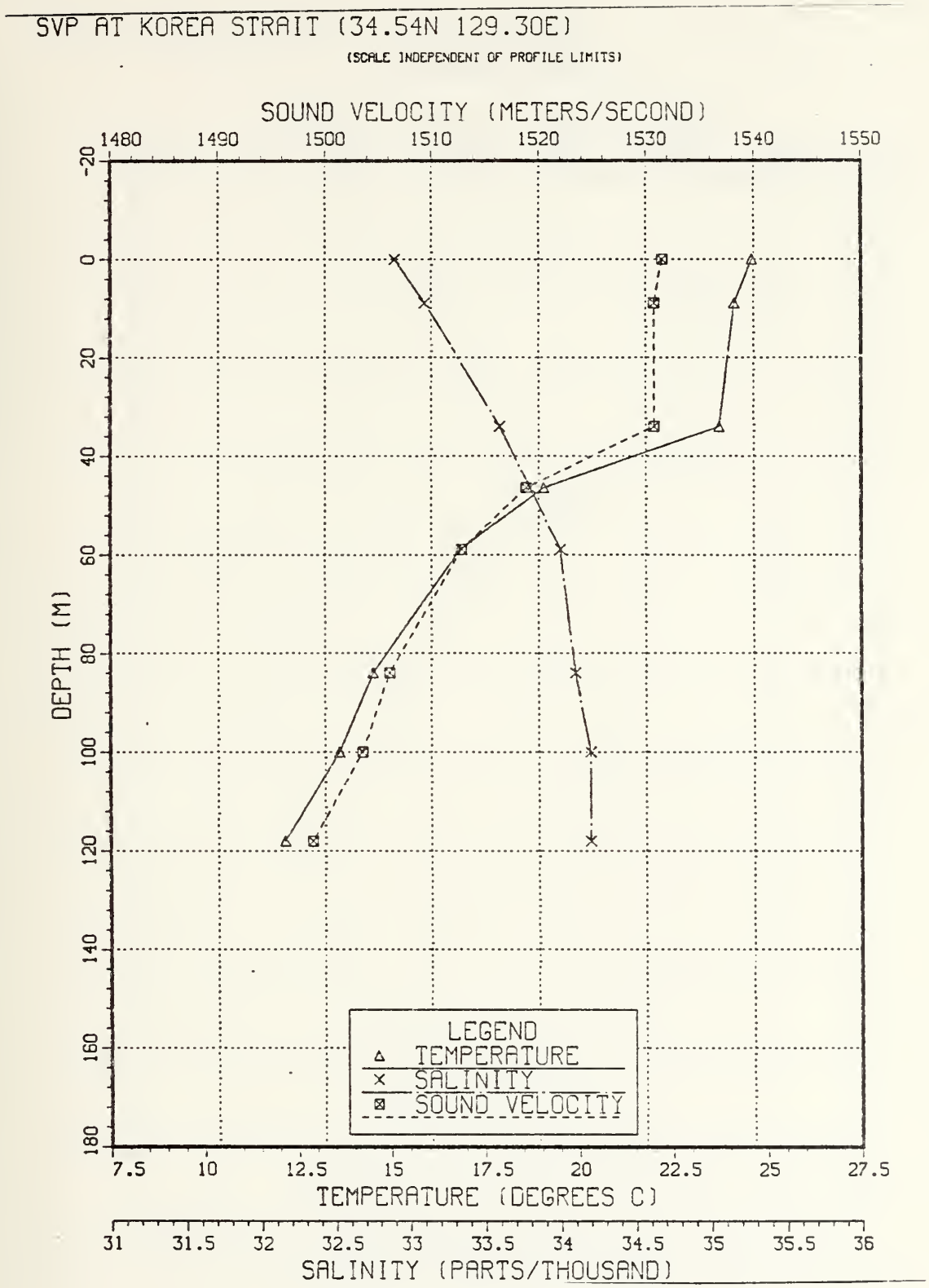

Figure B-2. Historical SVP in September (34.9N-129.5E).

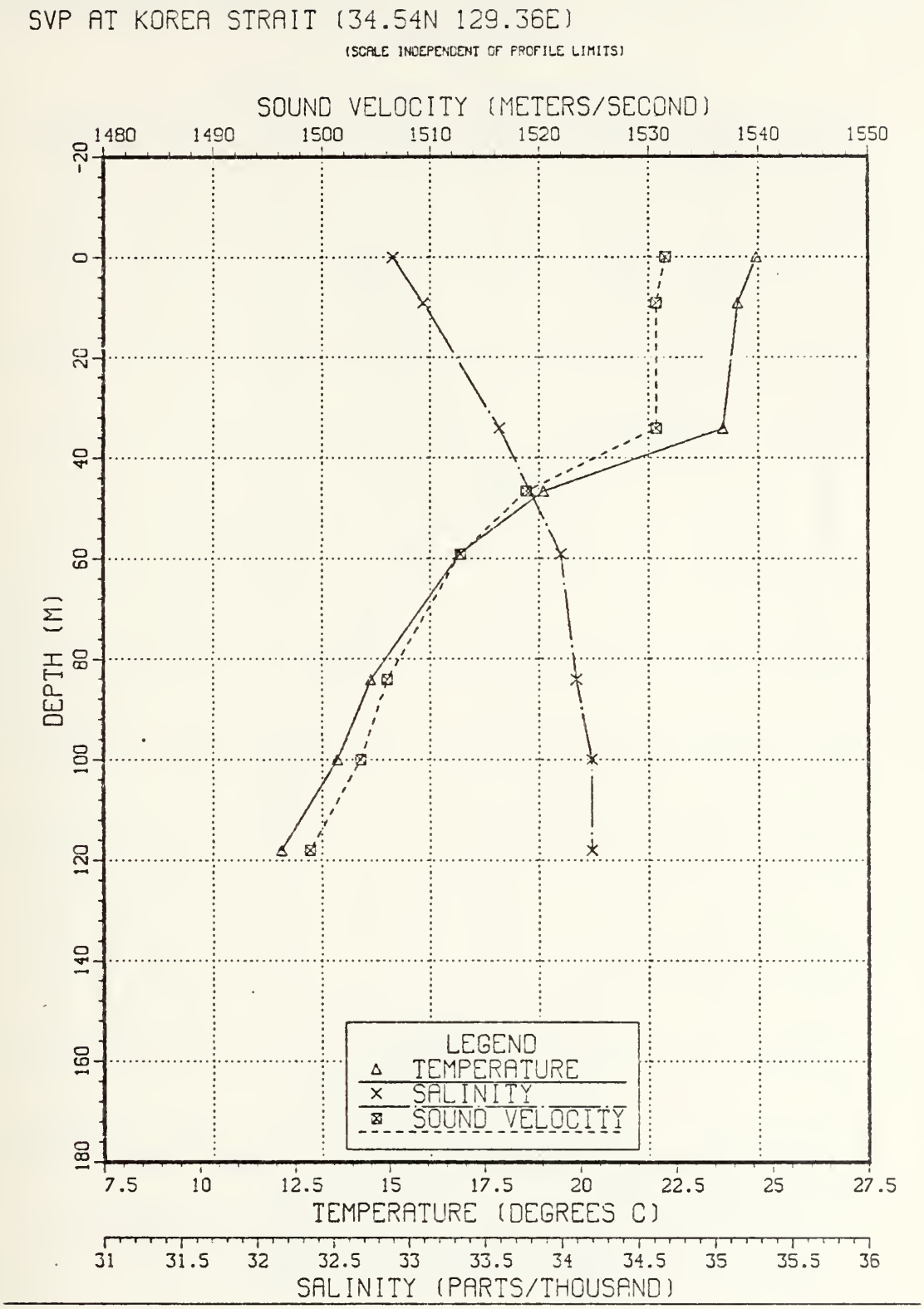

Figure B-3. Historical SVP in September (34.9N-129.6E).

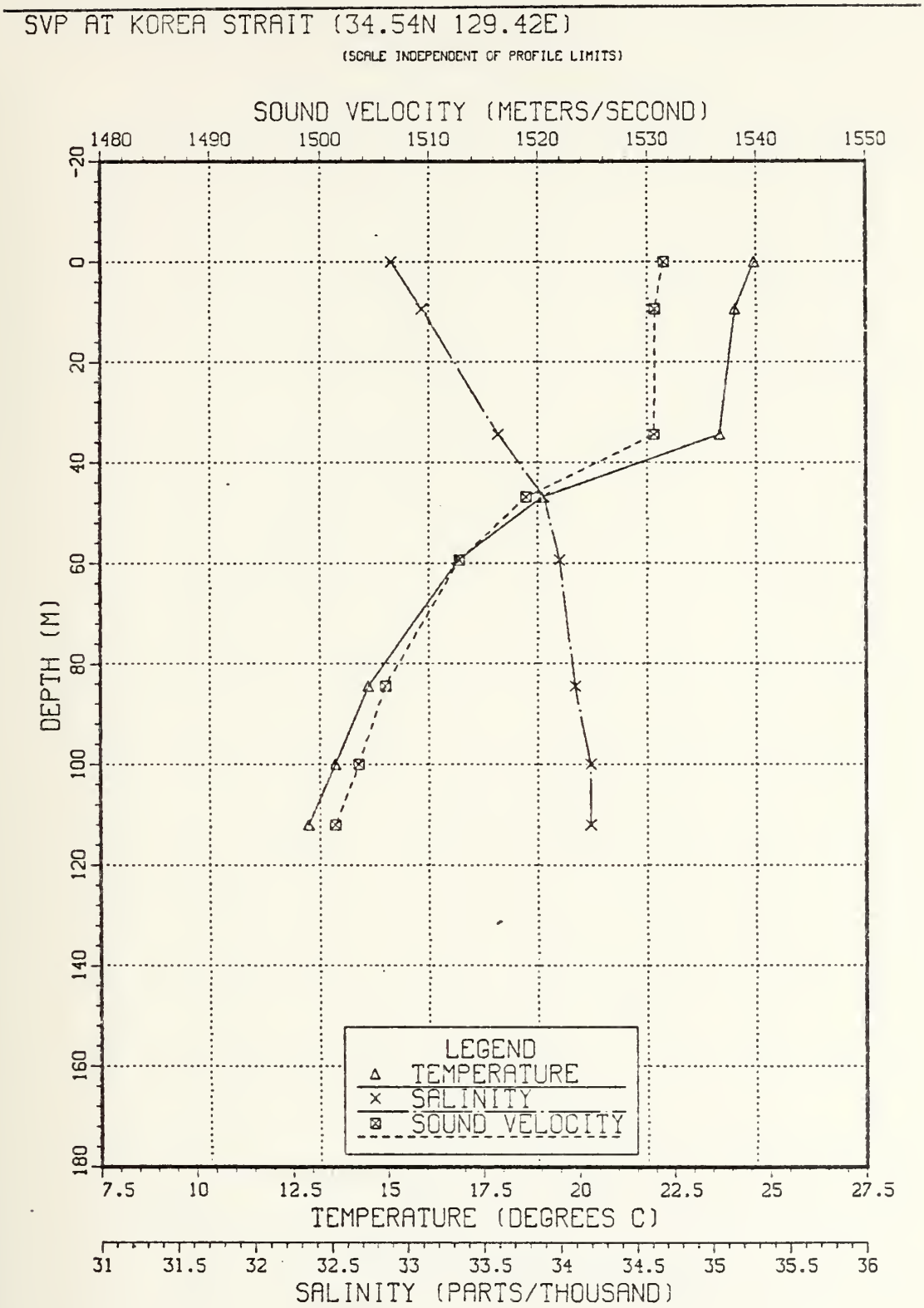

Figure B-4. Historical SVP in September (34.9N-129.7E)

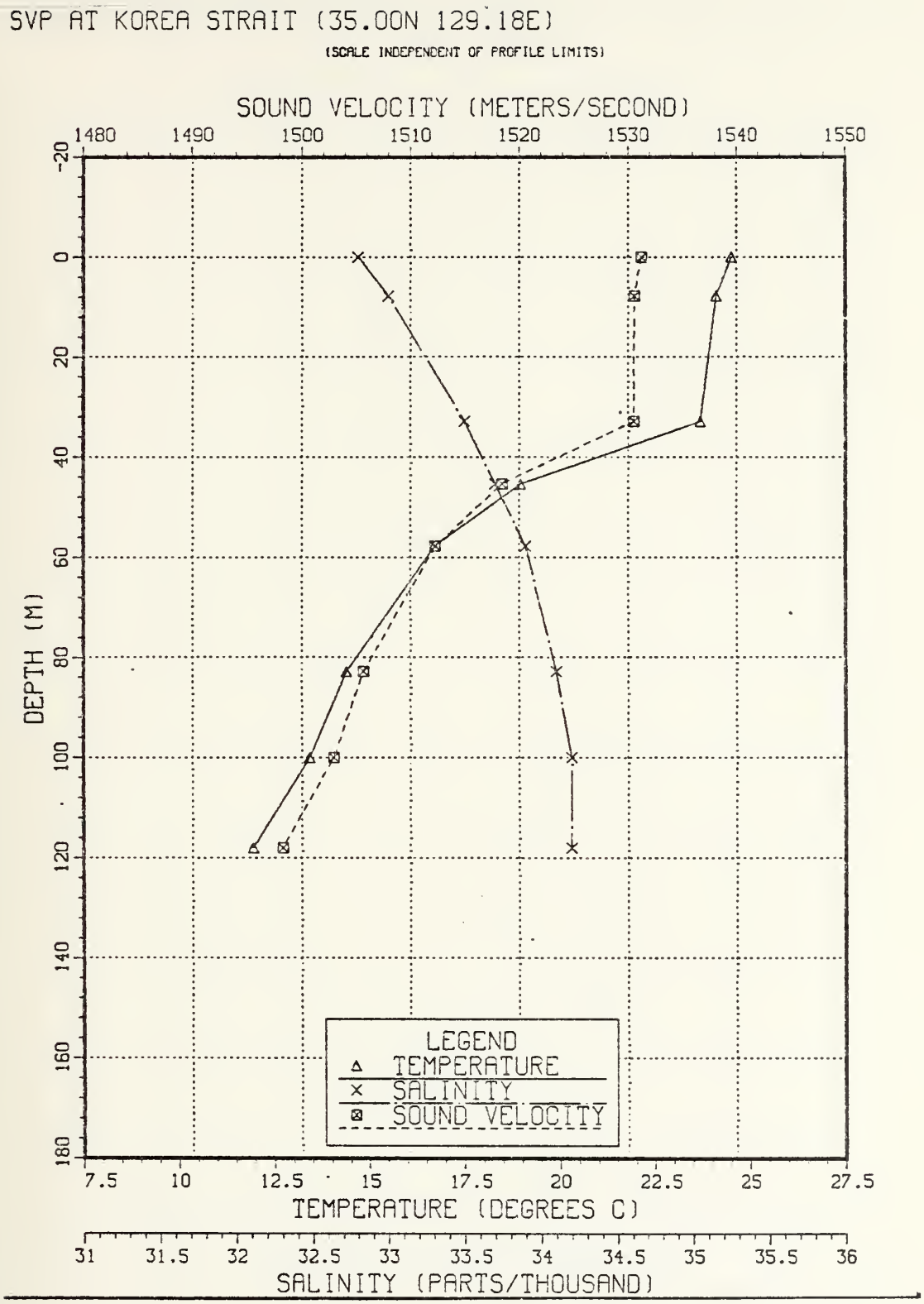

Figure B-5. Historical SVP in September (35.0N-129.3E).

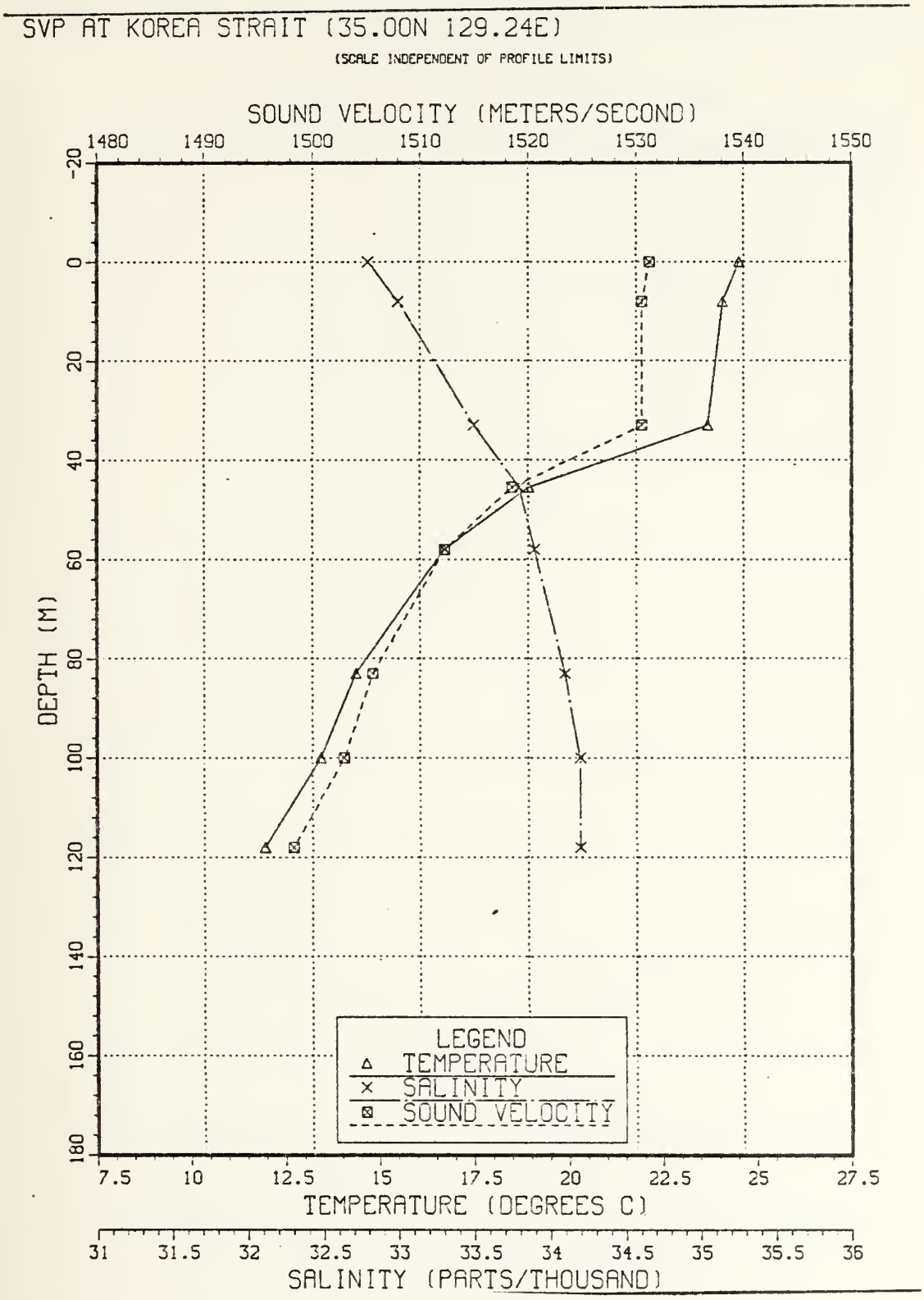

Figure B-6. Historical SVP in September (35.0N-129.4E).

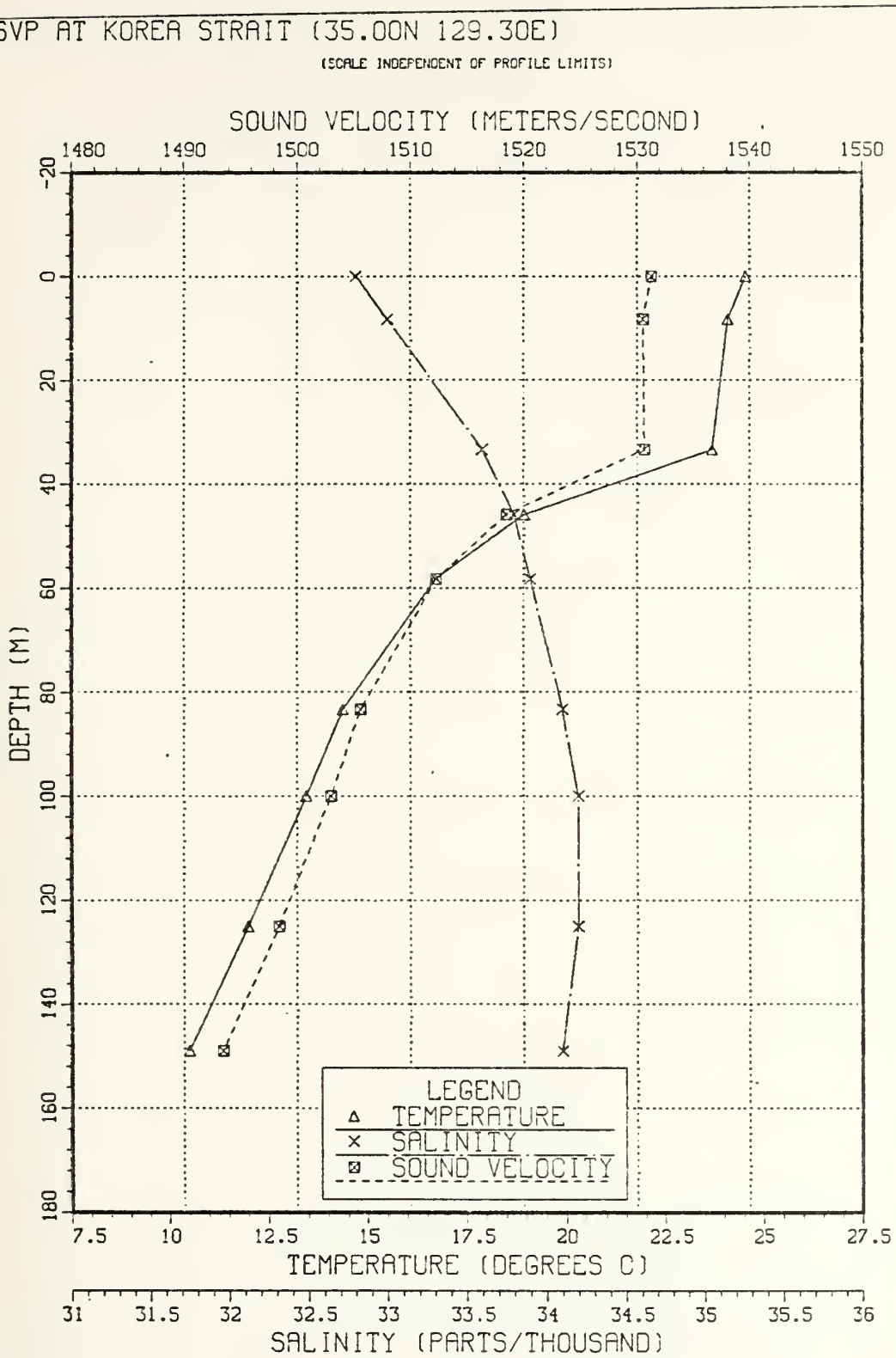

Figure B-7. Historical SVP in September (35.0N-129.5E).

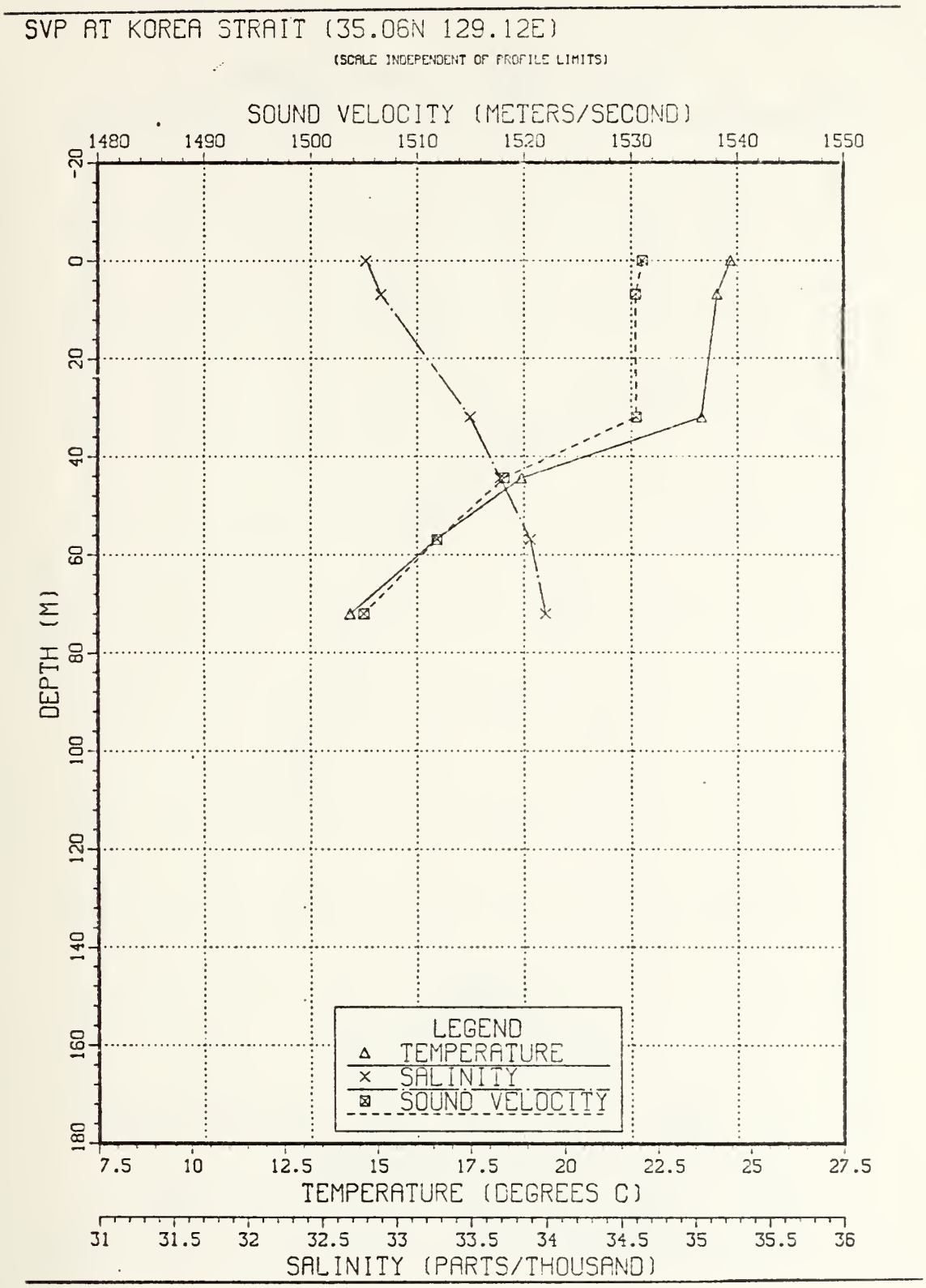

Figure B-8. Historical SVP in September (35.1N-129.2E)

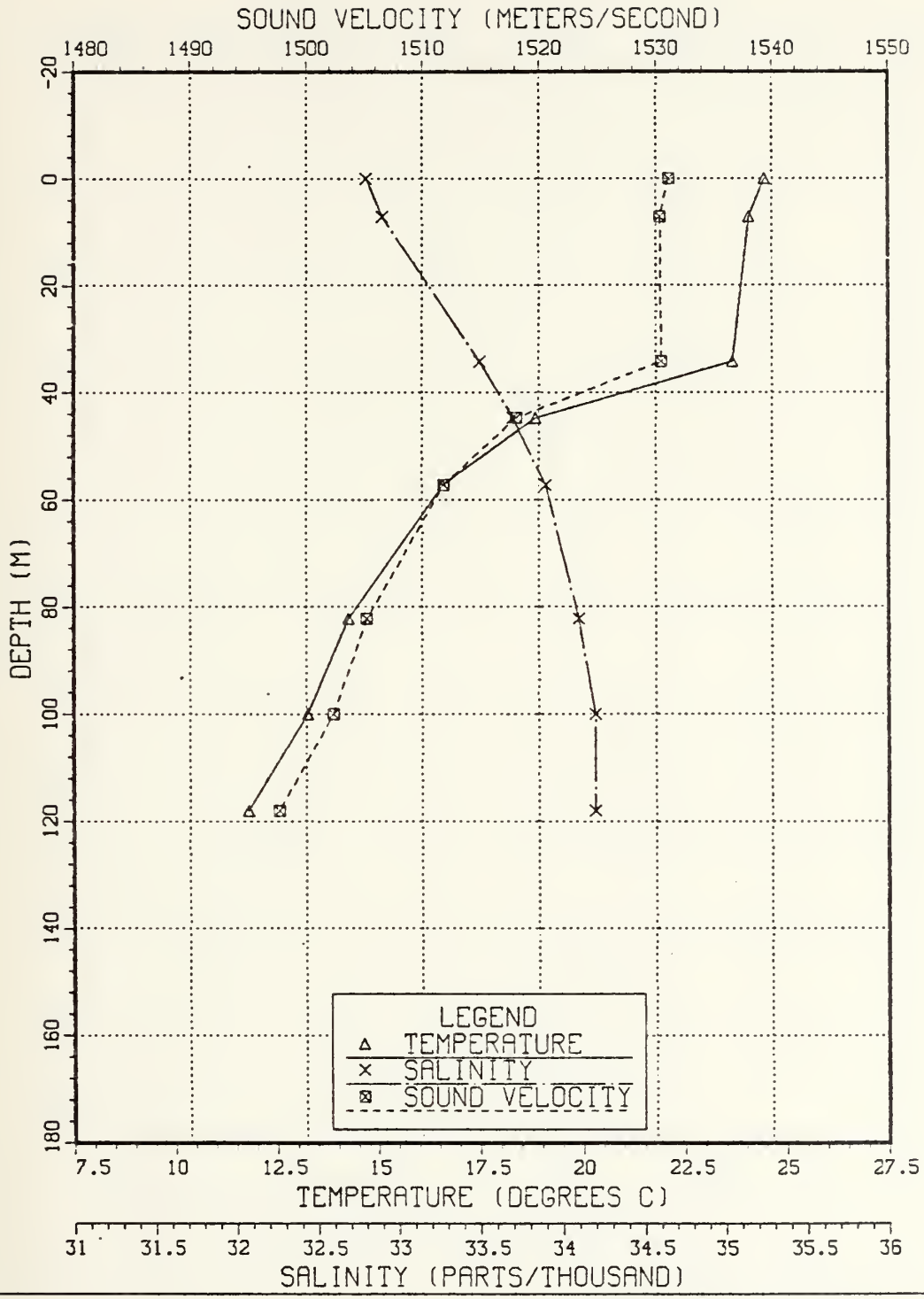

Figure B-9. Historical SVP in September (35.1N-129.3E).

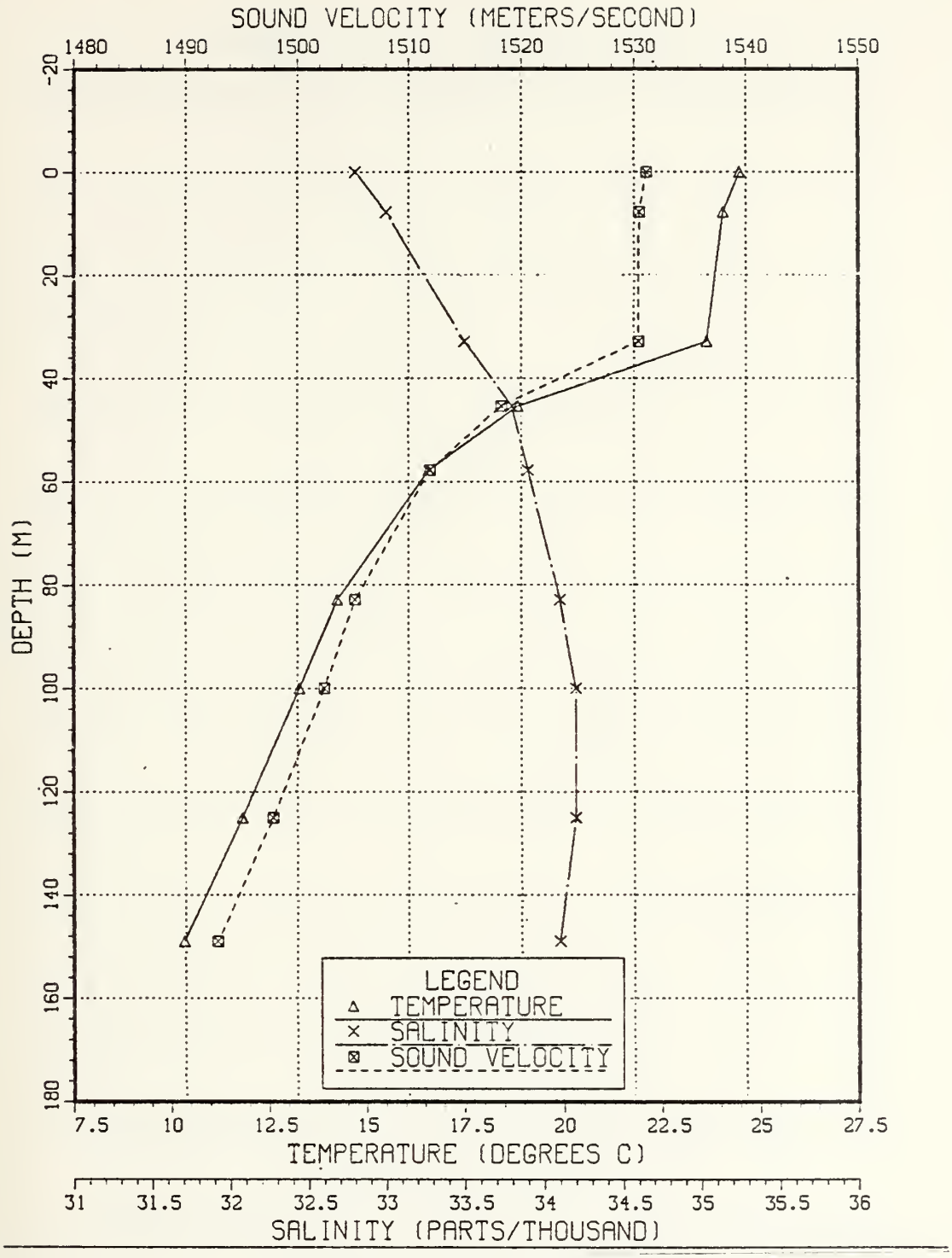

Figure B-10. Historical SVP in September (35.1N-129.5E).

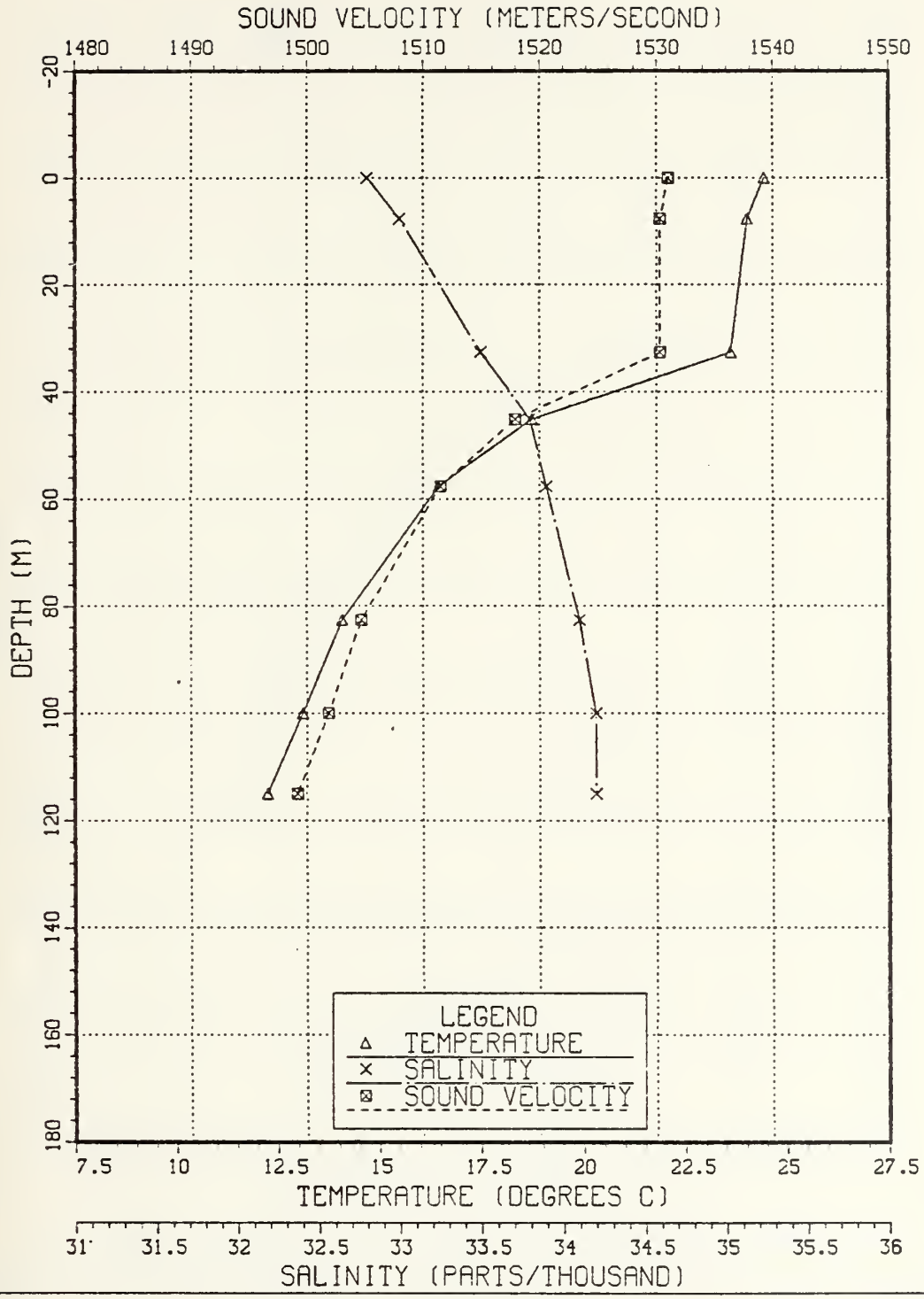

Figure B-11. Historical SVP in September (35.2N-129.6E).

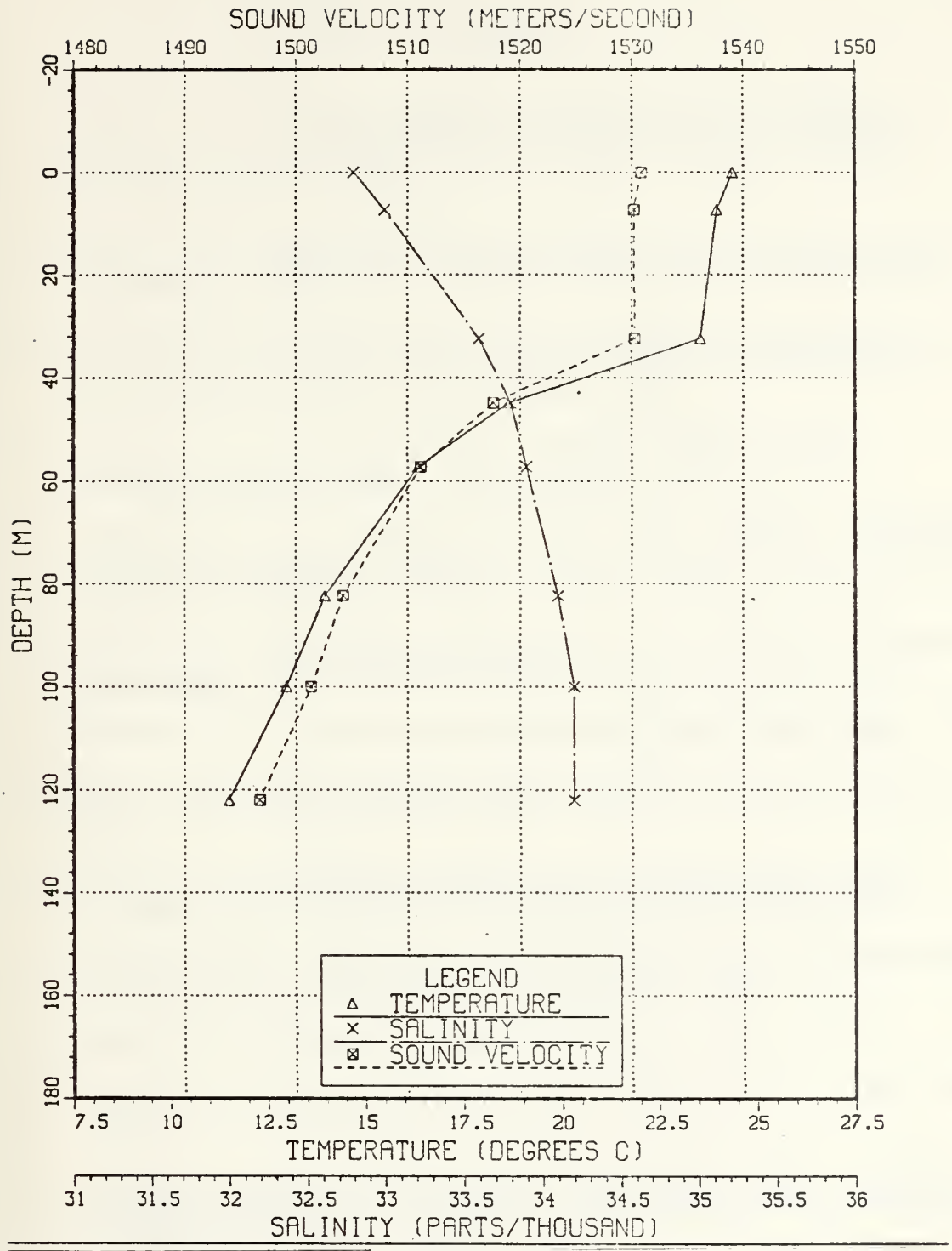

Figure B-12. Historical SVP in September (35.3N-129.7E).

LIST OF REFERENCES

1. Weston, D.C., Sound Propagation in the Presence of Bladder-Fish, Vol. 2, p. 55-88, 1967 In V.M. Albers (ed.), Underwater acoustics. Plenum Press, New York (Proc. 1966 NATO Advanced Study Institute, Copenhagen).

2. Weston, D.E., Fish as a Possible Cause of Low-Frequency Acoustic Attenuation in Deep Water (letter). JASA, 40, p. 1588, 1966.

3. Weston, D.E., Horrigan, A.A., Thomas, S.J.L., and Revie, J., Studies of Sound Transmission Fluctuations in Shallow Coastal Waters. Phil. Trans. Roy, Soc. A., p. 567-606, 1969.

4. Ching, H.P.A., and D. E. Weston., Shallow Water Acoustic Attenuation Due to Fish. In preparation, 1970.

5. Weston, D.E., K.J. Stevens, J. Revie, and M. Pengelly. Multiple Frequency Studies of Sound Transmission Fluctuations in Shallow Water. In preparation, 1970.

6. Weston, D.E., Fisheries Significance of the Acoustic Attenuation Due to Fish. In preparation, 1970

7. Weston, D.E., Contradiction Concerning Shallow Water Sound, 1967.

8. Nestor, M.J.R., RN, The Environment of South Korea and Adjacent Sea Area, NAVENVPREDRSCHFAC TR 77-03, 1977.

9. Lee, J.W., A Preliminary Report on the Environment of South Eastern Sector of Geojedo and Adjacent Sea Area, ADD, 1980.

10. Officer, C.B., Introduction to the Theory of Sound Transmission with Application to the Ocean, McGraw-Hill, 1958.

11. Urick, R.J., Sound Propagation in the Sea, DARPA, 1979.

12. Urick, R.J., Principles of Underwater Sound, 2nd Ed., McGraw-Hill, 1975.

13. Weston, D.E., and Pamela A. Ching., Sound Extinction by Fish in One-Way Shallow-Water Propagation, Admiralty Research Laboratory, Teddington, Middlesex, England, 1970.

14. Bedford, Anthony, and other, Acoustic Properties of Sediments, ARL-TR-82-47, 1982.

15. Piggot, C.D., Ambient Noise At Low Frequency in Shallow Water of the Scotian Shelf, JASA 36, p. 2152, 1965.

16. Summary of Synoptic Meterological Observations, U.S. Naval Weather Service Command, Vol. 9, 1971.

17. Kolpack, Ronald L., Temperature and Salinity Changes in the Tsushima Current, JECSS, p. 57, 1982.

18. Bannister, R.W., Denham, R.N. and Guthrie, K.M., Variability of Low-Frequency Ambient Sea Noise, JASA 65, No. 5, p. 1156-1163, 1979.

19. Arthur D. Little, Inc., Internal Waves; Their Influence Upon Naval Operation, Report No. 4090266, Department of Navy Bureau of Ship, 1966.

20. H. Francis, Eden, Arthur D. Little, Inc., and Michael Mohr., MIT, Acoustic Effect of Internal Waves in the Ocean, Third U.S. Navy Symposium on Military Oceanography, The Proceeding of the Symposium Vol. 2, p. 67, 1966.

21. Principles and Applications of Underwater Sound, Department of the Navy, Headquarters, Naval Material Command, Washington, D.C. 1968.

22. Huh, Oscar K., Satellite Observations and the Annual Cycle of Surface Circulation in the Yellow Sea, East China Sea, and Korea Strait, La Mer 20, 1982.

23. Kenzo Shuto., A Review of Sea Conditions in the Japan Sea, La Mer 20, p. 119-124, 1982.

24. Yoshiaki Toba, Kazumi Tomizawa, Yoshikazu Kurasawa, Kimio Hanawa., Seasonal and Year-to-Year Variability of the Tsushima-Tsugaru Warm Current System With Its Possible Cause, La Mer 20, 1982.

25. Ding Lee., George Botseas., An Implicit Finite-Difference Computer Model for Solving the Parabolic Equation, NUCS TR6659, 1982.

26. Foreman, Terry L., University of Texas Range Dependent Ray Model (MEDUSA), ARL TR 82-64, University of Texas, Austin, Texas, 1982.

27. Laevastu, T.,Capt. W.E. Hubert, USN. Analysis and Prediction of the Depth of the Thermocline and Near-Surface Thermal Structure. FNWF Technical Note. No. 10, August 1965.

28. Hamilton, Edwin L.,Geoacoustic Modeling of the Sea Floor, JASA 68, p. 1313-1340, 1980

BIBLIOGRAPHY

Banard, G.R., J.L. Bardin., W.B. Hempkins., Underwater Sound Reflection from Layered Media, JASA 36, P. 2119, 1964.

Brekhowskikh, L.M., Waves in Layered Media, Academic Press Inc., New York, 1960.

Cole, B.F., Marine Sediment Attenuation and Ocean-Bottom Reflected Sound, JASA 36, p. 1993 (A), 1964.

Faust, L.Y.; Seismic Velocity as a Function of Depth and Geologic Time, Geophics., 16, p. 192, 1951.

Liberman, L.N.; Reflection of Sound from Coastal Bottoms, JASA 20, p. 305, 1948.

MacKenzie, K.V.; Reflection of Sound From Coastal Bottoms, JASA 32, p. 221, 1960.

Marsh, H.W.; Reflection and Scattering of Sound by the Sea Bottom, JASA 36, p. 2003 (a), 1964. Complete Paper Avco Corporation, Marine Electronics Office, New London, Conn.

Mitchell, S.K., and K.C. Focke., The Role of the Attenuation Profile in Low Frequency Shallow Water Propagation, submitted to JASA (no date).

Perrone, A.J., Infrasonic and Low Frequency Ambient Noise Measurement in the Grand Banks , JASA 55, p. 754-758, 1974.

Rayleigh, Lord, The Theory of Sound, Vol. 2, Dover Publications, Inc., New York, 1945.

INITIAL DISTRIBUTION LIST

		No. of Copies
1.	Defense Technical Information Center Cameron Station Alexandria, Virginia 23314	2
2.	Library, Code 0142 Naval Postgraduate School Monterey, California 93943	2
3.	Chairman Code 68Mr) Department of Oceanography Naval Postgraduate School Monterey, California 93943	1
4.	Superintendent Republic of Korea Naval Academy Seuol, Korea	1
5.	Superintendent Naval Command and Staff College Republic of Korea Navy Seoul, Korea	1
6.	Glenn, J. Jung, Code 68 Jq Naval Postgraduate School Monterey, California 93943	2
7.	James V. Sanders, Code 61Sd Naval Postgraduate School Monterey, California 93943	4
8.	Calvin R. Dunlap, Code 68 Du Naval Postgraduate School Monterey, CA 93943	2
9.	Eugene W. Brown NAVOCEANO Code 7300 NSTL Station Bay St. Louis, MS 39522	1
10.	Commander Fleet Air Wing Republic of Korea Navy, Pohang 768-78, Seoul, Korea	2

11. Commander 2
AIRASRON 101, 768-78
Republic of Korea Navy
Seoul, Korea

12. Director 2
Agency for Defense Development
Box 18, Chinhae 602-00
Seoul, Korea

13. LTJG Diane Durban, U.S.N. 1
NAVOCEANCOMFAC Keflavik, IC
Naval Station
FPO: New York, NY 09571

14. LCDR Sea Hun. Park 2
AIRASRON 101,768-78
Republic of Korea Navy
Seoul, Korea

15. A. B. Coppens, Code 61 Cz 1
Naval Postgraduate School
Monterey, California 93943

16. Commander (ECV) 1
ATTN: LT Larry JAEGER
Seventh Coast Guard District
Federal Building
51 S.W. 1st Avenue
Miami, Florida 33130

17. Dr. James Andrews 1
NSTL Station
Bay St. Louis, MS 39529

18. Chief of Naval Research 1
ATTN: Dr. Michael McKissick
800 N. Quincy St.
Arlington, VA 22217

19. LCDR Suk In Lee 1
Office of ADCNO for Education
Korea Naval Headquarters
Seoul, Korea

121-352

207396

Thesis
P157552 Park
c.1 Underwater acoustic propagation in the Korea strait.

JUL 20 85
30 MAR 88
13 SEP 89
13 SEP 89

33072
33575
80180

207396

Thesis
P157552 Park
c.1 Underwater acoustic propagation in the Korea strait.

AMERICAN BINDERY TOPEKA KANSAS

thesP157552
Underwater acoustic propagation in the K
3 2768 001 97208 6
DUDLEY KNOX LIBRARY